New Catalysts for the Renewable Production of Monomers for Bioplastics

Thesis by

Joshua J. Pacheco

In Partial Fulfillment of the Requirements for

the Degree of Doctor of Philosophy

California Institute of Technology

Pasadena, CA

2015

(Defended May 12, 2015)

ACKNOWLEDGMENTS

Many thanks and appreciation is given to my family for their never-ending love and support during my time as a Ph.D. student.

My fellow Ph.D. students and postdocs within the M.E. Davis group were indispensable during my graduate studies. It was truly a pleasure to have been able to work every day with some of the hardest working and brightest researchers in the field. Without the many great ideas that had arisen from discussions with them, this work would not have been possible.

To many others at Caltech, including Dr. Jay Labinger, Dr. Mona Shahgholi, Dr. Chi Ma, and Dr. David VanderVelde, I am greatly thankful for the advice and assistance that you offered me.

Lastly, I express my great appreciation to my advisor, Prof. Mark Davis, for bringing me into his research group and giving me the opportunity to join the exciting field of zeolite synthesis and catalysis.

ABSTRACT

Terephthalic acid (PTA) is one of the monomers used for the synthesis of the polyester, polyethylene terephthalate (PET), that is used for the large-scale manufacture of synthetic fibers and plastic bottles. PTA is largely produced from the liquid-phase oxidation of petroleum-derived p-xylene (PX). However, there are now ongoing worldwide efforts exploring alternative routes for producing PTA from renewable, biomass resources.

In this thesis, I present a new route to PTA starting from the biomass-derived platform chemical, 5-hydroxymethylfurfural (HMF). This route utilizes new, selective Diels-Alder-dehydration reactions involving ethylene and is advantageous over the previously proposed Diels-Alder-dehydration route to PTA from HMF via 2,5-dimethylfuran (DMF) since the H_2 reduction of HMF to DMF is avoided. Specifically, oxidized derivatives of HMF are reacted as is, or after etherification-esterification with methanol, with ethylene over solid Lewis acid catalysts that do not contain strong Brønsted acids in order to synthesize intermediates of PTA and its equally important diester, dimethyl terephthalate (DMT). The partially oxidized HMF, 5-(hydroxymethyl)furoic acid (HMFA) is reacted with high pressure ethylene over a pure-silica molecular sieve catalyst containing framework tin (Sn-Beta) to produce the Diels-Alder-dehydration product, 4-(hydroxymethyl)benzoic acid (HMBA), with ~30% selectivity at ~20% yield. If HMFA is protected with methanol to form methyl 5-(methoxymethyl)furan-2-carboxylate (MMFC), MMFC can react with ethylene in the presence of a pure-silica molecular sieve containing framework zirconium

(Zr-Beta) to produce methyl 4-(methoxymethyl)benzenecarboxylate (MMBC) with >70% selectivity at >20% yield. HMBA and MMBC can then be oxidized to produce PTA and DMT, respectively. When Lewis acid containing mesoporous silica (MCM-41) and amorphous silica, or Brønsted acid containing zeolites (Al-Beta), are used as catalysts, a significant decrease in selectivity/yield of the Diels-Alder-dehydration product is observed.

An investigation to elucidate the reaction network and side products in the conversion of MMFC to MMBC was performed, and the main side products are found to be methyl 4-formylcyclohexa-1,3-diene-1-carboxylate and the ethylene Diels-Alder adduct of this cyclohexadiene. These products presumably form by a different dehydration pathway of the MMFC/ethylene Diels-Alder adduct and should be included when determining the overall selectivity to PTA or DMT since, like MMBC, these compounds are precursors to PTA or DMT.

Fundamental physical and chemical information on the ethylene Diels-Alder-dehydration reactions catalyzed by the Lewis acid-containing molecular sieves was obtained. Madon-Boudart experiments using Zr-Beta as catalyst show that the reaction rates are limited by chemical kinetics only (physical transport limitations are not present), all the Zr^{4+} centers are incorporated into the framework of the molecular sieve, and the whole molecular sieve crystal is accessible for catalysis. Apparent activation energies using Zr-Beta are low, suggesting that the overall activation energy of the system may be determined by a collection of terms and is not the true activation energy of a single chemical step.

TABLE OF CONTENTS

LIST OF FIGURES

LIST OF TABLES

CHAPTER 1

PRODUCTION OF RENEWABLE TEREPHTHALIC ACID USING DIELS-ALDER REACTIONS WITH ETHYLENE

1.1 Motivation for renewable terephthalic acid and overview of current approaches for its production.

Purified terephthalic acid (PTA) and ethylene glycol (EG) are used as monomers in the production of the important and large-scale polymeric material, poly(ethylene) terephthalate (PET). PET is used in a wide range of applications, from food and drink packaging to synthetic fibers for clothing and textiles. PTA and EG have been historically produced from petroleum. PTA is almost solely produced from the oxidation of p-xylene (PX) in the liquid phase by the Amoco process[1,2], and PX is produced by the catalytic reforming of gasoline-type streams in oil refineries. Ethylene produced from catalytic cracking processes in oil refineries can be oxidized to ethylene oxide, which in turn is hydrolyzed to EG.

The rising price of crude oil has influenced the choice of feedstock for chemical producers and has led to the development of processes for the production of renewable, biomass-derived chemicals.[3] These chemicals can be grouped into two families of bio-chemicals: (1) a “drop-in” chemical that is chemically identical to a petroleum-based chemical and is meant to supplement or replace it, or (2) a chemical that is new and different than any petroleum-based chemical on the market. The first family of biochemicals are generally easier to develop and produce on a commercial scale since a market for the chemical is already in place.

Renewable bio-PET is one example of a chemical belonging to this first family. The successful use of corn and sugarcane-based ethanol as a feedstock for the production of bio-EG for the production of PET has allowed for a PET material that is ~30 wt % biobased. In this process, the bio-ethanol is converted to ethylene by dehydration followed by oxidization to ethylene oxide and hydrolysis to EG, analogous to how EG is normally produced. PET producers have been able to sell and market this material as "bio-PET", although only the EG portion is renewable. There is a desire to produce completely, 100% renewable PET and, therefore, a demand for new technologies for the production of renewable, biomass-derived PTA.[4]

One important technology that has been developed by a Colorado-based company, Gevo, Inc., is a process to produce PX from sugars using a biological conversion step.[4] Gevo utilizes a microorganism that has been engineered for the fermentation of glucose into isobutanol. Isobutanol is dehydrated to isobutene and dimerized to diisobutylene. Diisobutylene undergoes dehydrocyclization to PX that is finally converted to PTA via the traditional oxidation process. Although the dehydrocyclization step can produce PX from diisobutylene at >85% selectivity, the overall theoretical mass yield of PTA is only 46% since 1/3 of the carbon in the initial glucose is lost as CO_2 in the fermentation step to produce isobutanol. Ultimately, this results in two glucose molecules being required to make only one PTA molecule.

Another important technology being pursued commercially by the California-based company, Micromidas, and the Michigan Molecular Institute

(MMI) is the production of PX from cellulosic biomass and utilizes Diels-Alder reactions between ethylene and a biomass-derived intermediate, 2,5-dimethylfuran (DMF). The company has developed methods of converting inexpensive waste cellulosic biomass into the intermediates, 5-(hydroxymethyl)furfural (HMF) and 5-(chloromethyl)furfural (CMF), by using hydrochloric acid as catalyst.[5] HMF and CMF undergo a H_2 reduction step to DMF, and DMF is further reacted with ethylene gas at high pressure (30 – 70 bar) and temperature (225-300 ^{o}C) to produce PX through a Diels-Alder-dehydration reaction (Fig. 1.1). The Diels-Alder-dehydration reaction has been optimized with the use of a homogeneous Lewis acid catalyst to produce PX in high yields (>95% based on DMF) within short reaction times.[6] If the ethylene gas used in the Diels-Alder step is derived from biomass (e.g., dehydration of bio-ethanol), then the final PX and PTA is 100% biobased. This route is able to efficiently convert HMF/CMF and ethylene to PX by conserving all the carbon in the HMF/CMF and ethylene molecules, giving a theoretical mass yield (for carbon) of 100%.

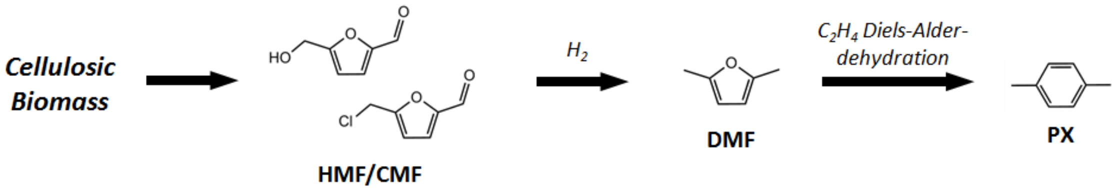

Fig. 1.1 Micromidas/MMI pathway from biomass to PX.

The Diels-Alder-dehydration reaction actually consists of two steps: (1) a reversible Diels-Alder cycloaddition between DMF and ethylene and (2) a dehydrative aromatization of the oxabicyclic cycloadduct (Fig. 1.2). A UOP patent first reported the conversion using a variety of catalytic materials.[7] The use of Bronsted acid zeolites[8-15] and WO_x-ZrO_2[16] as catalysts for the conversion have been the focus of several recent investigations.

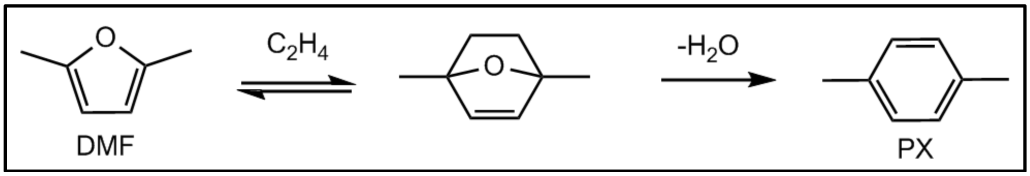

Fig. 1.2 Diels-Alder-dehydration reaction for the conversion of DMF and ethylene to PX.

The one-step conversion of raw cellulosic biomass to the HMF/CMF intermediates that the Micromidas/MMI pathway utilizes is similar to another process that has been commercialized by a Swiss chemical company, AVA Biochem. AVA Biochem's process converts waste cellulosic biomass into 5-hydroxymethylfurfural (HMF) in a one-step hydrothermal carbonisation (HTC) process.[17] In early 2014, AVA Biochem announced that it was producing HMF in Switzerland at 20 tons per year for industrial and research customers. These examples of Micromidas/MMI and AVA Biochem producing HMF or CMF in a single hydrothermal step suggests good economic viability of producing biobased chemicals via the HMF/CMF intermediates, and may be more competitive than biological-based processes, such as Gevo's fermentation-based process for the production of the isobutanol intermediate.

There are numerous other reports in the literature of methods for producing the intermediate HMF from biomass feedstocks.[18,19] One recent example was published by the M.E. Davis group in 2011 for the production of HMF from glucose and starch.[20] The system utilized a two-step conversion that was performed in a single batch reactor. The first step was the isomerization of glucose to fructose in aqueous media catalyzed by a Lewis acidic Beta molecular sieve with tin incorporated into the framework (Sn-Beta) and the second step was the HCl-catalyzed dehydration of fructose to HMF. An organic extraction phase was present to remove HMF from the reacting aqueous phase as it was formed. This system was shown to produce HMF from glucose or starch with high selectivity (69-72 %) at high conversions (>75 %).

1.2 Current Diels-Alder routes for upgrading HMF and ethylene to PTA.

Most of the work relating to the conversion of HMF (or CMF) to PTA has involved the production of PX via the Diels-Alder-dehydration reaction between DMF and ethylene. As discussed above, Micromidas and MMI have developed an efficient process for this Diels-Alder-dehydration step using homogeneous Lewis acid catalysts.[6] Alternatively, this step may be catalyzed by a variety of other materials as well, including Bronsted acid zeolites (e.g., H-Y, H-Beta), acetic acid, WO_x-ZrO_2, activated carbon, silica gel and γ-alumina.[7-16, 21] The reactions are performed in batch pressure reactors in the liquid phase under an ethylene atmosphere. The temperatures are typically 200-300°C with pressures between 30-70 bar.

A significant disadvantage to a route involving DMF in the Diels-Alder-dehydration step is the requirement for the conversion of HMF (or CMF) to DMF. This step requires a source of H_2 gas for the reduction and expensive metal reduction catalysts (e.g., CuRu/C). The source of H_2 and the cost of the reduction catalyst is an important consideration. In one calculation, the reduction catalyst cost contributed to over 40% of the total capital cost of a PX plant utilizing the DMF intermediate.[22] A pathway to PTA that avoids a H_2 reduction step may be advantageous.

One route that has been proposed that avoids the reduction step to DMF has been published in the patent literature. This route begins with the *oxidation* of HMF, rather than reduction, to the intermediate 2,5-furandicarboxylic acid (FDCA).[21, 23] FDCA can be obtained quantitatively from HMF by air oxidation.[24]

Although FDCA has been shown to react with ethylene to produce PTA via the Diels-Alder-dehydration reaction (Fig. 1.3), only low yields have been reported. The benefits to this route compared to going through the DMF intermediate are (1) it does not require an expensive reduction step and (2) the Diels-Alder-dehydration product is PTA rather than PX.

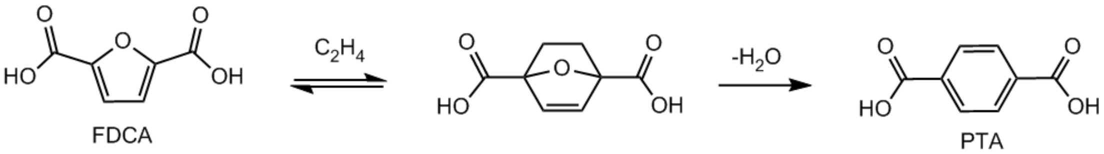

Fig. 1.3 Diels-Alder-dehydration reaction for the conversion of FDCA and ethylene to PTA.

Unfortunately, the conversion of FDCA and ethylene to PTA is very slow and only provides low yields of PTA. In one example, a PTA yield of 0.14 mol % is reported after reaction for 2 hours in aqueous solvent.[23] By performing the reaction in acetic acid, which behaves as both a solvent and weak dehydration catalyst, a 16.5 mol % yield of PTA was achieved after 32 hours of reaction.[21] The selectivity in both of these examples were not reported.

It is not surprising that the reaction between FDCA and ethylene is slow and difficult. The theory behind the mechanism of a Diels-Alder reaction describes the interaction of the molecular orbitals between the diene and the dienophile.[25] Diels-Alder cycloaddition reactions can be grouped into two types – Normal electron demand Diels-Alder reactions and Inverse electron demand Diels-Alder reactions. Normal electron demand reactions are the most common and involve an “electron-rich” diene and an “electron-poor” dienophile. In these reactions, the HOMO of the diene overlaps with the LUMO of the dienophile. The more efficient the overlap between the orbitals, or the more similar the energies, the easier the reaction proceeds, and substituents on the molecules contribute to the energies of these orbitals. Electron-donating groups bound to the diene will tend to raise the energy of the HOMO orbital of the molecule, and electron-withdrawing groups bound to the dienophile tend to lower the LUMO energy of the molecule. For example, ethylene is taken to be the simplest dienophile and, since it is lacking any electron-withdrawing groups, ethylene is also known to be quite inactive in Diels-Alder reactions, requiring elevated reaction temperatures and long reaction times. If an electron-withdrawing group is attached to the dienophile function (e.g., methyl acrylate), the dienophile becomes significantly more active in Diels-Alder reactions.

In the Diels-Alder cycloaddition between FDCA and ethylene, the dienophile, ethylene, is not the only inactive reactant. The diene in this case, FDCA, is also inactive due to the carboxylic acid groups (strongly electron withdrawing) on the 2- and 5- positions that cause the diene function to become “electron-poor” by lowering the energy of the HOMO. Examples of furan Diels-Alder chemistry in which the furanic diene contains carboxylate groups are rare.[26] Other than the above examples regarding the reaction of FDCA with ethylene to produce PTA in low yields, known examples that have been found in the literature involve (1) 5-amino furoates reacting with dienophiles at elevated temperatures[27,28] and (2) furoic acid reacting with monomeric cyclopentadienone.[29]

1.3 Research objective of the current thesis

Although the conversion of HMF to PTA based on the DMF/ethylene/PX Diels-Alder-dehydration reaction is possible and several effective catalysts exist for the Diels-Alder-dehydration step, the reduction step to convert HMF/CMF to DMF requires a H_2 source (three moles of H_2 per mol of HMF) and expensive metal reduction catalysts. A route that avoids the reduction step to DMF and, instead, converts HMF itself or a HMF derivative to the PTA presursor may be advantageous.

The main research objective in this thesis was to develop a new catalytic Diels-Alder route for the conversion of biomass-derived HMF to PTA, and avoid the reduction of HMF to DMF. Along with the production of biomass-derived EG, the new technology will allow for the production of 100% biobased PET.

The strategy for approaching this objective will involve exploratory research for (1) new Diels-Alder-dehydration reactions between oxygenated furans and ethylene and (2) new catalysts for these new reactions (Fig. 1.4). The following two sections will further discuss these areas, that is the proposed catalysts that were of particular interest and the new chemical reactions that were proposed to allow for novel routes to PTA from HMF.

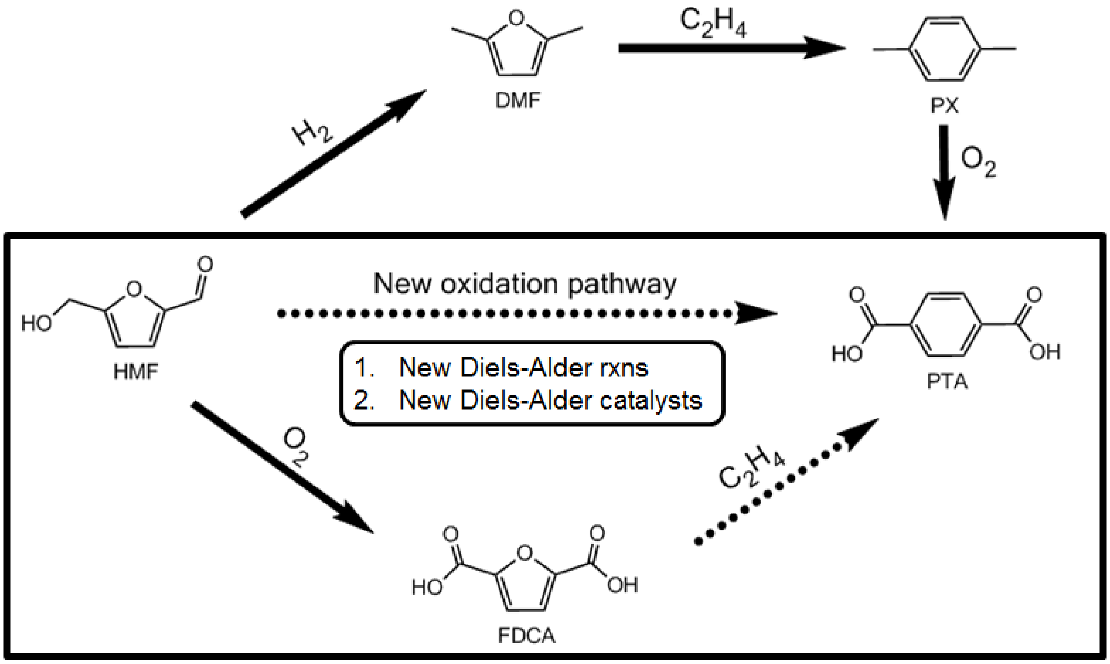

Fig. 1.4 Approach for developing new catalytic Diels-Alder route for the conversion of biomass-derived HMF to PTA.

1.4 Lewis acid molecular sieves as potential Diels-Alder-dehydration catalysts

The Diels-Alder-dehydration reaction between a furanic diene and ethylene to generate the substituted aromatic product and water involves two reactions in tandem. The Diels-Alder cycloaddition between the furan and ethylene produces an oxabicyclic intermediate, and is followed by the dehydrative aromatization of the oxabicyclic to generate the aromatic product and water. A catalyst for the overall Diels-Alder-dehydration reaction may participate in one or both of these steps.

One class of potential catalysts previously unreported were *pure Lewis acid molecular sieves*, specifically high-silica molecular sieves containing metal centers (Sn^{4+}, Ti^{4+}, Zr^{4+}) within the silica framework. These materials have been found to be useful in various Lewis acid-catalyzed processes, including isomerizations of carbohydrates[30,31] and the Meerwein-Ponndorf-Verley (MPV) reduction of carbonyl compounds.[32] Since homogeneous Lewis acids had already been shown to be effective for the Diels-Alder-dehydration between DMF and ethylene, it was reasoned that these solid Lewis acid microporous materials should also be useful. Furthermore, it was proposed that the Lewis acid molecular sieves would not only be effective catalysts for the reaction between DMF and ethylene, but may also be selective in Diels-Alder-dehydration reactions involving *oxygenated* furans, such as HMF or FDCA.[33]

The Diels-Alder-dehydration reaction conditions for using ethylene require high temperatures (150-300 ^{o}C) and pressures (30-70 bar) in the presence of an acid catalyst, and one main issue that was anticipated was the large number of side reactions and/or polymerizations that would be available to the oxygenated/functionalized furans at these conditions. Pure Lewis acidic molecular sieves were interesting potential catalysts for several reasons. First, Lewis acid molecular sieves may catalyze fewer side reactions than the Bronsted acid counterparts, H-Beta or H-Y zeolites, allowing for more selective catalysis for the Diels-Alder-dehydration reaction. Some side reactions that would be possible with HMF are dehydroxymethylation, etherification (by forming HMF dimers), and decarbonylation, and FDCA may undergo decarboxylation. Lewis acids were thought to be less effective than Bronsted acids in catalyzing some or all of these side reactions. Secondly, the microporous environment of the molecular sieve catalysts may prevent dimerizations/polymerizations of HMF from occuring due to spacial constraints at the acid site. Lastly, the micropores of the Lewis acid molecular sieves are hydrophobic (when synthesized in fluoride media) due to the low density of defect sites and nearly pure silica composition.[34] For reactions that produce water as a product, such as the Diels-Alder-dehydration reaction, the poisoning effect of water on Lewis acid catalysis is mitigated. The water is bound less strongly to the Lewis acid center in the hydrophobic, microporous environment and can be more easily displaced by an organic reactant molecule.[35] One interesting example of the exploitation of this property has been the use of these materials as Lewis acid catalysts for the isomerization of glucose to fructose in pure water solvent.[30]

1.5 Stategies for investigating novel Diels-Alder routes to PTA.

The investigation of new Diels-Alder routes to PTA from HMF and ethylene involved several strategies. First, the catalysis of a traditional Diels-Alder cycloaddition reaction between furan and acrylic acid using the proposed Lewis acid molecular sieves was studied (Chapter 3). The cycloaddition between furan and acrylic acid was successfully catalyzed by molecular sieves having the Beta topology containing Sn^{4+}, Zr^{4+}, and Ti^{4+} metal centers (Sn-Beta, Zr-Beta, Ti-Beta). The results show that these solid Lewis acids, under the reaction conditions used for this system ($50^{o}C$), successfully catalyze the cycloaddition but not the dehydrative aromatization of the Diels-Alder adduct to the substituted aromatic product (benzoic acid). The formation of benzoic acid was instead achieved by using a strong Bronsted acid (sulfuric acid). This work showed that the Lewis acid Beta molecular sieves can behave as selective Diels-Alder catalysts and further suggested their potential usefulness in Diels-Alder-dehydration reactions between oxygenated furans and ethylene.

Next, new Diels-Alder-dehydration reaction systems were explored using either (1) HMF with ethylene to produce the PTA intermediate 4-(hydroxymethyl)benzaldehyde (HMB), or (2) a protected derivative of HMF to react with ethylene to produce the PTA intermediate (Chapter 4). HMF may be protected through a variety of ways, such as converting the hydroxymethyl functionality to an alkoxymethyl group through etherification with alcohols or converting the aldehyde functionality to an acetal by reaction with diols or alcohols. During these reaction screening studies, the Lewis acid molecular sieves were applied mostly as possible catalysts.

The third approach to developing a pathway to PTA from HMF was to simply improve the yields of PTA from the Diels-Alder-dehydration reaction between FDCA and ethylene (Chapter 4). If the rate of PTA production from FDCA could be significantly improved, either by applying a catalyst or finding new reaction conditions, this would allow for a breakthrough in producing bio-PTA. Here, the Lewis acid molecular sieves were again used mostly as potential catalysts. The main outcome was the successful use of the Lewis acid Beta molecular sieves in producing small amounts of PTA from FDCA in a reaction system using *dioxane solvent*. Although FDCA yields of up to only ~3% were achieved, the reaction product solutions were “clean” with little humins/coke formation and low conversion of the FDCA reactant to side products. Conversely, when Bronsted acid zeolites and homogeneous Lewis acids were used as catalysts, the product solution was “dark” from significant humins formation without any PTA being produced.

The final approach taken for developing a new ethylene Diels-Alder-dehydration pathway to PTA from HMF was to *partially* oxidize HMF to 5-(hydroxymethyl)-2-furoic acid (HMFA) before reacting with ethylene to produce the PTA precursor, 4-(hydroxymethyl)benzoic acid (HMBA). HMBA may then be subsequently oxidized to PTA. This reaction was achieved using Sn-Beta with 20-30% selectivity to HMBA.[36,37] When HMFA was protected using an alcohol (methanol) to produce the ether/ester form, methyl 5-(methyoxymethyl)furan-2-

carboxylate (MMFC), MMFC reacted with ethylene over Zr-Beta to form the product, methyl 4-(methoxymethyl)benzene carboxylate (MMBC), with >70% selectivity at >20% yields after 6 hours of reaction. Chapters 5, 6 and 7 will be devoted to discussing the findings of the new ethylene Diels-Alder-dehydration reactions involving HMFA and MMFC that allow for a new oxidation pathway to bio-PTA from HMF.

1.6 References

[1] Tomas, R.A.F.; Bordado, J.C.M.; Gomes, J.F.P.; *Chem. Rev.* **2013**, *113* (10), 7421 – 7469.

[2] Landau, R.; Saffer, A.; *Chem. Eng. Prog.* **1968**, *64*(10), 20 – 26.

[3] Vennestrom, P.N.R.; Osmundsen, C.M.; Christensen, C.H.; Taarning, E.; *Angew. Chem. Int. Ed.* **2011**, *50*, 10502 – 10509.

[4] Collias, D.I.; Harris, A.M.; Nagpal, V.; Cottrell, I.W.; Schultheis, M.W.; *Industrial Biotechnology* **2014**, *10*(2), 91 – 105.

[5] Masuno, M.N.; Bissell, J.; Smith, R.L.; Higgins, B.; Wood. A.B.; Foster, M.; Utilizing a multiphase reactor for the conversion of biomass to produce substituted furans. U.S. Patent Appl. No. 14/124,240, **2014**.

[6] Masuno, M.N.; Smith, P.B.; Hucul, D.A.; Dumitrascu, A.; Brune, K.; Smith, R.L.; Bissell, J.; Foster, M.; Methods of producing para-xylene and terephthalic acid. U.S. Patent Appl. No. 13/838,761, **2013**.

[7] Brandvold, T.A.; Carbohydrate route to para-xylene and terephthalic acid. U.S. Patent 8,314,267, **2012**.

[8] Williams, C.L.; Chang C-C.; Do, P.; Nikbin, N.; Caratzoulas, S.; Vlachos, D.G.; Lobo, R.F.; Fan, W.; Dauenhauer, P.J.; *ACS Catal.* **2012**, *2*, 935 – 939.

[9] Do, P.T.M.; McAtee, J.R.; Watson, D.A.; Lobo, R.F.; *ACS Catal.* **2013**, *3*, 41 – 46.

[10] Nikbin, N.; Do, P.T.; Caratzoulas, S.; Lobo, R.F.; Dauenhauer, P.J.; Vlachos, D.G.; *J. Catal.* **2013**, *297*, 35 – 43.

[11] Xiong, R.; Sandler, S.I.; Vlachos, D.G.; Dauenhauer, P.J.; *Green. Chem.* **2014**, *16*, 4086 – 4091.

[12] Chang, C-C.; Green, S.K.; Williams, C.L.; Dauenhauer, P.J.; Fan, W.; *Green. Chem.* **2014**, *16*, 585 – 588.

[13] Nikbin, N.; Feng, S.; Caratzoulas, S.; Vlachos, D.G.; *J. Phys. Chem. C* **2014**, *118*, 24415 – 24424.

[14] Li, Y-P.; Head-Gordon, M.; Bell, A.T.; *J. Phys. Chem. C* **2014**, *118*, 22090 – 22095.

[15] Patet, R.E.; Nikbin, N.; Williams, C.L.; Green, S.K.; Chang, C-C.; Fan, W.; Caratzoulas, S.; Dauenhauer, P.J.; Vlachos, D.G.; *ACS. Catal.* **2015**, DOI: 10.1021/cs5020783.

[16] Wang, D.; Osmundsen, C.M.; Taarning, E.; Dumesic, J.A.; *ChemCatChem* **2013**, *5*, 2044 – 2050.

[17] Krawielitzki, S.; Klausli, T.M.; *Industrial Biotechnology* **2015**, *11*(1), 1 – 3.

[18] Zhao, H.; Holladay, J.E.; Brown, H.; Zhang, Z.C.; *Science* **2007**, *316*(5831), 1597 – 1600.

[19] Pagán-Torres, Y.J.; Wang, T.; Gallo, J.M.R.; Shanks, B.H.; Dumesic, J.A.; *ACS Catal.* **2012**, *2*(6), 930 – 934.

[20] Nikolla, E.; Roman-Leshkov, Y.; Moliner, M.; Davis, M.E.; *ACS Catal.* **2011**, *1*, 408 – 410 .

[21] Wang, B.; Gruter, F.J.M.; Dam, M.A.; Kriegel, R.M.; Process for the preparation of benzene derivatives from furan derivatives. WO Patent Appl. PCT/NL2013/050740, **2013**.

[22] Lin, Z.; Ierapetritou, M.; Nikolakis, V.; *AIChE Journal* **2013**, *59*(6), 2079 – 2087.

[23] Gong, W.H.; Terephthalic acid composition and process for the production thereof. U.S. Patent 8,299278, **2012**.

[24] Casanova, O.; Iborra, S.; Corma, A.; *ChemSusChem* **2009** *2*(12), 1138 – 1144.

[25] Fringuelli, F. and Taticchi, A. (Eds.). (2002). *The Diels-Alder Reaction: Selected Practical Methods.* West Sussex, England: John Wiley & Sons, Ltd.

[26] Dauben, W.G.; Krabbenhoft, H.O.; *J. Am. Chem. Soc.* **1976**, *98*(7), 1992 – 1993.

[27] Cochran, J.E.; Wu, T.; Padwa, A.; *Tetrahedron Lett.* **1996** *37*(17), 2903 – 2906.

[28] Padwa, A.; Dimitroff, M.; Waterson, A.G.; Wu, T.; *J. Org. Chem.* **1997**, *62*, 4088 – 4096.

[29] Gavina, F.; Costero, A.M.; Gil, P.; Palazon, B.; Luis, S.V.; *J. Am. Chem. Soc.* **1981**, *103*, 1797 – 1798.

[30] Moliner, M.; Román-Leshkov, Y.; Davis, M.E.; *Proc. Natl. Acad. Sci. USA* **2010**, *107*(14), 6164 – 6168.

[31] Román-Leshkov, Y.; Moliner, M.; Labinger, J.A.; Davis, M.E.; *Angew. Chem. Int. Ed. Engl.* **2010**, *49*(47), 8954 – 8957.

[32] Corma, A.; Domine, M.E.; Nemeth, L.; Valencia, S.; *J. Am. Chem. Soc.* **2002**, *124*(13), 3194 – 3195.

[33] Roman-Leshkov, Y.; Davis, M.E.; *ACS Catal.* **2011**, *1*(11), 1566 – 1580.

[34] Blasco, T.; Camblor, M.A.; Corma, A.; Esteve, P.; Martinez, A.; Prieto, C.; Valencia, S.; *Chem. Commun.* **1996**, 2367 – 2368.

[35] Gounder, R.; Davis, M.E.; *AIChE Journal* **2013**, *59*(9), 3349 – 3358.

[36] Pacheco, J.J.; Davis, M.E.; *Proc. Natl. Acad. Sci. USA* **2014**, *111*(23), 8363 – 8367.

[37] Davis, M.E.; Pacheco, J.J.; Diels-Alder reactions catalyzed by Lewis acid containing solids: Renewable production of bio-plastics. U.S. Patent Appl. 14/282,099, 2014.

CHAPTER 2

MATERIALS AND METHODS FOR INVESTIGATING NEW DIELS-ALDER-DEHYDRATION ROUTES TO PTA

2.1 Preparation of catalyst materials

Three types of catalysts were chosen for investigating the Diels-Alder reactions: (1) a Bronsted acid zeolite (Al-Beta), (2) a homogeneous Lewis acid (scandium triflate, $Sc(OTf)_3$), and (3) various Lewis acid-containing silica-based molecular sieves and mesoporous silicas having the BEA, MFI and MCM-41 topologies.

The Al-Beta (or H-Beta) zeolite had a SiO_2/Al_2O_3 molar ratio of 27 and was obtained from Tosoh Corporation (Product # HSZ-930NHA). The material was received in the NH_4^+ form and calcined in air to convert to the H^+ form before use in reaction experiments.

Scandium triflate ($Sc(OTf)_3$) was used as received from Sigma-Aldrich.

Lewis acid-containing molecular sieves and mesoporous silicas were synthesized in the laboratory using the following methods:

Sn-Beta molecular sieve was prepared as follows: 7.46 g of an aqueous tetraethylammonium hydroxide (TEAOH) solution [Sigma-Aldrich, 35% (wt/wt)] was diluted with 15 g of water. 6.98 g of tetraethylorthosilicate (TEOS) [Sigma-Aldrich, 98% (wt/wt)] was added and stirred on a magnetic stirplate until the mixture became a single phase (normally, 30-90 minutes). A separate solution was prepared by dissolving 0.094 g of tin (IV) chloride pentahydrate ($SnCl_4 \cdot 5H_2O$) [Sigma-Aldrich, 98% (wt/wt)] in 1 g of water, and this solution was added dropwise to the first solution under stirring conditions. The resulting mixture was covered and stirred overnight to allow complete hydrolysis of the TEOS. The following day the desired water ratio in the gel was obtained by complete evaporation of ethanol and some water. The gel was transferred to a Teflon-liner before 0.739 g of hydrofluoric acid (HF) solution [Sigma-Aldrich, 48% (wt/wt)] was added, resulting in a thick gel with a composition of SiO_2/0.01 $SnCl_4$/0.54 TEAOH/0.54 HF/6.75 H_2O. Finally, 0.6 g of a mixture of dealuminated zeolite Beta crystals in water, prepared according to the method reported by Chang, et al.,[1] was added to the gel. The Teflon-liner was sealed in a stainless steel autoclave and heated at 140°C under rotating conditions for 5-7 days. The solids were recovered by centrifugation, washed with water (3x) and acetone (1x), and dried at 100°C overnight.

Zr-Beta molecular sieve was prepared as follows: 7.46 g of an aqueous tetraethylammonium hydroxide (TEAOH) solution [Sigma-Aldrich, 35% (wt/wt)] was diluted with 15 g of water. 6.98 g of tetraethylorthosilicate (TEOS) [Sigma-Aldrich, 98% (wt/wt)] was added and stirred on a magnetic stirplate until the mixture became a single phase (normally, 30-90 minutes). Zirconium was added to the gel as either zirconyl chloride octahydrate [$ZrOCl_2 \cdot 8\ H_2O$, Sigma-Aldrich, 98% (wt/wt)] or zirconium (IV) propoxide [Sigma-Aldrich, 70% (wt/wt) in propanol]. A separate solution was prepared by either (1) diluting zirconyl chloride octahydrate in 3-4 g of water or (2) zirconium (IV) propoxide in 2 g of ethanol, and this solution was added dropwise to the first solution under stirring conditions. Samples with gel Si/Zr = 63-400 were prepared using zirconium (IV) propoxide (Chapter 7) and the amount varied depending on the desired Si/Zr ratio. The resulting mixture was covered and stirred overnight to allow complete hydrolysis of the TEOS. The desired water ratio in the gel was obtained by complete evaporation of ethanol, propanol and some water. The gel was transferred to a Teflon-liner before 0.739 g of hydrofluoric acid (HF) solution [Sigma-Aldrich, 48% (wt/wt)] was added, resulting in a thick gel with a composition of SiO_2/0.003-0.016 ZrO_2/0.54 TEAOH/0.54 HF/6.75 H_2O. Finally, 0.6 g of a mixture of dealuminated zeolite Beta crystals in water, prepared according to the method reported by Chang, et al.,[1] was added to the gel. The Teflon-liner was sealed in a stainless steel autoclave and heated at 140^{o}C under rotating conditions for 5-7 days. The solids were recovered by centrifugation, washed with water (3x) and acetone (1x), and dried at 100^{o}C overnight.

Ta-Beta molecular sieve was prepared as follows: 7.47 g of an aqueous tetraethylammonium hydroxide (TEAOH) solution [Sigma-Aldrich, 35% (wt/wt)] was diluted with 15 g of water. 6.99 g of tetraethylorthosilicate (TEOS) [Sigma-Aldrich, 98% (wt/wt)] was added and stirred on a magnetic stirplate for 60 min. A separate solution was prepared by diluting 0.084 g $Ta(OC_2H_5)_5$ [Sigma-Aldrich, 99.98%] in 1 g of ethanol, and this solution was added dropwise to the first solution under stirring conditions. The resulting mixture was covered and stirred overnight to allow complete hydrolysis of the TEOS. The desired water ratio in the gel was obtained by complete evaporation of ethanol, propanol and some water. The gel was transferred to a Teflon-liner before 0.75 g of hydrofluoric acid (HF) solution [Sigma-Aldrich, 48% (wt/wt)] was added, resulting in a thick gel with a composition of SiO_2/0.007 TaO_2/0.54 TEAOH/0.54 HF/6.67 H_2O. Finally, 0.6 g of a mixture of dealuminated zeolite Beta crystals in water, prepared according to the method reported by Chang, et al.,[1] was added to the gel. The Teflon-liner was sealed in a stainless steel autoclave and heated at 140°C under rotating conditions for 5 days. The solids were recovered by centrifugation, washed with water (3x) and acetone (1x), and dried at 100°C overnight.

Nb-Beta molecular sieve was prepared as follows: 7.48 g of an aqueous tetraethylammonium hydroxide (TEAOH) solution [Sigma-Aldrich, 35% (wt/wt)] was diluted with 15 g of water. 6.99 g of tetraethylorthosilicate (TEOS) [Sigma-Aldrich, 98% (wt/wt)] was added and stirred on a magnetic stirplate for 65 min. A separate solution was prepared by diluting 0.099 g $Nb(OC_2H_5)_5$ [Sigma-Aldrich, 99.95%] in 1 g of ethanol, and this solution was added dropwise to the first solution under stirring conditions The resulting mixture was covered and stirred overnight to allow complete hydrolysis of the TEOS. The desired water ratio in the gel was obtained by complete evaporation of ethanol, propanol and some water. The gel was transferred to a Teflon-liner before 0.74 g of hydrofluoric acid (HF) solution [Sigma-Aldrich, 48% (wt/wt)] was added, resulting in a thick gel with a composition of SiO_2/0.01 NbO_2/0.54 TEAOH/0.54 HF/6.67 H_2O. Finally, 0.6 g of a mixture of dealuminated zeolite Beta crystals in water, prepared according to the method reported by Chang, et al.,[1] was added to the gel. The Teflon-liner was sealed in a stainless steel autoclave and heated at 140°C under rotating conditions for 5 days. The solids were recovered by centrifugation, washed with water (3x) and acetone (1x), and dried at 100°C overnight.

Ti-Beta molecular sieve was prepared as follows: 3.53 g of tetraethylammonium fluoride hydrate [Alfa Aesar, 97% (wt/wt)] was dissolved in 7 g of water. 7 g of tetraethylorthosilicate (TEOS) [Sigma-Aldrich, 98% (wt/wt)] was then added and the mixture was stirred for 30 min. A separate solution was prepared by diluting 0.123 g of titanium (IV) isopropoxide [Sigma-Aldrich, 99%] in 2 g of ethanol, and this solution was added dropwise to the first solution under stirring conditions. The resulting mixture was covered and stirred overnight to allow complete hydrolysis of the TEOS. The desired water ratio in the gel was obtained by complete evaporation of ethanol, isopropanol and some water, resulting in a gel with composition 1 SiO_2/0.013 TiO_2/0.55 TEAF/8.07 H_2O. Finally, 0.15 g of pure silicon zeolite Beta seeds was added to the gel. The gel was transferred to a Teflon-lined stainless steel autoclave and heated at 140^{o}C under static conditions for 14 days. The solids were recovered by centrifugation, washed with water (3x) and acetone (1x), and dried at 100^{o}C overnight.

Tin and aluminum-containing Beta molecular sieve (Sn-Al-Beta) was prepared as follows: 7.75 g of an aqueous tetraethylammonium hydroxide (TEAOH) solution [Sigma-Aldrich, 35% (wt/wt)] was diluted with 15.65 g of water, followed by the addition of 1.24 g of hydrogen peroxide solution [Sigma-Aldrich, 30% (wt/wt)]. 7 g of tetraethylorthosilicate (TEOS) [Sigma-Aldrich, 98% (wt/wt)] was added and stirred on a magnetic stirplate for about 30 min. A separate solution was prepared by dissolving 0.113 g of tin (IV) chloride pentahydrate ($SnCl_4 \cdot 5H_2O$) [Sigma-Aldrich, 98% (wt/wt)] in 1 g of water, and this solution was added dropwise to the first solution under stirring conditions. After about 20 min of stirring, 0.056 g of aluminum isopropoxide powder was added to the gel while stirring. The resulting mixture was covered and stirred overnight to allow complete hydrolysis of the TEOS. The desired water ratio in the gel was obtained by complete evaporation of ethanol, isopropanol and some water. The gel was transferred to a Teflon-liner before 0.74 g of hydrofluoric acid (HF) solution [Sigma-Aldrich, 48% (wt/wt)] was added, resulting in a thick gel with a composition of SiO_2/0.01 SnO_2/0.0042 Al_2O_3/0.56 TEAOH/0.56 HF/7.22 H_2O. Finally, 0.6 g of a mixture of dealuminated zeolite Beta crystals in water, prepared according to the method reported by Chang, et al.,[1] was added to the gel. The Teflon-liner was sealed in a stainless steel autoclave and heated at 140^oC under rotating conditions for 8 days. The solids were recovered by centrifugation, washed with water (3x) and acetone (1x), and dried at 100^oC overnight.

Sn-MCM-41 was prepared as follows: 1.98 g of hexadecyltrimethylammonium bromide (CTAB) [Sigma-Aldrich, 98% (wt/wt)] was dissolved in 10 g of water. Next, 3.15 g of tetramethylammonium hydroxide solution (TMAOH) [Sigma-Aldrich, 25% (wt/wt) in water] was added. A separate solution was prepared by diluting 0.12 g of tin (IV) chloride pentahydrate ($SnCl_4{\cdot}5H_2O$) [Sigma-Aldrich, 98% (wt/wt)] in 1.89 g of water, and this solution was added dropwise to the first solution under stirring conditions. Finally, 2 g of fumed silica [Cab-O-Sil EH-5, 99.9% purity] was added, resulting in a thick gel with composition 1 SiO_2/0.01 $SnCl_4$/0.16 CTAB/0.26 TMAOH/24.3 H_2O. The homogeneous gel was transferred to a Teflon-lined stainless steel autoclave and heated at 140^oC under static conditions for 25 hours. The solids were recovered by centrifugation, washed with water (3x) and acetone (1x), and dried at room temperature under flowing air.

Zr-MCM-41 was prepared as follows: 1.98 g of hexadecyltrimethylammonium bromide (CTAB) [Sigma-Aldrich, 98% (wt/wt)] was dissolved in 10 g of water. Next, 3.15 g of tetramethylammonium hydroxide solution (TMAOH) [Sigma-Aldrich, 25% (wt/wt) in water] was added. A separate solution was prepared by diluting 0.055 g of zirconyl chloride octahydrate [$ZrOCl_2$ ▪ 8 H_2O, Sigma-Aldrich, 98% (wt/wt)] in 2.13 g of water, and this solution was added dropwise to the first solution under stirring conditions. Finally, 2 g of fumed silica [Cab-O-Sil M5, 99.9% purity] was added, resulting in a thick gel with composition 1 SiO_2/0.005 ZrO_2/0.16 CTAB/0.26 TMAOH/24.3 H_2O. The homogeneous gel was transferred to a Teflon-lined stainless steel autoclave and heated at 140^oC under static conditions for 22 hours. The solids were recovered by centrifugation, washed with water (3x) and acetone (1x), and dried at room temperature under flowing air.

An amorphous SiO_2 material containing Sn^{4+} (Sn-SiO_2) was prepared by a xerogel method: 6.989 g of tetraethylorthosilicate (TEOS) [Sigma-Aldrich, 98% (wt/wt)] was diluted with 8.682 g of water. 1.904 g of HCl solution (J.T. Baker, 0.1 N) was added and the resulting solution was stirred for 2 hours. Next, a second solution of 0.199 g of tin (IV) chloride pentahydrate ($SnCl_4 \cdot 5H_2O$) [Sigma-Aldrich, 98% (wt/wt)] in 2 g of water was prepared and added dropwise to the first solution. After an additional hour of stirring, a tetrapropylammonium hydroxide

(TPAOH) solution [Alfa Aesar, 40% (wt/wt)] was added dropwise until the gel hardened to a soft, colorless solid. The hardened gel was allowed to dry in a 100°C oven overnight to produce the "as-made" xerogel solid. The resulting solid was calcined at 580°C for 6 h.

Sn-MFI was prepared using a solid transformation of the "as-made" xerogel solid described above in the synthesis of the amorphous Sn-SiO_2 material: A tetrapropylammonium hydroxide (TPAOH) solution [20% (wt/wt)] was prepared by diluting a 40% (wt/wt) TPAOH solution (Alfa Aesar) with water. The 20% (wt/wt) TPAOH solution was added to the "as-made" xerogel solid (described above) in a ratio of 1.6 g TPAOH (20%) : 1 g xerogel solid, and this mixture was transferred to a Teflon-lined stainless steel autoclave and heated at 175°C under static conditions for 24 hours. The solids were recovered by centrifugation, washed with water (3x) and acetone (1x), and dried at 100°C overnight.

Zr-MFI was prepared as follows: 7.36 g of tetrapropylammonium hydroxide (TPAOH) solution [20% (wt/wt)] was diluted in 22.05 g of water. Next, 7 g of tetraethylorthosilicate (TEOS) [Sigma-Aldrich, 98% (wt/wt)] was added and the solution was stirred for 30 min. A separate solution was prepared by diluting 0.085 g of zirconyl chloride octahydrate [$ZrOCl_2 \cdot 8\ H_2O$, Sigma-Aldrich, 98% (wt/wt)] in 4 g of water, and this solution was added dropwise to the first solution under stirring conditions. The resulting mixture was covered and stirred overnight to allow complete hydrolysis of the TEOS. The desired water ratio in the gel was obtained by complete evaporation of ethanol and some water, resulting in a gel with composition 1 SiO_2/0.008 ZrO_2/0.44 TPAOH/30 H_2O. The gel was transferred to a Teflon-lined stainless steel autoclave and heated at 180^oC under static conditions for 48 hours. The solids were recovered by centrifugation, washed with water (3x) and acetone (1x), and dried in a 100^oC oven overnight.

All materials were calcined in a muffle furnace with flowing air (breathing grade). The as-made material was placed in a ceramic dish and heated in the oven using the following temperature program: ramp at 1^oC/min from ambient to 150^oC and hold for 3 hours, followed by ramping at 1^oC/min from 150^oC to 580^oC and holding for 6 hours.

2.2 Characterization of materials

Powder x-ray diffraction (XRD) patterns of the synthesized materials confirmed the BEA, MFI, and MCM-41 topologies and indicated high crystallinity of the samples. XRD patterns were collected using a Rigaku Miniflex II diffractometer and Cu Kα radiation. See Figures 2.1-A to 2.5-A in the appendix for XRD patterns.

Scanning electron microscopy (SEM) images with energy dispersive x-ray spectroscopy (EDS) measurements were used to determine crystal size and silicon/metal (Si/M) atom ratios, respectively. SEM and EDS were recorded on a LEO 1550 VP FE SEM at an electron high tension (EHT) of 15 or 20 kV.

2.3 Suppliers for furans and other organic reagents

Table 2.1 List of suppliers for dienes and Diels-Alder-dehydration product standards.

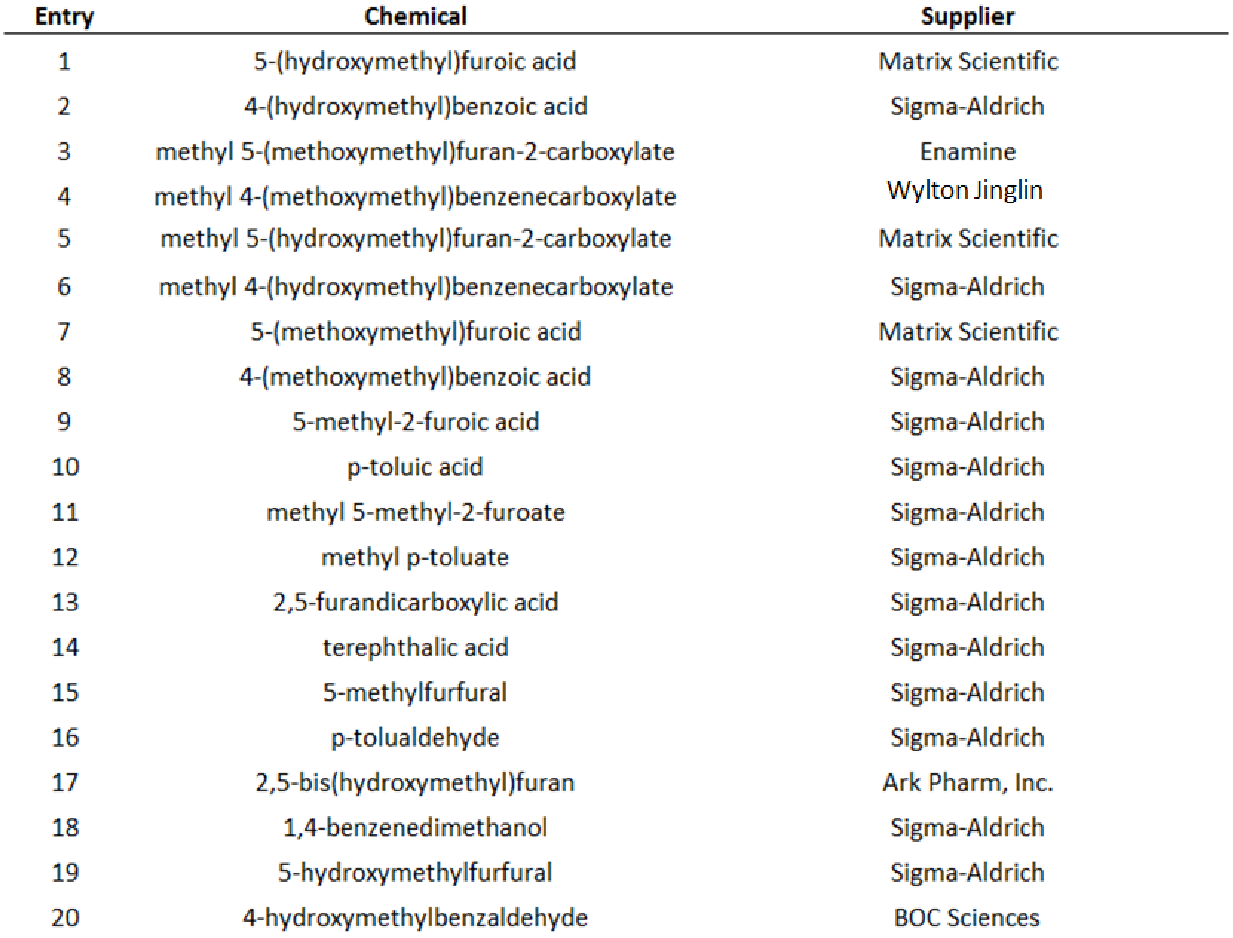

Entry	Chemical	Supplier
1	5-(hydroxymethyl)furoic acid	Matrix Scientific
2	4-(hydroxymethyl)benzoic acid	Sigma-Aldrich
3	methyl 5-(methoxymethyl)furan-2-carboxylate	Enamine
4	methyl 4-(methoxymethyl)benzenecarboxylate	Wylton Jinglin
5	methyl 5-(hydroxymethyl)furan-2-carboxylate	Matrix Scientific
6	methyl 4-(hydroxymethyl)benzenecarboxylate	Sigma-Aldrich
7	5-(methoxymethyl)furoic acid	Matrix Scientific
8	4-(methoxymethyl)benzoic acid	Sigma-Aldrich
9	5-methyl-2-furoic acid	Sigma-Aldrich
10	p-toluic acid	Sigma-Aldrich
11	methyl 5-methyl-2-furoate	Sigma-Aldrich
12	methyl p-toluate	Sigma-Aldrich
13	2,5-furandicarboxylic acid	Sigma-Aldrich
14	terephthalic acid	Sigma-Aldrich
15	5-methylfurfural	Sigma-Aldrich
16	p-tolualdehyde	Sigma-Aldrich
17	2,5-bis(hydroxymethyl)furan	Ark Pharm, Inc.
18	1,4-benzenedimethanol	Sigma-Aldrich
19	5-hydroxymethylfurfural	Sigma-Aldrich
20	4-hydroxymethylbenzaldehyde	BOC Sciences

2.4 Methods for studying the Diels-Alder reaction between furan and acrylic acid

The Diels-Alder cycloaddition reaction between furan and acrylic acid was investigated using the Lewis acid Beta molecular sieves and scandium triflate homogeneous Lewis acid as catalysts. The reactions were performed in batch operation and the liquid phase was analyzed using quantitative ^{1}H NMR. Reaction experiments were conducted in a thick-walled glass reactor with a crimp-top seal. The glass reactor was loaded with a magnetic stir bar, catalyst, and 3 grams (44 mmol) of furan (Sigma-Aldrich). The catalyst amount was added to meet a target molar ratio of ~360 acrylic acid:metal atoms. Next, 0.3 grams (4.2 mmol) of acrylic acid (Sigma-Aldrich) was added, and the reactor was immediately sealed and placed in a 50^{o}C water bath. The reaction system was under autogeneous pressure due to the low boiling point (32^{o}C) of the furan solvent/reactant. Aliquots (20 μl) were collected at different times during the reaction by using a syringe needle through the crimp-top seal. Each aliquot was diluted in a known mass of $CDCl_3$ containing a known concentration of tetraethylsilane (TES) as external standard, transferred to an NMR tube through a filter pippette (to remove the solid catalyst), and a ^{1}H NMR spectrum was collected at room temperature. Figure 2.6-A in the appendix shows an example ^{1}H NMR spectrum of the product solution of the Diels-Alder (DA) reaction between furan and acrylic acid with each of the peaks identified. By using the tetraethylsilane peaks, the acrylic acid and DA product concentrations in the furan solvent/reactant were measured.

The DA product, 7-oxa-bicyclo[2.2.1]hept-5-ene-2-carboxylic acid, was dehydrated to the aromatic product, benzoic acid, by treatment with concentrated sulfuric acid. The procedure was adapted from Shiramizu and Toste.[2] In a small screwtop sample vial, concentrated sulfuric acid (98%, 400 μl) was added to the solid DA product (30 mg, Matrix Scientific) while stirring in an ice bath. After 15 minutes, the reaction mixture was quenched with an aqueous sodium bicarbonate solution. The organic products were extracted several times with ethyl acetate, and the organic phases were combined into a round bottom flask. The mixture was dried with addition of magnesium sulfate, the solids separated by filtration, and the ethyl acetate and other volatiles were removed by rotary evaporation. The remaining solids were dissolved in $CDCl_3$ and the ^1H NMR spectrum was taken at room temperature.

2.5 Methods for studying Diels-Alder-dehydration reactions using ethylene and various substituted furans

High-pressure ethylene gas was used in the screening of Diels-Alder-dehydration reactions with various furanic dienes. Experiments were carried out in a 50 ml high-pressure stainless steel batch reactor (Parr Series 4590) equipped with a magnetic stirrer and heater. The o-ring material that was chosen to seal the reactor cylinder to the reactor head was Kalrez® Sprectrum^{TM} 7090 perfluoroelastomer. The reactor setup allowed for ethylene gas (Matheson, 1200 psig, 99.995% purity) or helium to be charged to the reactor. A high-pressure oxygen/moisture trap (Agilent OT3) was also installed on the inlet line.

In a typical experiment, the catalyst and reaction solution were loaded into the Parr reactor. About 10 ml of reaction solution were used in the experiments since this was the minimal volume that allowed for contact of the stirrer with the liquid. This ensured mixing during the reactions while minimizing the usage of catalyst and reagent. If a quantitative analysis of the reaction was being performed, an initial aliquot (~0.5 g) of the feed solution was collected and analyzed with the final product solution after reaction. The magnetic stirrer was operated at ~200 rpm and the head space of the reactor was purged with helium gas with a fill/vent cycle (10x). Next, the reactor was pressurized to ~10-40 bar (room temperature) with ethylene gas, the inlet valve was closed, and the reaction was performed in batch operation. The reactor was heated to the reaction temperature (150-300^{o}C) while the pressure increased autogenously. For example, when the reactor was pressurized to 37 bar and heated to 190^{o}C, the pressure increased autogenously to 70 bar. At the end of the reaction time, the reactor was allowed to cool to room temperature and the reactor gases were vented. The reactor vessel was opened and the liquid/solids were then collected into a 20 ml glass scintillation vial before analysis by ^{1}H NMR, GC/FID, GC/MS, and/or HPLC.

Before each experiment, the reactor was cleaned using the following procedure. The Parr reactor cylinder, stirrer, thermocouple, inlet diptube, and o-ring were cleaned by hand with acetone and Kim-Wipe. Then, about 25 ml of the solvent that was planned for use in the next experiment was added to the reactor and sealed to the head. For example, if dioxane was planned to be used in the next experiment, dioxane was used in this step. The reactor was purged with helium gas with a fill/vent cycle (10x). This process was performed in order to make an effort to rinse clean the inlet diptube of the reactor head and replace any residual liquid in the diptube with the same solvent that was being used for the next experiment. Following the fill/vent cycle, the reactor was opened and the cylinder was emptied and rinsed clean with acetone and Kim-Wipe.

2.6 Analysis of ethylene/furan Diels-Alder products by ^{1}H NMR

The liquid product solutions were analyzed by ^{1}H NMR to identify products (by comparing to known product standards) and to quantify conversion, product yield, and selectivity. This analysis method was used primarily in the exploratory portion of the project due to the convenience of the method, particulary when analyzing a variety of reactions during screening investigations.

Typically, an aliquot (~ 0.2 g) of the crude product mixture was diluted in $CDCl_3$ or DMSO-d_6 NMR solvent (~1.0 g) and transferred to an NMR tube using a filter pipette to remove catalyst and/or any solid reaction products. The ^{1}H NMR spectrum was collected at room temperature. If a quantitative analysis was being performed, the NMR solvent contained tetraethylsilane (TES) as external standard at a known concentration. Both the feed solution and product solution were analyzed to determine reactant and product concentrations and conversion, product yield, and selectivity. For example, the signals used for calculating the conversion of methyl 5-methoxymethyl-furan-2-carboxylate (MMFC) and the yield of methyl 4-(methoxymethyl)benzene carboxylate (MMBC) in DMSO-d_6: tetraethylsilane $\delta = 0.49$ ppm (q, 8 H); MMFC $\delta = 6.63$ ppm (d, 1 H) and $\delta = 7.26$ ppm (d, 1 H); MMBC $\delta = 7.46$ ppm (d, 2 H) and $\delta = 7.95$ ppm (d, 2 H).

During the course of investigating the Diels-Alder-dehydration reaction between MMFC and ethylene to produce MMBC, an alternative technique to quantify the reaction results using ^{1}H NMR was also used. Rather than using TES as external standard, it was found that the dioxane solvent could be used as an internal standard reference. The procedure involved simply calculating the area ratios of the MMFC [δ = 6.63 ppm (d, 1 H) and δ = 7.26 ppm (d, 1 H)] and MMBC [δ = 7.46 ppm (d, 2 H) and δ = 7.95 ppm (d, 2 H)] peaks to the dioxane solvent peak for both the feed and product solutions, and measure the MMFC conversion and MMBC yield by comparing these area ratios. This method was used for determining the reaction results in Table 5.5. Fig. 2.7-A in the appendix shows the use of the dioxane peak in the ^{1}H NMR as internal standard reference gives accurate determination of MMFC and MMBC concentrations in dioxane for a series of calibration solutions of known concentrations. Table 2.1-A compares reaction results measured using the TES external standard and the dioxane solvent as internal standard, showing that both methods give similar results.

2.7 Analysis of reaction products by GC/FID

GC/FID analysis was performed on an Agilent 7890B GC system equipped with a flame ionization detector (FID). The column used was an Agilent HP-5 (30 m x 0.32 mm x 0.25 μm) with N_2 as carrier gas (6 ml/min flow through column). The injection samples were typically prepared by filtering a small aliquot of the product solution through a filter pipette before diluting in dichloromethane (DCM) in a ratio of 30 mg sample:170 mg of DCM. Volumes of 1 μL were injected into the GC using a Hamilton 5 μL GC injection syringe. Split mode was used with a 7:1 split ratio. A typical oven temperature program was as follows: Hold 75^{o}C for 0.3 min, ramp to 90^{o}C at 10^{o}C/min and hold for 4.5 min, ramp to 300^{o}C at 50^{o}C/min and hold for 3 min.

2.8 Analysis of reaction products by GC/MS

GC/MS analysis was performed on an Agilent 5890 GC interfaced with a 5970 Mass Selective Detector. The column used was an DB-5 (30 m x 0.25 mm x 0.25 μm). The MSD was set to scan 50 to 550 m/z at 1.61 scans/s. The ionization mode was electron ionization and the instrument was tuned using standard manufacturer autotune procedures using PFTBA (perfluorotributylamine) standard.

GC/TOF-MS analysis was performed by JEOL on a AccuTOF GCv 4G system. The MS ion source was a EI/FI/FD Combination Ion Source (EI+: 70eV, 300μA, 280 ^{o}C; FI+: -10kV, 40mA(30msec), JEOL emitter, Heater OFF). GC-interface temperature of 280^{o}C used with 1 Hz data acquisition rate.

2.9 Analysis of reaction products by HPLC

HPLC separation and analysis was performed on an Agilent HPLC system with an Agilent Hi-Plex H column using a pure water mobile phase flowing at 0.6 ml/min. The column temperature was held at 65°C. The injection samples were prepared by transferring a small aliquot through a 0.2 µm filter into an HPLC vial (Waters), and injection volumes of 2 µL were used. A diode array detector (DAD) was used with wavelength signals of 205 and 228 nm.

2.10 References

[1] Chang, C-C.; Wang, Z.; Dornath, P.; Cho, H.J.; Fan, W.; *RSC Adv.* **2012**, *2*, 10475 – 10477

[2] Shiramizu, M.; Toste, F.D.; *Chem. Eur. J.* **2011**, *17*, 12452 – 12457.

CHAPTER 3

LEWIS ACID MOLECULAR SIEVES AS DIELS-ALDER CYCLOADDITION CATALYSTS: REACTION OF FURAN WITH ACRYLIC ACID

3.1 Diels-Alder cycloaddition between furan and acrylic acid

The Diels-Alder reaction between furan and acrylic acid was studied using the series of Lewis acid molecular sieves as catalysts. These molecular sieve materials have not been previously reported as Diels-Alder catalysts, and so the aim of this work was to investigate the usefulness of these materials for improving the rates of the cycloaddition reaction. The target reaction is shown in Fig. 3.1 and did not involve the dehydration of the Diels-Alder adduct to the aromatic product, benzoic acid.

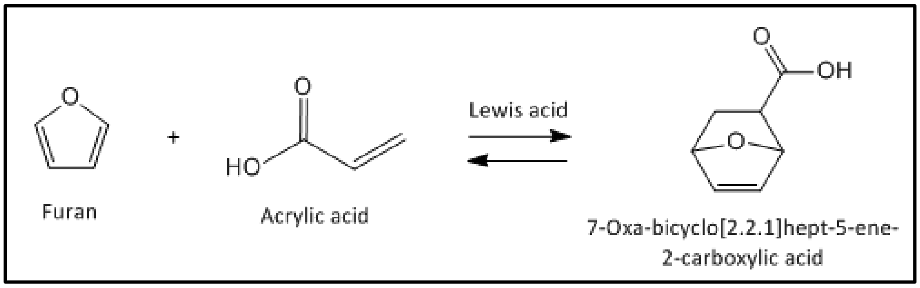

Fig. 3.1 Lewis acid-catalyzed Diels-Alder cycloaddition between furan and acrylic acid.

Lewis acid-containing solids are known to catalyze Diels-Alder reactions.[1] For example, Corma et al. have studied the Diels-Alder cycloaddition between cyclopentadiene and p-benzoquinone catalyzed by a series of silica-based Lewis acid-containing solids similar to the of Lewis acid molecular sieves that are proposed here, that is Sn- and Ti-containing MCM-41 and ITQ-2.[2] MCM-41 is a mesoporous silica and ITQ-2 is a delaminated zeolitic material.

Molecular sieves can have both acid catalysis[2] and molecular confinement[3] effects on improving rates and selectivities. Since these cycloaddition reactions are bi-molecular and have a negative change in entropy, the spatial confinement within the micropores of zeolites alone is expected to lead to improved rates.[3,4]

The uncatalyzed cycloaddition reaction between furan and acrylic acid is very slow at ambient temperature, taking weeks to reach equilibrium conversions.[5] It can be catalyzed by various homogenous Lewis acids, such as $ZnCl_2$, $FeCl_3$, $AlCl_3$, and borane complexes,[6] decreasing the time to reach equilibrium at ambient temperature to within 24 hr. When the methyl ester of acrylic acid was used as the dienophile, $ZnCl_2$ and ZnI_2 supported on silica gel were shown to catalyze the reaction heterogeneously.[7]

Here, Lewis acid Beta molecular sieves and scandium(III) triflate were tested as catalysts in the Diels-Alder reaction between furan and acrylic acid. Scandium(III) triflate was chosen as a reference homogeneous Lewis acid catalyst since Toste and Shiramizu successfully used scandium(III) triflate to catalyze a very similar and related Diels-Alder reaction between 2,5-dimethylfuran and acrolein.[8]

An example of the concentration profiles for furan, acrylic acid, and the Diels-Alder adduct using scandium(III) triflate as catalyst at 50°C is shown in Fig.3.2. High (>95%) selectivity to the Diels-Alder adduct was achieved and acrylic acid conversions reached equilibrium conversions of ~40% at reaction times of 4 hours.

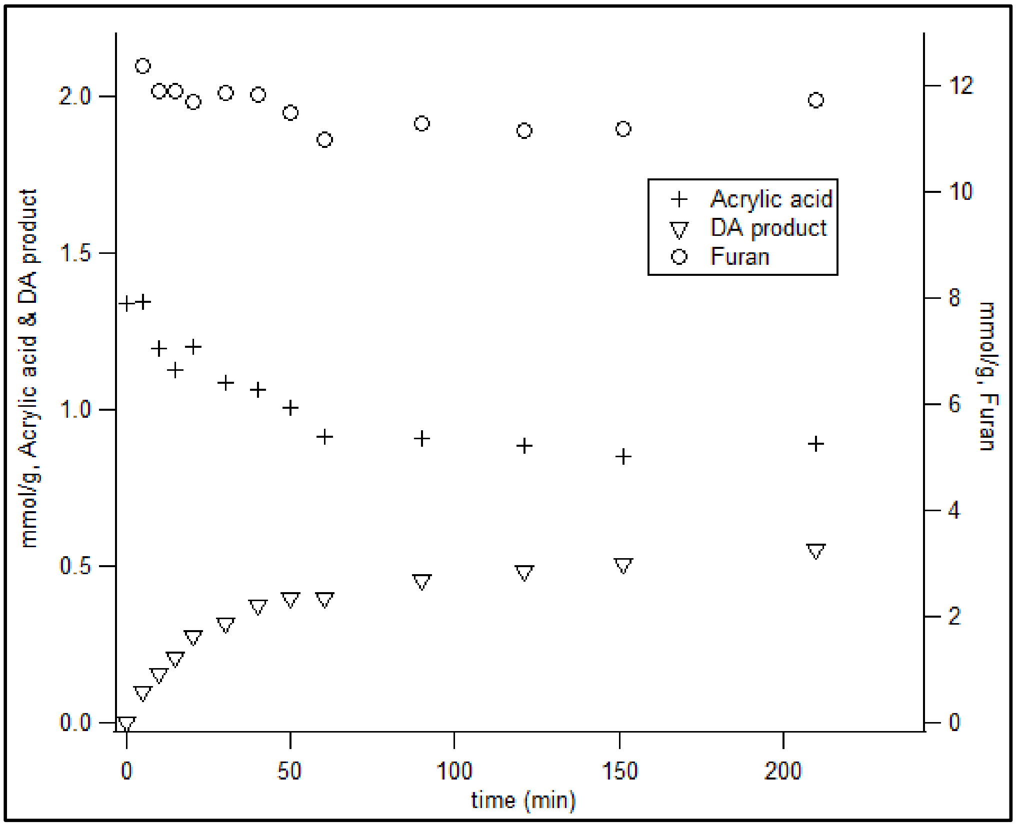

Fig. 3.2 Concentration profiles [mmol/(g solution)] of the furan and acrylic acid Diels-Alder reaction using Sc(OTf)$_3$ as catalyst. Reaction conditions: T=50^{o}C, 3.0 g furan, 0.3 g acrylic acid, 6 mg catalyst.

Fig. 3.3 compares the Diels-Alder product concentration profiles over time for the Sc(OTf)$_3$ and Lewis acid Beta molecular sieve (Sn-Beta, Zr-Beta, Ti-Beta) catalysts. A pure silica Beta molecular sieve (Si-Beta) was included as a control. The results clearly indicate that the solid Lewis acids, Sn-Beta and Zr-Beta, are catalysts for producing the Diels-Alder product and are comparable to the homogeneous Lewis acid. Ti-Beta is only marginally active when compared to the Si-Beta control. At this reaction temperature (50^{o}C), the dehydration of the Diels-Alder product to form benzoic acid was not observed.

This is the first time this series of Lewis acid Beta molecular sieve materials have been shown to be catalysts for any Diels-Alder reaction. In addition, this finding supports further investigation of using these materials as catalysts for the Diels-Alder reactions involving ethylene as the dienophile.

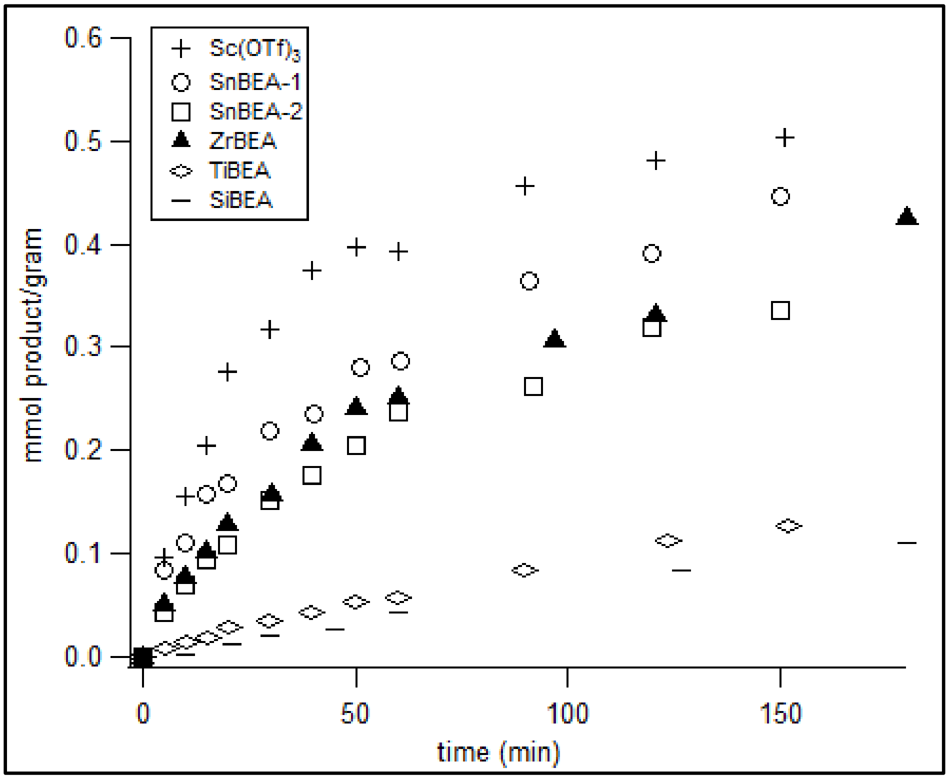

Fig. 3.3 Diels-Alder product concentration profiles using Sn-Beta, Zr-Beta, Ti-Beta, and Sc(OTf)$_3$ catalysts. Reaction conditions: T=50^{o}C, 3.0 g furan, 0.3 g acrylic acid, 360 acrylic acid:metal molar ratio. Sn-BEA-2 profile used 784 acrylic acid:metal ratio.

The conversion of the Diels-Alder adduct to benzoic acid (Fig. 3.4) was not accomplished using the Sn-Beta or Zr-Beta catalysts under the reaction conditions used for the cycloaddition, but here it is shown that the conversion can be performed using a strong Bronsted acid.   Toste and Shiramizu[8] reported methods for the conversion of a similar 7-oxabicyclo[2.2.1]hept-2-ene compound using concentrated sulfuric acid at 0°C (Fig. 3.5).

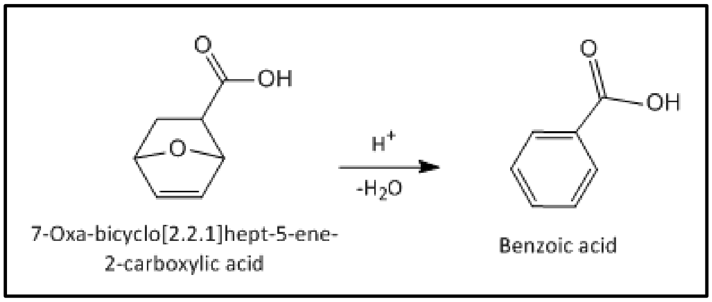

Fig. 3.4 Bronsted acid-catalyzed conversion of the Diels-Alder adduct, 7-oxa-bicyclo[2.2.1]hept-5-ene-2-carboxylic acid, to benzoic acid.

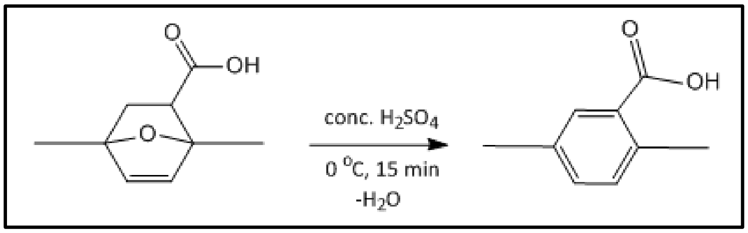

Fig. 3.5 Dehydrative aromatization example from Toste and Shiramizu.[8]

When these conditions were applied to the current Diels-Alder adduct, the formation of benzoic acid was confirmed by ^{1}H NMR. The product NMR spectrum obtained is given in the appendix (Fig. 3.1-A). This shows that the Diels-Alder adduct, 7-oxa-bicyclo[2.2.1]hept-5-ene-2-carboxylic acid, is capable of undergoing dehydrative aromatization to the substituted aromatic product under strong Bronsted acid conditions at low temperatures, but the Lewis acid

Beta molecular sieves were unable to perform the dehydration under the low temperature conditions.

3.2 References

[1] Cativiela, C.; Fraile, J.M.; Garcia, J.I.; Mayoral, J.A.; Pires, E.; Royo, A.J.; *Tetrahedron* **1993**, *49*(19), 4073 – 4084.

[2] Gomez, M.V.; Cantin, A.; Corma, A.; de la Hoz, A.; *J. Mol. Catal. A* **2005**, *240*, 16 – 21.

[3] Dessau, R.M.; *J. Chem. Soc., Chem. Commun.* **1986**, 1167 – 1168.

[4] Fringuelli, F. and Taticchi, A. (Eds.). (2002). *The Diels-Alder Reaction: Selected Practical Methods.* West Sussex, England: John Wiley & Sons, Ltd.

[5] Moore, J.A.; Partain, E.M.; *J. Org. Chem.* **1983**, *48*, 1105 – 1106.

[6] Kuwayama, T.; Ujita, K.; Shimizu, K.; Terashima, S.; Process for preparation of 7-oxabicyclo[2.2.1]hept-5-ene-2-carboxylic acid derivatives. US Patent 6,677,464, **2004**.

[7] Fraile, J.M.; Garcia, J.I.; Massam, J.; Mayoral, J.A.; Pires,E.; *J. Mol. Catal.* **1997**, *123*, 43 – 47.

[8] Shiramizu, M.; Toste, F.D.; *Chem. Eur. J.* **2011**, *17*, 12452 – 12457.

CHAPTER 4

USING ETHYLENE AS A DIENOPHILE IN DIELS-ALDER-DEHYDRATION REACTIONS WITH VARIOUS FURANS: SUMMARY OF EXPLORATORY WORK

Results from reaction screening studies involving ethylene and various furanic dienes, with the objective of finding novel Diels-Alder-dehydration reactions that would allow for an oxidation route from HMF to PTA, are summarized in this chapter. The known DMF to PX conversion was investigated and will be discussed first. The use of HMF, protected derivatives of HMF, and FDCA (fully oxidized HMF) as dienes in the ethylene Diels-Alder-dehydration reaction will also be summarized and discussed.

4.1 Conversion of DMF and ethylene to p-Xylene

Here, the conversion of DMF and ethylene to p-xylene was investigated. Since this reaction has been previously reported to be catalyzed by Bronsted acid zeolites[1-8] and homogeneous Lewis acids,[9] some of these reports have been reproduced and, in addition, the DMF/PX reaction was used as an initial screening reaction for using the proposed Lewis acid molecular sieves as Diels-Alder-dehydration catalysts.

The main objectives of the work included:

- Reproduce results from previous reports using Bronsted acid zeolites and homogeneous Lewis acids for the conversion of DMF to p-xylene.
- Determine if heterogeneous Lewis acid molecular sieves (e.g., Sn-BEA, Zr-BEA, Sn-MFI) are catalysts for this reaction.

Bronsted acid-containing zeolites, H-Al-BEA (Tosoh Corp.) and H-Al-Sn-BEA, a homogeneous Lewis acid, scandium triflate [$Sc(OTf)_3$], and pure Lewis acid Beta molecular sieves, Sn-BEA and Zr-BEA, were tested and the results are summarized in Table 4.1. Heptane was chosen as the reaction solvent for experiments using the Bronsted acid-containing zeolites since previous studies found the aliphatic solvent to give higher PX selectivities. Dioxane solvent was used when testing $Sc(OTf)_3$ since this was reported to be a preferable solvent when using the homogeneous Lewis acid catalysts.[9] Little effort was made to optimize the reaction systems for maximum p-xylene yield since the objective was to screen the various catalysts for p-xylene production from DMF and ethylene.

Table 4.1 Reaction results for PX synthesis via Diels-Alder-dehydration of DMF and ethylene. Reaction temperature = 250°C.

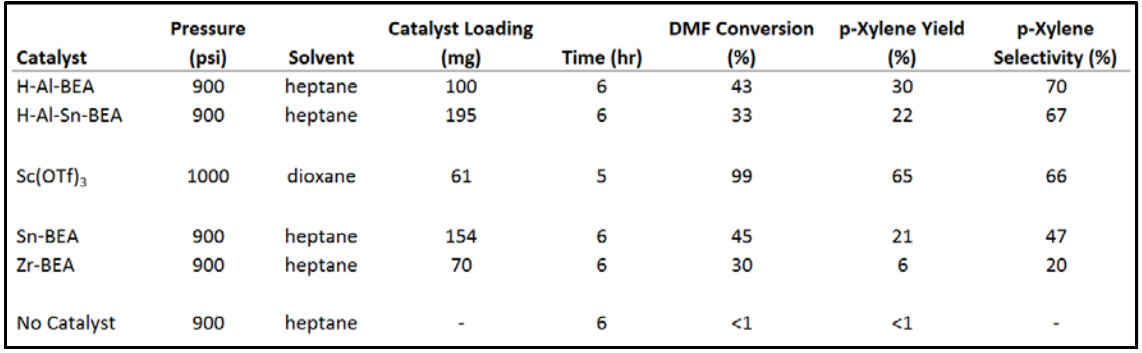

Catalyst	Pressure (psi)	Solvent	Catalyst Loading (mg)	Time (hr)	DMF Conversion (%)	p-Xylene Yield (%)	p-Xylene Selectivity (%)
H-Al-BEA	900	heptane	100	6	43	30	70
H-Al-Sn-BEA	900	heptane	195	6	33	22	67
$Sc(OTf)_3$	1000	dioxane	61	5	99	65	66
Sn-BEA	900	heptane	154	6	45	21	47
Zr-BEA	900	heptane	70	6	30	6	20
No Catalyst	900	heptane	-	6	<1	<1	-

The H-Al-BEA and H-Al-Sn-BEA catalysts made PX at 30 % and 22 % yields, respectively, after 6 hours of reaction time with about 70 % selectivity. Scandium triflate in dioxane produced PX at 65 % yield with similar selectivity (66 %). These results are in agreement with previous reports that these materials are active in catalyzing PX production. In addition, Table 4.1 shows that Sn-BEA and Zr-BEA were also able to successfully produce p-xylene with 21 % and 6 % yield, respectively, although the selectivity was lower (20-47 %) than the Bronsted acid zeolites and homogeneous Lewis acid. This is the first example of the Lewis acid Beta molecular sieves, Sn-BEA and Zr-BEA, used as catalysts to perform the Diels-Alder-dehydration reaction between DMF and ethylene.

An interesting observation from using the Lewis acid Beta molecular sieve catalysts was that the reaction product mixtures using these materials appeared “cleaner” after reaction compared to the solutions that were generated using the

H-Al-BEA, H-Al-Sn-BEA, and $Sc(OTf)_3$. Fig. 4.1 shows the product mixtures produced using each of the different catalysts. The conditions for each experiment are summarized in Table 4.2.

There are differences in the color of the solid catalyst between the left (Sn-BEA) and right (H-Al-Sn-BEA) vials. Under these conditions, the aluminum present in the BEA zeolite causes blackening of the solid while the pure Sn-BEA is only slightly discolored. Similarly, the liquid phase becomes more discolored when using the H-Al-Sn-BEA zeolite compared to the Sn-BEA. The scandium triflate catalyst produces a dark brown and opaque solution.

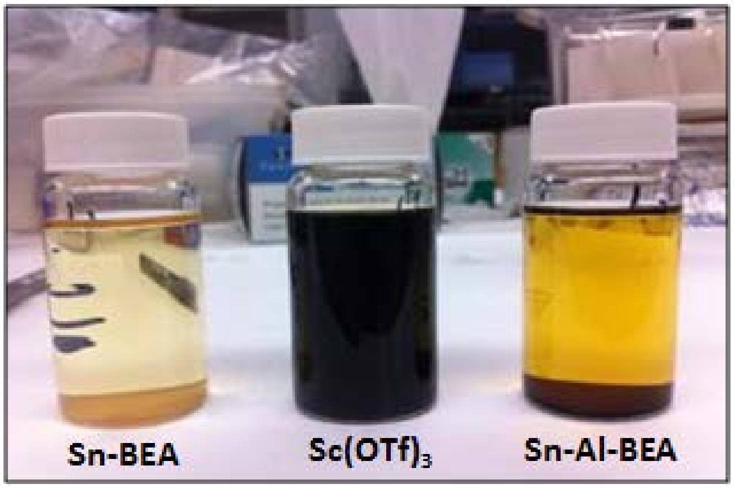

Fig. 4.1 Product solutions using Sn-BEA (left), $Sc(OTf)_3$ (center), and Sn-Al-BEA (right) catalysts. Reaction conditions are given in Table 4.2.

Table 4.2 Reaction results for PX synthesis via Diels-Alder-dehydration of DMF and ethylene using Sn-BEA, $Sc(OTf)_3$, and Sn-Al-BEA catalysts.

Vial	**Catalyst**	**DMF Conc. (Molar)**	**Temperature (^oC)**	**Pressure (psig)**	**Reaction time (hr)**	**PX Yield**
Left	Sn-BEA	0.5	150	850	42	10%
Center	$Sc(OTf)_3$	0.5	150	850	42	20%
Right	Sn-Al-BEA	0.5	150	850	42	15%

Although each of the three product solutions were not further analyzed to better understand each reaction system (e.g., the number of side reactions, organic deposition onto catalyst), the simple observations made at this point from comparing the color of the solutions and catalyst after reaction may suggest that certain side reactions (polymerizations, insoluble solids formation, catalyst coking, etc.) are avoided with the pure Lewis acidic molecular sieves, even though the measured selectivities in Table 4.1 for these materials were lower. This encouraged further testing of these materials as catalysts for the Diels-Alder-dehydration reaction of other furanic dienes with additional functionality (HMF, FDCA, etc.).

4.2 Conversion of 5-hydroxymethyl furfural (HMF) and ethylene to 4-hydroxymethyl benzaldehyde (HMB)

This section provides the results and discussion for the experiments aimed at finding reaction conditions for performing the Diels-Alder-dehydration reaction (Fig. 4.2) between HMF and ethylene to product the PTA precursor, 4-hydroxymethyl benzaldehyde (HMB). Since the product, HMB, can be oxidized to form PTA, this reaction pathway would allow for a novel oxidation route to PTA from HMF.

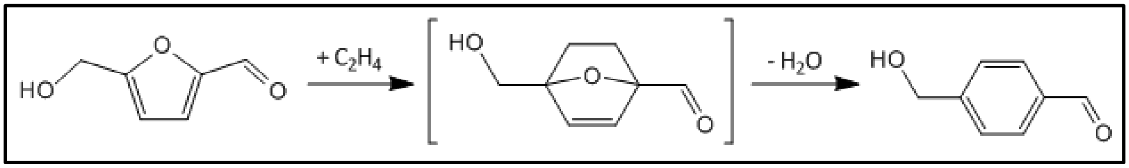

Fig. 4.2 Diels-Alder-dehydration of HMF and ethylene to form HMB.

The aldehyde functionality on HMF was a concern for two reasons. First, the aldehyde group was expected to react readily in undesired side reactions at the conditions required for the Diels-Alder reaction with ethylene. Second, the aldehyde group is electron withdrawing and is predicted to deactivate the diene functionality towards cycloadditions, making the reaction with ethylene very slow.

A strategy proposed to improve the reactivity of the furan in the Diels-Alder step while removing the aldehyde group was to “protect” HMF by forming the acetal derivative with alcohols or diols (Fig 4.3). This strategy was investigated by (1) using alcohols (methanol, propanol) or diols (ethylene glycol) in the reaction solvent to perform the acetalization and Diels-Alder-dehydration in the same reactor, and (2) by using a two step process in which the acetalization and Diels-Alder-dehydration reactions are done in separate reactors.

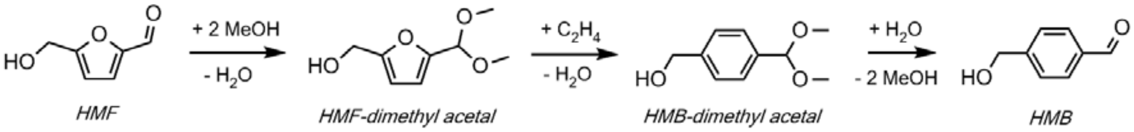

Fig. 4.3 Converting HMF to acetal before Diels-Alder-dehydration with ethylene.

A variety of reaction conditions were tested by varying solvents, catalysts, reaction temperature, reaction time, and HMF concentration. Table 4.3 provides a summary of the system conditions that were used during the investigation of finding methods for converting HMF to HMB.

Table 4.3 List of solvents, catalysts, reaction temperatures, and reaction times used to investigate the HMF to HMB reaction.

Catalysts	H-Al-Beta Sn-Beta Zr-Beta Si-Beta $Sc(OTf)_3$
Solvents	Heptane Ethylene glycol Methanol i-Propanol n-Propanol Dioxane
Temperatures	150 - 250 °C
Reaction times	0.3 - 24 hours

The screening reactions and results are summarized in Tables 4.4 and 4.5. The experiments utilizing alcohols or ethylene glycol in the reaction solvent to perform the acetalization of HMF and the ethylene Diels-Alder-dehydration in the same reactor are given in Table 4.4. Aluminum-containing (Bronsted acid) catalysts were screened (entries 1-4, Table 4.4) since it was expected that both acetalization and Diels-Alder-dehydration reactions would be Bronsted acid catalyzed. Ethylene glycol was added to the reaction solution (entries 1 & 3) to form the acetal, and alcohols (isopropanol, methanol) were also used (entries 2 & 4). Lewis acid Beta molecular sieves were screened in entries 5 & 6. In each case, no aromatic products were observed. When a lower temperature (160^{o}C) was used in entry 4, some HMF-dimethyl acetal was detected along with other unidentified side products. For the other reactions that used temperatures between 220-250 ^{o}C, dark product solutions were obtained with significant catalyst coking.

Experiments in which the reactor was initially charged with the acetal to attempt only the ethylene Diels-Alder-dehydration are summarized in Table 4.5. Most of the entries in Table 4.5 are for experiments that used furfural-derived acetals, since these compounds could be obtained from a commercial vendor (Sigma-Aldrich). It was reasoned that any ethylene Diels-Alder-dehydration reaction conditions found with the furfural-acetal should also be applicable with the HMF-acetal.

Table 4.4 Summary of screening experiments for the acetalization and ethylene Diels-Alder-dehydration of HMF. Results determined by ^{1}H NMR.

Entry	Diene	Reaction conditions	Result
1	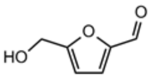	4 wt % HMF 14 wt % ethylene glycol 82 wt % heptane T = 250°C P = 900 psig C_2H_4 t = 2 hours 100 mg H-Al-Beta (Tosoh)	No HMB or aromatic product formation. Black product solution with significant catalyst coking.
2	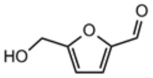	9 wt % HMF 12 wt % isopropanol 79 wt % heptane T = 250°C P = 900 psig C_2H_4 t = 4 hours 200 mg H-Al-Sn-Beta	No HMB or aromatic product formation. Product solution contained mostly unreacted HMF. Significant catalyst coking.
3	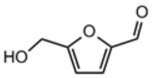	5 wt % HMF 95 wt % ethylene glycol T = 250°C P = 900 psig C_2H_4 t = 2 hours 100 mg H-Al-Beta (Tosoh)	No HMB or aromatic product formation. Black product solution with significant catalyst coking.
4	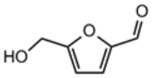	15 wt % HMF 46 wt % methanol 39 wt % heptane T = 160°C P = 850 psig C_2H_4 t = 6 hours H-Al-Beta (Tosoh)	No HMB or aromatic product formation. Some HMF-dimethyl acetal produced. Many unidentified side product peaks in ^{1}H NMR.
5	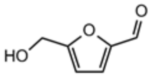	4 wt % HMF 22 wt % n-propanol 74 wt % heptane T = 250°C P = 900 psig C_2H_4 t = 4 hours 100 mg Sn-Beta	No HMB or aromatic product formation. Black product solution with significant catalyst coking.
6	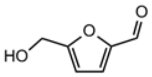	5 wt % HMF 95 wt % ethylene glycol T = 220°C P = 900 psig C_2H_4 t = 2 hours 100 mg Zr-Beta	No HMB or aromatic product formation. Black product solution with significant catalyst coking.

Table 4.5 Summary of screening experiments for the ethylene Diels-Alder-dehydration of HMF-acetal and furfural-acetal dienes. Results determined by ^{1}H NMR.

Entry	Diene	Reaction conditions	Result
1	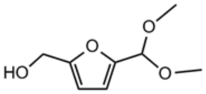	25 wt % HMF-dimethyl acetal 75 wt % heptane T = 250°C P = 900 psig C_2H_4 t = 6 hours 150 mg Sn-Beta	No aromatic product formation. Nearly complete HMF-dimethyl acetal conversion. Black product solution with significant catalyst coking. Black solids coated on reactor walls.
2	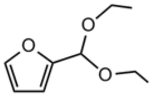	15 wt % furfural-diethyl acetal 85 wt % heptane T = 250°C P = 900 psig C_2H_4 t = 2.5 hours 100 mg Sn-Beta	No aromatic products. Acetal hydrolysis to furfural. Solid humins/coke formation.
3	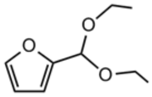	15 wt % furfural-diethyl acetal 85 wt % heptane T = 250°C P = 900 psig C_2H_4 t = 6 hours 100 mg H-Al-Beta (Tosoh)	No aromatic products. Acetal hydrolysis to furfural. Solid humins/coke formation.
4	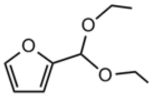	15 wt % furfural-diethyl acetal 85 wt % heptane T = 250°C P = 900 psig C_2H_4 t = 6 hours 100 mg H-Al-Ti-Beta	No aromatic products. Significant catalyst coking.
5	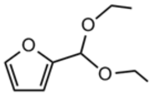	15 wt % furfural-diethyl acetal 85 wt % heptane T = 250°C P = 900 psig C_2H_4 t = 6 hours 100 mg Si-Beta	No aromatic products. Acetal hydrolysis to furfural.
6	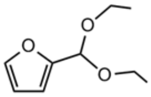	35 wt % furfural-diethyl acetal 65 wt % heptane T = 150°C P = 900 psig C_2H_4 t = 11 hours No catalyst	No aromatic products.

Table 4.5 Continued

Entry	Diene	Reaction conditions	Result
7	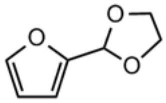	12 wt % furfural-EG acetal 88 wt % dioxane T = 250°C P = 900 psig C_2H_4 t = 5 hours 100 mg Sn-Beta	No aromatic products. Acetal hydrolysis to furfural. Solid humins/coke formation.
8	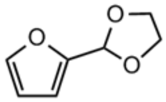	12 wt % furfural-EG acetal 88 wt % dioxane T = 250°C P = 900 psig C_2H_4 t = 24 hours 100 mg Si-Beta	No aromatic products.
9	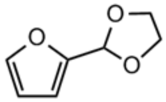	5 wt % furfural-EG acetal 95 wt % dioxane T = 250°C P = 800 psig C_2H_4 t = 15 hours 200 mg $Sc(OTf)_3$	No aromatic products. Solid humins/coke formation.
10	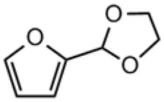	5 wt % furfural-EG acetal 95 wt % dioxane T = 250°C P = 1050 psig C_2H_4 t = 0.3 hr 5 mg $Sc(OTf)_3$	No aromatic products. Acetal hydrolysis to furfural. Solid humins/coke formation.

The HMF-dimethyl acetal (entry 1, Table 4.5) was tested in heptane solvent with Sn-Beta present, and nearly complete HMF-dimethyl acetal conversion with no aromatic product formation was observed. Instead, significant catalyst coking and black solid formation occurred. For the experiments using the furfural-acetals, catalyst coking and solid humins/coke formation occurred for all experiments that utilized high temperatures (250°C) or an acid catalyst. Heavy catalyst coking and solid humins/coke formation was avoided when the acid catalyst was removed (entries 5-6 & 8, Table 4.5).

The main challenges found for using the acetals as substrates to react with ethylene at the high temperature/pressure conditions expected for the Diels-Alder-dehydration reaction to occur was (1) minimizing the hydrolysis reaction of the acetal back to the aldehyde, and (2) minimizing humins or coke formation on the catalyst and reactor walls. Since water is produced in the desired Diels-Alder-dehydration reaction, the hydrolysis of the acetal to the aldehyde is expected to be difficult to avoid. The cause for the significant humins and coke formation was assumed to be the reactive aldeyhde functionality.

Some other general conclusions from this work on converting HMF to HMB include the following:

- HMF and the HMF-acetal derivatives were found to be reactive towards humins and/or coke formation under the conditions expected for the Diels-Alder-dehydration reaction to occur (T=150-250^{o}C, P=800-1000 PSI, Bronsted or Lewis acid catalysts), and no yield to the target HMB product was observed.
- When zeolite catalysts are used (Bronsted acid or Lewis acid), significant carbon deposition or coking of the catalyst occurred. Typically several peaks in the ^{1}H NMR spectra were present in addition to HMF or furfural peaks, most of which were unidentified.

- When a homogeneous Lewis acid (scandium triflate) was used, black solid or humins formation was observed. HMF peaks typically were not present in the liquid-phase ^{1}H NMR spectra, indicating nearly full conversion of the HMF reactant.

4.3 Conversion of 2,5-bis(hydroxymethyl)furan (BHMF) to 1,4-bis(hydroxymethyl)benzene (BHMB)

It is suspected that the aldehyde substituent on HMF is the cause for the high reactivity of HMF towards undesired side reactions, resulting in no HMB formation. The next diene that was investigated was 2,5-bis(hydroxymethyl)furan (BHMF) which is obtained by a partial reduction of HMF. Since BHMF has only hydroxymethyl [-CH_2OH] funtions on the furan ring we thought that the number of side reactions available would be less and would allow for a higher chance of achieving the desired Diels-Alder-dehydration product, in this case 1,4-bis(hydroxymethyl)benzene (BHMB) . The reaction scheme is shown in Fig. 4.4. This reaction was studied using two different solvent systems – dioxane and acetic acid.

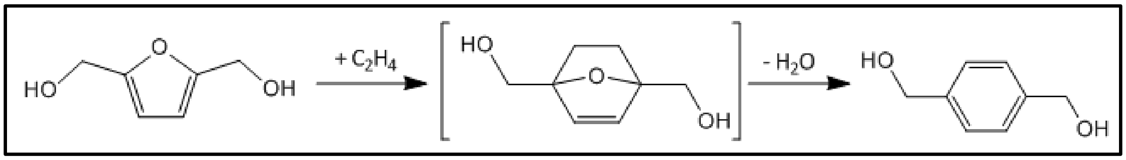

Fig. 4.4 Diels-Alder-dehydration of BHMF and ethylene to BHMB.

a. Dioxane solvent system

The first issue that was addressed with the BHMF/dioxane system was to determine the temperature up to at which BHMF was thermally stable in the absence of a catalyst. Further experimentation using proposed catalysts would be performed below this temperature to minimize side reactions occurring in the solution phase. A series of four experiments are summarized in Table 4.6 that varied the reaction temperature between 150-300°C and the reaction time between 1-15 hours. It was found that BHMF was stable (did not react) in the dioxane liquid phase at 250°C for at least 15 hours. When the temperature was raised to 300°C the diene began to undergo side reactions, mainly the dehydroxymethylation of BHMF to form furfuryl alcohol, furan, and formaldehyde as shown in Fig 4.5. Solids and humins also began to form in the reactor at the 300°C temperature.

Table 4.6 Experiment conditions and results for determining temperature that BHMF is thermally stable. Reaction conditions: 0.1 M BHMF in dioxane, 1000 psig C_2H_4, no catalyst. Results obtained by ^{1}H NMR analysis.

Entry	Temperature (°C)	Reaction time (hr)	Result
1	150	1	No reaction.
2	250	2	No reaction.
3	250	15	No reaction.
4	300	6	Thermal degradation reactions occur. Mainly, furan and formaldehyde formation (dehydroxymethylation), and solids/hummins formation.

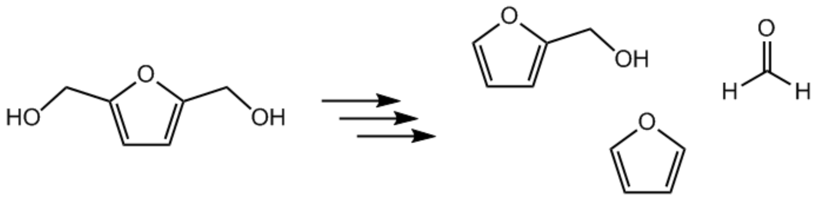

Fig. 4.5 Dehydroxymethylation of BHMF: a significant side reaction.

Based on the results above, proposed catalysts were tested using temperatures no greater than 250^oC. The two catalysts that were studied in the BHMF/dioxane system are (1) scandium triflate and (2) Sn-BEA molecular sieve.

Several attempts were made to finding conditions that scandium triflate was able to achieve yields of the desired Diels-Alder-dehydration product. In all cases, significant degradation of the BHMF diene occurred, producing mainly solid humins and a black, opaque product mixture. It appears that the homogeneous Lewis acid is very reactive with BHMF towards these degradation reactions under the 150-250^oC reaction temperatures and the result was no yield of the aromatic Diels-Alder-dehydration product.

Numerous experiments were also done using the Sn-BEA catalyst in the BHMF/dioxane system (Table 4.7). Initial tests were done at 250^oC (entry 1) and it was found that Sn-BEA at this temperature results in significant catalyst coking and dehydroxymethylation of BHMF as observed by formaldehyde and furan formation.

Table 4.7 Experiment conditions and results for BHMF in dioxane solvent with Sn-BEA catalyst. Reaction conditions: Dioxane solvent, Sn-Beta catalyst, 1000 psig C_2H_4. Results obtained using ^1H NMR analysis.

Entry	BHMF Concentration (M)	Temperature (^oC)	Reaction time (hr)	Result
1	0.1	250	16	Dark/black liquid and catalyst. Significant dehydroxymethylation.
2	0.1	150	1	Low BHMF conversion. Some dehydroxymethylation.
3	0.1	150	6	Some dehydroxymethylation. **Low yields of BHMB.**
4	0.25	150	42	BHMF completely converted. **Low yields of BHMB.**

Next, experiments were performed at 150^{o}C with Sn-BEA catalyst (entries 2-4). At these conditions the undesired dehydroxymethylation reaction was significantly slowed, and the BHMF was still present and mostly unconverted after 6 hours of reaction. After 6 hours (entry 3), low amounts of BHMB were detected by ^{1}H NMR (NMR peaks matched that of BHMB product standard). The product solution was a light green color and not black like that observed for the system using scandium triflate. The reaction at 150 ^{o}C was allowed to proceed for 42 hours (entry 4) and BHMB was still observed in the product ^{1}H NMR spectrum while the BHMF peaks were gone indicating complete conversion.

To provide further support that the target BHMB product was forming, the product solutions were analyzed by GC/FID. Supporting the ^{1}H NMR results, there was a trace product peak in the chromatograms obtained for the solutions in entries 3-4 that matched the elution time of the BHMB product standard. The conversion and selectivity was not quantified, but based on the ^{1}H NMR and GC/FID analyses, it appeared the ethylene Diels-Alder-dehydration reaction was achieved with only trace yield and selectivity.

The main findings from this portion of the study are:

- A reaction system was found using BHMF and dioxane solvent that allowed high reaction temperatures (150-250^{o}C) and pressures (1000 PSIG) to be held for long times (>6 hours) in the presence of the Lewis acid molecular sieve, Sn-Beta, without significant degradation of the furan.

- Sn-BEA molecular sieves were used to form the Diels-Alder-dehydration product between an oxygenated furan (BHMF) and ethylene, although only low yields and selectivities were achieved. The main side reaction was the dehydroxymethylation to form furfuryl alcohol, furan, and formaldehyde.

b. Acetic acid solvent system

Some reaction testing with BHMF was performed using acetic acid as solvent. Reasons for investigating acetic acid as a solvent system included (1) acetic acid was shown to catalyze the Diels-Alder-dehydration reaction between DMF and ethylene to produce p-xylene [5], and (2) the acetic acid solvent would react with BHMF to produce the di-ester (Fig. 4.6) that may be more stable and less susceptible to the dehydroxymethylation side reaction (Fig. 4.5). Several tests using acetic acid as solvent are summarized in Table 4.8.

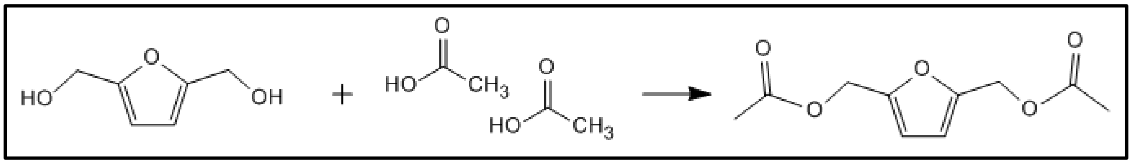

Fig. 4.6 Esterification of BHMF with acetic acid to form di-ester.

Table 4.8 Experiment conditions and results for BHMF in acetic acid solvent. Reaction conditions: 1000 psig C_2H_4. Results obtained by ^{1}H NMR analysis.

Entry	Catalyst	Temperature (°C)	Reaction time (hr)	Result
1	none	150	1	Low BHMF conversion. Some dehydroxymethylation.
2	none	175	23	High BHMF conversion. Significant dehydroxymethylation.
3	$Sc(OTf)_3$	150	1	No product peaks in ^{1}H NMR. Significant solids formation.
4	$Sc(OTf)_3$	150	1	No product peaks in ^{1}H NMR. Significant solids formation.
5	$Sc(OTf)_3$	250	1	No product peaks in ^{1}H NMR. Significant solids formation.
6	$Sc(OTf)_3$	250	1	No product peaks in ^{1}H NMR. Significant solids formation.
7	Sn-BEA	150	2	High BHMF conversion. Significant dehydroxymethylation.

The main conclusions from these experiments are:

- Acetic acid increases the rate of dehydroxymethylation to produce furan and formaldehyde.
- Similarly to when dioxane is used as solvent, adding scandium triflate to the reaction mixture results in solids/humins formation. No peaks (other than solvent) remain in the ^{1}H NMR spectra of the liquid product.
- Adding Sn-BEA catalyst to the acetic acid system does not change the result from the case of no catalyst, that is significant production of furan and formaldehyde.

4.4 Conversion of 2,5-furandicarboxylic acid (FDCA) to terephthalic acid (PTA)

The Diels-Alder-dehydration between FDCA and ethylene to produce PTA, shown in Fig. 4.7, was investigated using the Lewis acid molecular sieves as catalysts. This conversion was first reported in a BP patent that describes methods for producing PTA using water as solvent and no catalyst, although only very low yields (0.14 mol %) were achieved.[10] The product of this reaction consists of a solid "cake" phase and a liquid phase, and the PTA product was reported to be present in both phases. PTA production from FDCA and ethylene was again reported recently in a Furanix/Coca-Cola patent application that shows PTA yields of up to 16.5%.[11] The higher yields were achieved by using acetic acid, phosphoric acid, acetic acid anhydride or benzoic acid anhydride as desiccating agent, and long reaction times (32 hours). Table 4.9 summarizes the conditions of the reaction systems used in these patents.

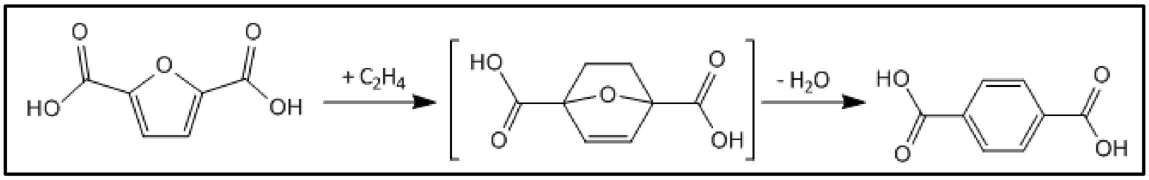

Fig. 4.7 Diels-Alder-dehydration reaction of FDCA and ethylene to PTA.

Table 4.9 Experiment conditions and PTA yields reported in BP patent[10] and Furanix/Coca-Cola patent appl.[11]

	BP patent (2009)	**Furanix/Coca-Cola patent (2014)**
FDCA concentration (molar)	0.3-0.6	~1.0
PTA yield (mol %)	0.14	6.8-16.5
Solvents	water	acetic acid, acetic acid anhydride
Catalyst	none	acetic acid, phosphoric acid
Desiccating agent	none	acetic acid anhydride, benzoic acid anhydride
Ethylene Pressure	100-250 PSIG	430 PSIG (room temperature)
Temperature (°C)	100-200	240
Reaction time (hrs)	2	32

To begin this investigation, several experiments were performed using the aqueous reaction conditions reported in the BP patent. The reaction product consisted of solid and liquid phases that were both analyzed using ^{1}H NMR in DMSO-d_6 solvent (the solid phase extracted using DMSO-d_6, and the liquid phase dissolved in DMSO-d_6). No measurable PTA was found in any of the products. Experiments reproducing the Furanix/Coca-Cola patent reaction conditions were not performed.

The use of DMSO as a reaction solvent was considered since DMSO was the only solvent found that could completely solubilize FDCA as room temperature. The main difficulty with using DMSO solvent is that solvent degradation at temperatures above ~150°C occur in the presence of an acid catalyst.

Dioxane was applied next as a solvent for two main reasons: (1) dioxane was found to be a preferable solvent in the Micromidas patent application for the production of PX from DMF and ethylene [9], and (2) low yields of BHMB was obtained from BHMF and ethylene when using dioxane with Sn-Beta catalyst.

Sc(OTf)$_3$, H-BEA, and Sn-BEA catalysts were tested and compared using 0.1 molar FDCA solutions in dioxane at 250^{o}C (Table 4.10). The H-BEA and Sc(OTf)$_3$ both produced high conversions of FDCA with no measurable PTA yield. In addition, the product solutions for both experiments were black or brown, and black solids formed when Sc(OTf)$_3$ was used.

Table 4.10 Experiment conditions and results for FDCA in dioxane solvent using Sc(OTf)$_3$, H-BEA, and Sn-BEA catalysts. Reaction conditions: 0.1 M FDCA in dioxane, 250^{o}C, 1000 psig C_2H_4, 14 hours reaction time. Results obtained by ^{1}H NMR analysis.

Catalyst	Catalyst amount (mg)	Result
Sc(OTf)$_3$	60	High conversion of FDCA. No PTA yield. Black liquid product and solids formation.
H-BEA	200	High conversion of FDCA. No PTA yield. Dark brown product solution and coked (black) catalyst.
Sn-BEA	200	Low conversion of FDCA. Estimated PTA yield 1-3 mol % based on ^{1}H NMR. Clear product solution. Catalyst only slightly discolored.

A very different result was obtained when Sn-BEA was tested as catalyst. The product solution was clear and only slightly discolored, and the solid catalyst was an off-white color (Fig. 4.8). Additionally, PTA formation was observed (estimated 1-3 mol% yields) and FDCA conversions appeared low based on the large FDCA peak remaining in the product NMR. The ^{1}H NMR spectra of the different product solutions are compared to the PTA standard in Fig. 4.9.

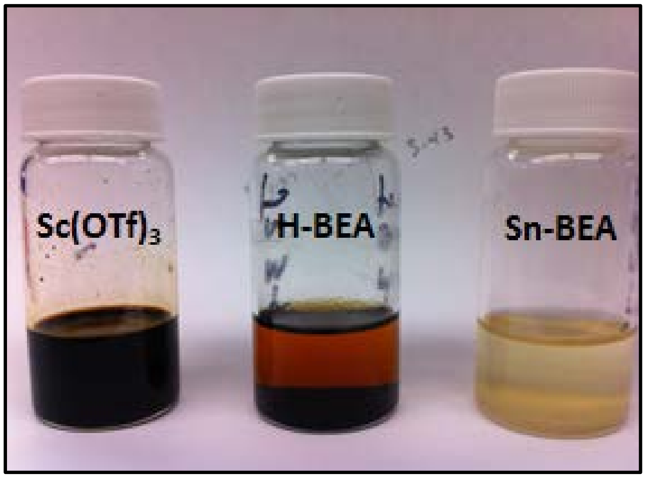

Fig. 4.8 Product solutions using $Sc(OTf)_3$ (left), H-BEA (center), and Sn-BEA (right) catalysts. Reaction conditions summarized in Table 4.10.

FDCA conversions could not be accurately measured since the FDCA was highly insoluble in the dioxane solvent making it difficult to collect a homogeneous aliquot of the product for analysis. The PTA yield was estimated by dissolving a small aliquot of the mixture (of known mass) in DMSO-d_6 containing an external standard (tetraethylsilane), and collecting a ^{1}H NMR to quantify the amount of PTA in the solid/liquid product. The yield was calculated from dividing by the initial FDCA amount charged in the reactor.

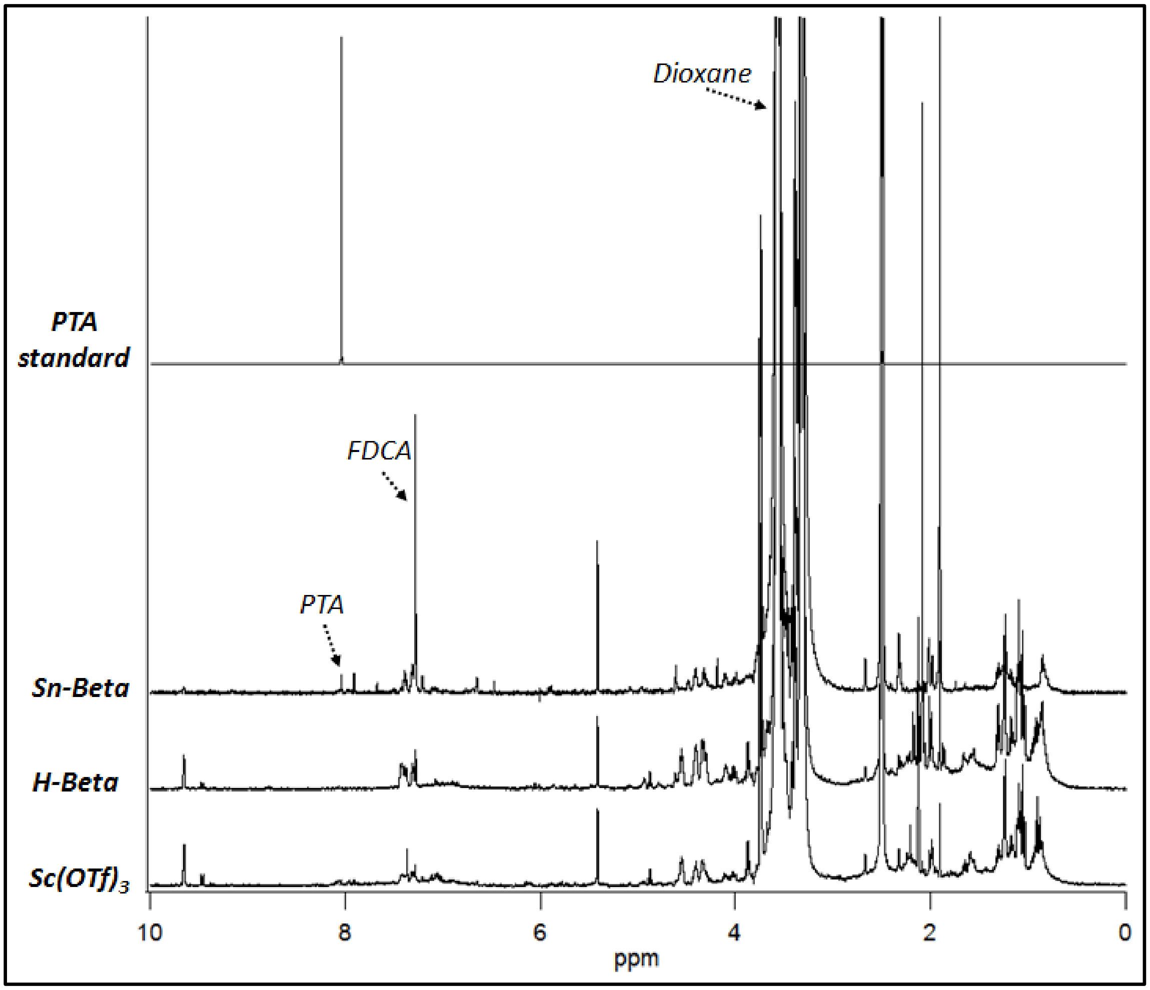

Fig. 4.9 ^{1}H NMR spectra of the different product solutions compared to the PTA standard. Reaction conditions summarized in Table 4.10.

Since the peak assigned to PTA in the ^{1}H NMR spectrum was small, two tests were done to further confirm that PTA was being formed. In one test, a small amount of PTA standard was added to the product solution, and ^{1}H NMR spectra before and after the addition of PTA were compared (Fig 4.1-A in appendix). The peak assigned to PTA became larger after addition of the standard, providing further confirmation that PTA was formed. In a second test, HPLC analysis was used to identify a product with identical elution time as the

PTA standard (Fig 4.2-A in appendix), providing further support for the presence of PTA in the product.

To address the possibility that PTA was undergoing secondary reactions that were resulting in low PTA yields, a control experiment was performed that used PTA as the starting reagent instead of FDCA. After 14 hours of reaction, ^{1}H NMR analysis showed only PTA present in the dioxane solvent with no other product peaks. This suggested that if higher PTA yields were achieved from the reaction between FDCA and ethylene, then the PTA would be stable under reaction conditions and would not be converted in secondary reactions.

The Lewis acid Beta molecular sieve/dioxane reaction system was tested using other Lewis acid molecular sieves, Zr-Beta and Ti-Beta (Table 4.11). These catalysts showed similar results to Sn-Beta, that is, a “clean” product solution with estimated PTA yields of 1-3 %. Lowering the temperature from 250^{o}C to 225^{o}C and increasing the effective FDCA concentration from 0.1 M to 1.0 M was found to produce an NMR spectrum with even fewer side products along with the PTA product (Fig. 4.10).

Table 4.11 Reaction results for PTA synthesis via Diels-Alder-dehydration of FDCA and ethylene in dioxane. Reaction conditions: 1 M FDCA in dioxane, 225^{o}C, 1000 psig C_2H_4, 16 hours. Results obtained by ^{1}H NMR analysis.

Entry	Catalyst	Catalyst amount (mg)	PTA Yield (%)
1	Sn-Beta	200	1-3
2	Zr-Beta	122	1-3
3	Ti-Beta	200	1-3

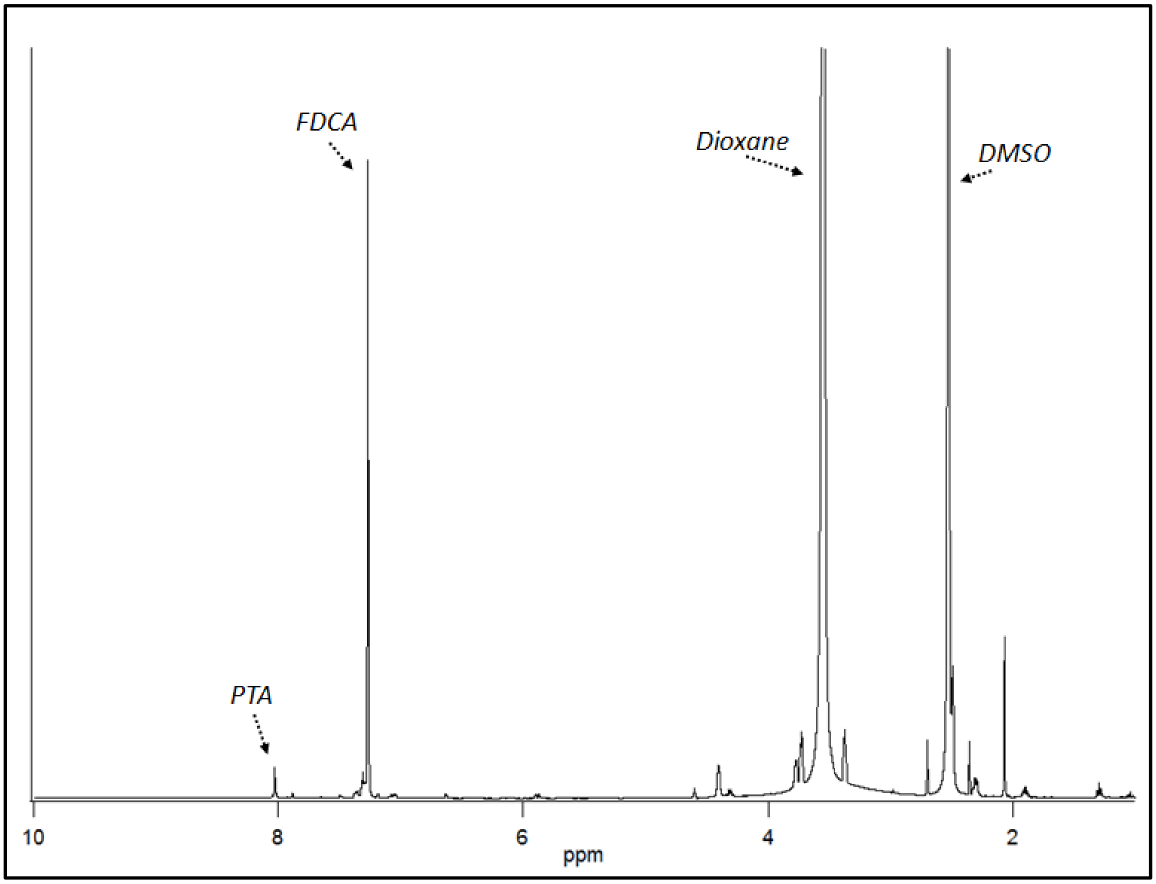

Fig. 4.10 ^{1}H NMR (in DMSO-d_6) of Sn-Beta catalyzed Diels-Alder-dehydration of FDCA and ethylene to PTA. Reaction conditions: 1 M FDCA in dioxane, 200 mg Sn-Beta, 225^{o}C, 1000 psig C_2H_4, 16 hours.

Although PTA was being produced, the yields were low even after long reaction times. Efforts were made to increase yield. One hypothesis for the low yields in the dioxane solvent system was the low solubility of FDCA in dioxane. A low FDCA concentration in the reacting liquid phase would help explain the slow PTA formation. At room temperature, FDCA is nearly insoluble and it is unclear how much of the FDCA is solubilized at reaction conditions (225-250^{o}C, 1000 psig). To help understand whether the low solubility of FDCA in dioxane was resulting in the slow reaction kinetics, a series of experiments were performed using the dimethyl ester of FDCA (dimethyl-FDCA) as the diene (Fig. 4.11), since dimethyl-FDCA is completely soluble in dioxane at room temperature at the ~0.1-1.0 M concentrations that were being tested. The product of this reaction is dimethyl terephthalate (DMT).

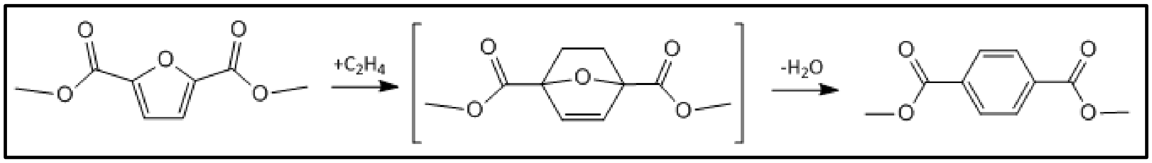

Fig. 4.11 Diels-Alder-dehydration of dimethyl-FDCA and ethylene to dimethyl terephthalate.

Table 4.12 Reaction results for Diels-Alder-dehydration experiments between dimethyl-FDCA and ethylene. Reaction conditions: 0.4 M dimethyl-FDCA solution in dioxane, 200 mg catalyst, 800 psig C_2H_4. Results obtained by ^1H NMR analysis.

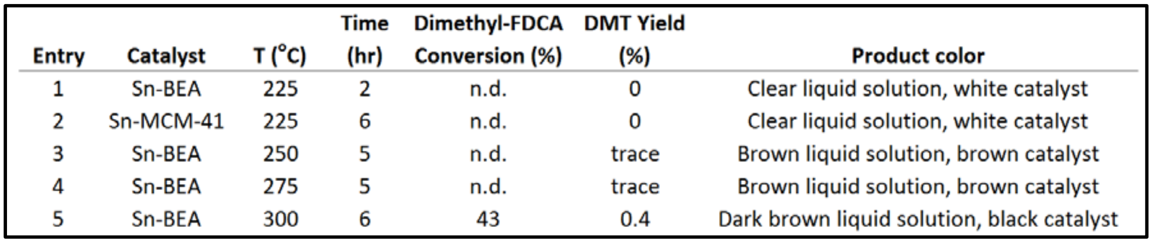

Entry	Catalyst	T (°C)	Time (hr)	Dimethyl-FDCA Conversion (%)	DMT Yield (%)	Product color
1	Sn-BEA	225	2	n.d.	0	Clear liquid solution, white catalyst
2	Sn-MCM-41	225	6	n.d.	0	Clear liquid solution, white catalyst
3	Sn-BEA	250	5	n.d.	trace	Brown liquid solution, brown catalyst
4	Sn-BEA	275	5	n.d.	trace	Brown liquid solution, brown catalyst
5	Sn-BEA	300	6	43	0.4	Dark brown liquid solution, black catalyst

Several experiments were performed using Sn-BEA, as well as the Lewis acid-containing mesoporous material, Sn-MCM-41, as catalysts (Table 4.12). Temperatures of 225-300°C were screened. The di-ester was stable in the present of Sn-BEA and Sn-MCM-41 at 225°C, resulting in a clear liquid solution and white catalyst (entries 1 & 2). When the temperature was increased to 250°C and 275°C, degradation reactions began to occur, indicated by the light brown liquid phase and catalyst, and only a trace amount of DMT was detected (entries 3 & 4). When the temperature was raised to 300°C the liquid solution was dark brown and the catalyst was black, and only 0.4 mol % DMT yield was produced at 43% dimethyl-FDCA conversion (entry 5). Clearly, dimethyl-FDCA is very unreactive with ethylene under these conditions, and as the temperature was increased other undesired degradation reactions took place. Since the completely soluble di-ester was very unreactive with ethylene, this suggests that the slow rates for the conversion of FDCA and ethylene to PTA are not due to low solubility.

Another possibility for the low PTA yields may be a very difficult and slow Diels-Alder cycloaddition reaction between FDCA and ethylene. The two strong electron-withdrawing groups (-COOH) attached to the furanic diene and the lack of any electron-withdrawing groups on the dienophile (ethylene) are factors that may contribute to a high activation barrier for the cycloaddition step. In an effort to make the –COOH groups of FDCA less electron withdrawing to improve the reactivity of the furan in the Diels-Alder cycloaddition, the disodium salt of FDCA was prepared and tested for the Diels-Alder-dehydration reaction with ethylene (Fig. 4.12). The product, disodium terephthalate, was not produced and, instead, sodium furoate was formed by decarboxylation.

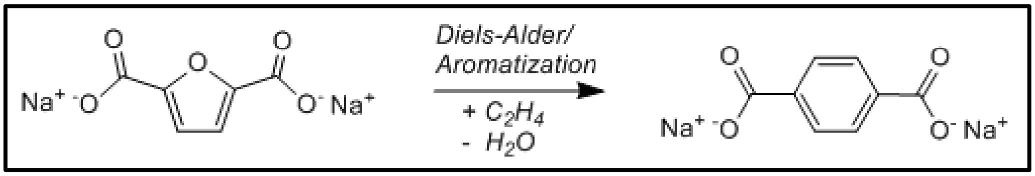

Fig. 4.12 Diels-Alder-dehydration of disodium-FDCA and ethylene to disodium terephthalate.

The Lewis acid molecular sieve/dioxane system reported here for the conversion of FDCA to PTA is an improvement over the previously reported methods in the BP patent using aqueous conditions and no catalyst, mainly due to the significant reduction in side degradation reactions (that lead to a black/brown product containing solid coke/humins) and improved yields (up to ~3% compared to 0.14%). Efforts to further increase the production rates and yield were unsuccessful, and so bio-PTA synthesis by this new method is still unlikely to be practical for commercial application.

The main findings and outcomes from this chapter include the following:

- The experiment conditions published in the BP patent were replicated, but no measurable PTA yield was obtained per ^{1}H NMR analysis. The products obtained from these reaction conditions using water solvent are highly discolored (black/brown), indicating humins formation from FDCA.
- Sn-BEA, Ti-BEA, and Zr-BEA molecular sieves in dioxane solvent are shown to be catalysts for the conversion of FDCA and ethylene to PTA. Although the PTA yields are low (1-3 mol%), the system appears to be more selective for PTA synthesis than previously reported methods, and degradation reactions that result in dark solutions and humins formation are avoided.

4.5 References

[1] Williams, C.L.; Chang C-C.; Do, P.; Nikbin, N.; Caratzoulas, S.; Vlachos, D.G.; Lobo, R.F.; Fan, W.; Dauenhauer, P.J.; *ACS Catal.* **2012**, *2*, 935 – 939.

[2] Do, P.T.M.; McAtee, J.R.; Watson, D.A.; Lobo, R.F.; *ACS Catal.* **2013**, *3*, 41 – 46.

[3] Nikbin, N.; Do, P.T.; Caratzoulas, S.; Lobo, R.F.; Dauenhauer, P.J.; Vlachos, D.G.; *J. Catal.* **2013**, *297*, 35 – 43.

[4] Xiong, R.; Sandler, S.I.; Vlachos, D.G.; Dauenhauer, P.J.; *Green. Chem.* **2014**, *16*, 4086 – 4091.

[5] Chang, C-C.; Green, S.K.; Williams, C.L.; Dauenhauer, P.J.; Fan, W.; *Green. Chem.* **2014**, *16*, 585 – 588.

[6] Nikbin, N.; Feng, S.; Caratzoulas, S.; Vlachos, D.G.; *J. Phys. Chem. C* **2014**, *118*, 24415 – 24424.

[7] Li, Y-P.; Head-Gordon, M.; Bell, A.T.; *J. Phys. Chem. C* **2014**, *118*, 22090 – 22095

[8] Patet, R.E.; Nikbin, N.; Williams, C.L.; Green, S.K.; Chang, C-C.; Fan, W.; Caratzoulas, S.; Dauenhauer, P.J.; Vlachos, D.G.; *ACS. Catal.* **2015**, DOI: 10.1021/cs5020783.

[9] Masuno, M.N.; Smith, P.B.; Hucul, D.A.; Dumitrascu, A.; Brune, K.; Smith, R.L.; Bissell, J.; Foster, M.; Methods of producing para-xylene and terephthalic acid. U.S. Patent Appl. No. 13/838,761, **2013**.

[10] Gong, W.H.; Terephthalic acid composition and process for the production thereof. U.S. Patent 8,299278, **2012**.

[11] Wang, B.; Gruter, F.J.M.; Dam, M.A.; Kriegel, R.M.; Process for the preparation of benzene derivatives from furan derivatives. WO Patent Appl. PCT/NL2013/050740, **2013**.

CHAPTER 5

DISCOVERY OF NEW SELECTIVE DIELS-ALDER REACTIONS USING ETHYLENE: PRODUCTION OF PTA FROM HMF VIA OXIDATION ROUTE

5.1 New ethylene Diels-Alder-dehydration reactions using 5-methyl-2-furoic acid (MFA) and methyl 5-methyl-2-furoate (MMF) as dienes

In Chapter 4, the synthesis of PTA from FDCA (fully oxidized HMF) and ethylene was accomplished using the Lewis acid molecular sieve catalysts in dioxane solvent, although maximum PTA yields of only ~3 mol % were obtained. This chapter discusses further efforts to improve the reactivity of the furanic diene containing the electron-withdrawing carboxylic acid groups (–COOH) in the ethylene Diels-Alder-dehydration reaction. These efforts resulted in the discovery of a series of new ethylene Diels-Alder-dehydration reactions catalyzed by Lewis acid-containing molecular sieves and mesoporous silicas, and these new reactions open a new route to renewable PTA from HMF that avoid reduction steps.

As hypothesized in Chapter 4, the slow reactivity of FDCA in the Diels-Alder reaction with ethylene is likely due to the deactivation of the diene function towards cycloadditions with a dienophile by the two carboxylic acid groups (–COOH). Attempts were made to make these groups less deactivating by using the Na^+ salt of FDCA, since the (–COONa) group would be less electron withdrawing than the (–COOH) groups. Here, another strategy was successfully applied and was the use of furanic dienes that contain only one (–COOH) or (–COOR) group on the 2- position and a methyl, hydroxymethyl, or alkoxymethyl group on the 5- position. This substitution of the functionality on the 5- position replaces an electron-withdrawing group (–COOH) with a slightly electron-donating group (-CH_3, -CH_2OH, -CH_2OR), resulting in a more active diene in the Diels-Alder reaction with ethylene.

The next dienes tested were 5-methyl-2-furoic acid (MFA) and the corresponding methyl ester, methyl 5-methyl-2-furoate (MMF). The corresponding Diels-Alder-dehydration products with ethylene are p-toluic acid (TA) and methyl p-toluate (MPT) (Fig. 5.1). These dienes have similar functionality to FDCA and dimethyl-FDCA, but they should be more active in Diels-Alder reactions due to having only one carboxylic acid function. Therefore, these furans were used as model dienes in the effort to understand if the presence of two carboxylic acid functions was the cause of the slow reaction rates with ethylene.

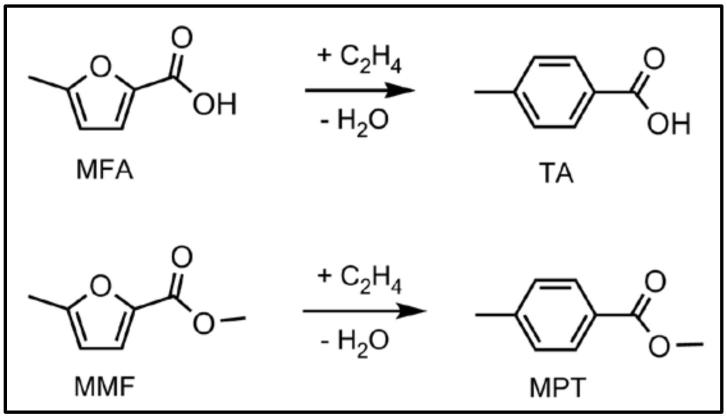

Fig. 5.1 Ethylene Diels-Alder-dehydration reactions of MFA to TA and MMF to MPT.

Table 5.1 Ethylene Diels-Alder-dehydration reaction results for conversion of MFA/MMF to TA/MPT. Reaction conditions: 0.4 M solution in dioxane, 200 mg catalyst, T=225^{o}C, 1000 psig C_2H_4, 6 hours. Results determined by ^{1}H NMR.

Entry	Diene	Product	Catalyst	Conversion (%)	Yield (%)	Selectivity (%)
1	MFA	TA	Sn-BEA	82	14	17
2	MMF	MPT	Sn-BEA	13	13	~100
3	MMF	MPT	Sn-MCM-41	12	12	~100
4	MMF	MPT	Sn-SiO_2 (amorphous)	11	11	~100
5	MMF	MPT	Si-BEA	0	0	n/a

These dienes were tested for reaction with ethylene using dioxane solvent in the presence of various Lewis acid (Sn^{4+})-containing silica materials (Table 5.1). Sn-BEA was found to catalyze the Diels-Alder-dehydration reaction between MFA and ethylene to produce 14 mol % yield of TA at 82% conversion after 6 hours at 225^{o}C and 1000 psig C_2H_4 pressure (entry 1). Although the selectivity to TA in this system was low, the catalyst after reaction was an off-white color and not significantly coked. The methyl ester, MMF, reacted with ethylene in the presence of a variety of Lewis acidic silicas to produce the aromatic product, MPT, with nearly 100% selectivity. Sn-BEA molecular sieve, Sn-MCM-41 mesoporous silica, and a Sn^{4+}-containing amorphous silica (Sn-SiO_2) all produced similar results, that is 11-13 % yield of MPT at nearly 100% selectivity (entries 2-4). A control experiment using a pure silica Beta (Si-BEA, entry 5) confirmed that the Sn^{4+} sites were required for catalysis and that the silica surface is not catalyzing the reaction.

Zirconium (Zr^{4+})-containing Beta molecular sieves were also shown to be effective and selective catalysts for the conversion of MMF and ethylene to MPT

(Table 5.2). Different Zr-Beta samples were used for the two reactions (entries 1-2), both producing MPT with high selectivity. The gas chromatograms of both product solutions (Fig. 5.2 and Fig 5.3) indicate very few side products.

Table 5.2 Reaction results for Zr-Beta as catalyst in ethylene Diels-Alder dehydration of MMF to MPT. Reaction conditions: 0.1 M MMF in dioxane, 100 mg Zr-Beta, 190^{o}C, 1000 psig C_2H_4, 6 hours. A Si/Zr atom ratio of 123 was measured for both Zr-Beta-1 and Zr-Beta-2 samples by energy-dispersive x-ray spectroscopy (EDS). Conversions and yields measured by ^{1}H NMR in entry 1 and by GC-FID (decane as external standard) in entry 2.

Entry	Catalyst Sample	MMF Conversion (%)	MPT Yield (%)	MPT Selectivity (%)
1	Zr-Beta-1	23.0	22.3	97
2	Zr-Beta-2	15.8	16.0	101

The finding that MFA and MMF can react with ethylene in the Diels-Alder-dehydration reaction to produce the aromatic product was a significant breakthrough in the research project. Unfortunately, MFA and MMF are not particularly useful intermediates in the transformation of HMF to PTA. A route involving MFA or MMF would be impractical, mainly because the synthesis of MFA from HMF would be difficult as one of the substituents of HMF would need to be selectively reduced while the other selectively oxidized (Fig. 5.4).

In the next section, a new route is proposed for the transformation of HMF to PTA that avoid reduction steps and utilize Diels-Alder-dehydration reactions similar to those described here.

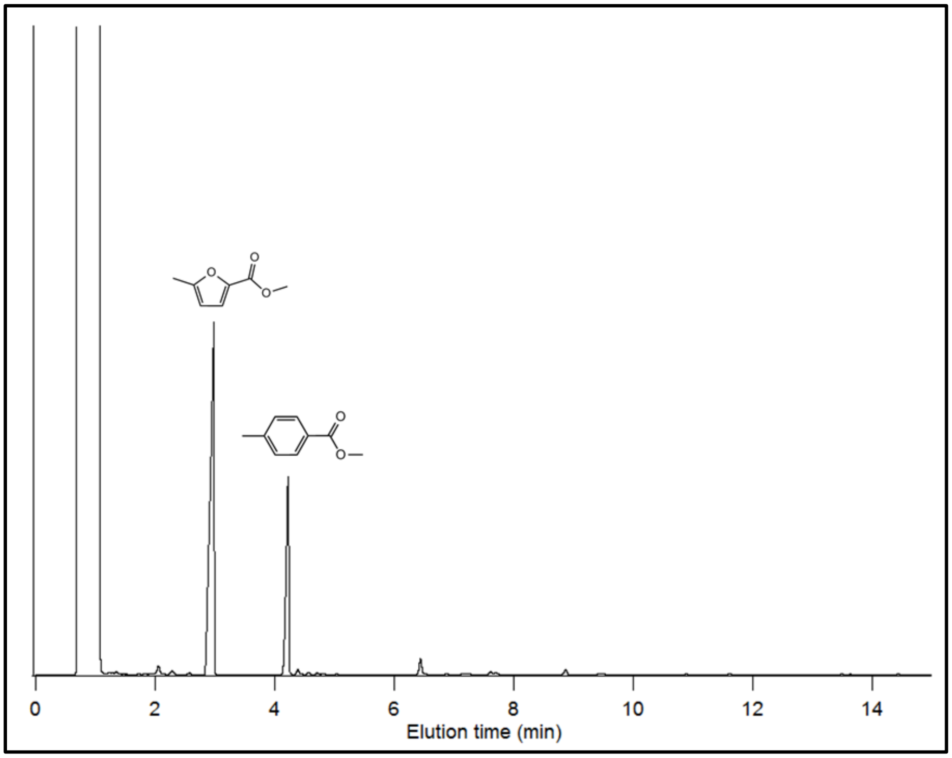

Fig. 5.2 Gas chromatogram of product in Table 5.2, Entry 1.

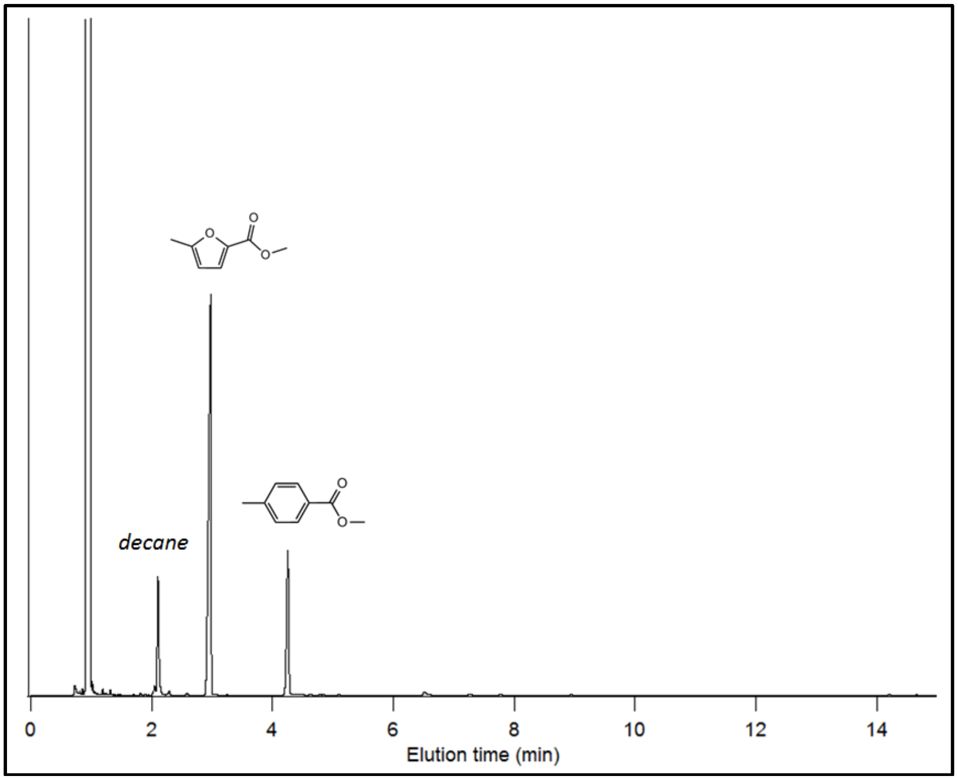

Fig. 5.3 Gas chromatogram of product in Table 5.2, Entry 2.

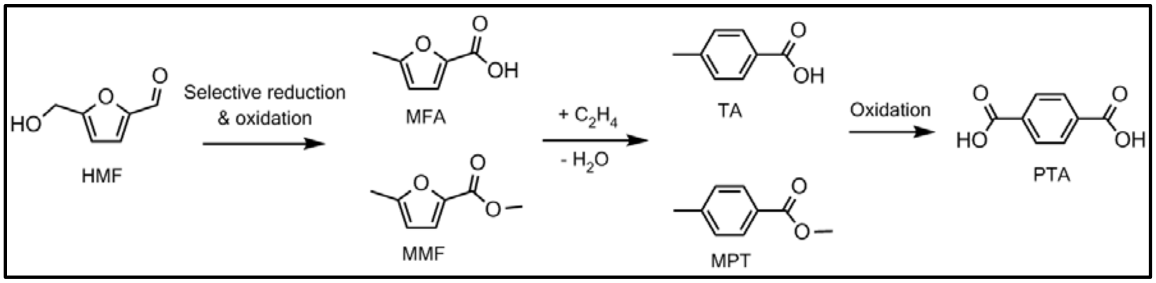

Fig. 5.4 Pathway to PTA from HMF via ethylene Diels-Alder-dehydration of MFA/MMF to TA/MPT.

5.2 Methyl 5-methoxymethyl-furan-2-carboxylate (MMFC) as a diene in the ethylene Diels-Alder-dehydration reaction

The MFA and MMF dienes are unique from the dienes tested in Chapter 4 in that these substrates have one carboxylic acid or carboxylate ester functionality. Based on this observation, a pathway from HMF to PTA was proposed that involved the partial oxidation of HMF to the carboxylic acid, 5-hydroxymethyl-2-furoic acid (HMFA). The HMFA intermediate may then react with ethylene to form the PTA precursor, 4-(hydroxymethyl)benzoic acid (HMBA), that could be further oxidized to PTA (Fig.5.5). Since HMFA can be easily obtained through the air oxidation of HMF,[1] HMFA was a HMF derivative of high interest for the ethylene Diels-Alder-dehydration reaction. Since in the previous section the most selective conversion was achieved when MFA was protected with methanol to form the ester MMF, the methanol protected form of HMFA, methyl 5-methoxymethyl-furan-2-carboxylate (MMFC), was also an attractive substrate for testing. The reaction of MMFC with ethylene would produce methyl 4-(methoxymethyl)benzene carboxylate (MMBC), a precursor to both PTA and dimethylterephthalate (DMT). In this section, the Diels-Alder-dehydration reaction results for the conversion of MMFC to MMBC will be summarized and discussed. The results for using HMFA will be presented in the following section.

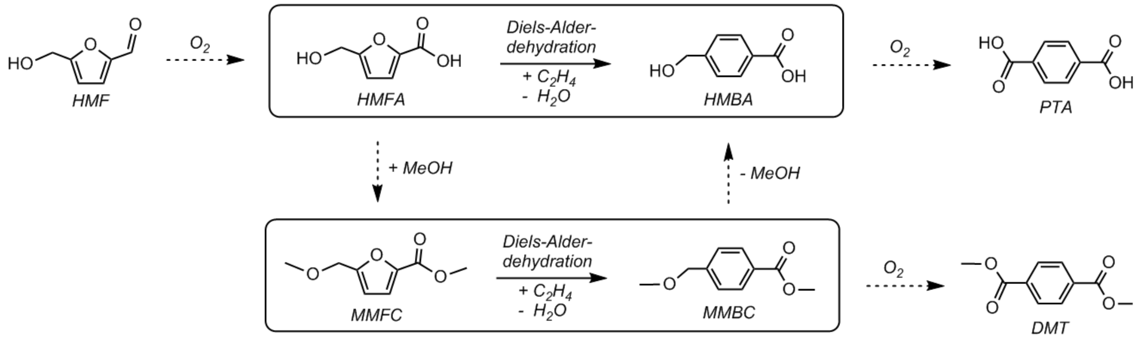

Fig. 5.5 Proposed pathway from HMF to PTA via the Diels-Alder-dehydration of HMFA/MMFC and ethylene.

Several materials were screened for catalytic activity in the conversion of MMFC and ethylene to MMBC (Table 5.3). The MMFC substrate was stable in dioxane solvent at 190^{o}C and stable in the presence of Si-Beta (entries 1 & 2). A series of Lewis acid Beta molecular sieves with different Lewis acid centers in the silica framework were tested (entries 3-7). Out of all five different materials Sn-Beta and Zr-Beta were the only ones active for the Diels-Alder-dehydration reaction, and while both Sn-Beta and Zr-Beta produced MMBC at similar yields (24 and 21 %, respectively) the Zr-Beta was significantly more selective (48 and 81 %, respectively). These results show that the proposed reaction to convert MMFC and ethylene to MMBC is possible, and high selectivity can be achieved using Zr-Beta as catalyst. The Ti-, Ta-, and Nb-containing Beta molecular sieves were essentially inactive. When Sn- and Zr-containing MCM-41 (mesoporous silica), MFI (medium-pore silica molecular sieve), and amorphous silica materials were tested (entries 8-12), little or no MMBC was detected. Recall, Sn-MCM-41 and amorphous Sn-SiO$_2$ were active catalysts for the conversion of MMF and ethylene to TA. This suggests that a possible effect due to the confinement within the microporous environment of the large-pore Beta molecular sieve may be important for the Diels-Alder-dehydration reaction between MMFC and ethylene. The solid Bronsted acid, H-Al-Beta, was screened (entry 13), and after the 6 hour reaction period MMFC was fully converted with only 2 % yield of MMBC, clearly indicating the importance of using a Lewis acidic material to avoid significant side reaction and degradation of the oxygenated substrate under the reaction conditions.

Table 5.3 Reaction results for ethylene Diels-Alder dehydration of MMFC to MMBC. Reaction conditions: 0.1 M MMFC in dioxane, 100 mg catalyst, 190^{o}C, 1000 psig C_2H_4. Conversions and yields determined by ^{1}H NMR.

Entry	Catalyst	Time (hr)	MMFC conversion (%)	MMBC yield (%)	MMBC selectivity (%)
1	None	6	1	0	0
2	Si-Beta	6	2	0	0
3	Sn-Beta	6	50	24	48
4	Zr-Beta	6	26	21	81
5	Ti-Beta	12	2	1	50
6	Ta-Beta	2	9	1	11
7	Nb-Beta	2	n.d.	0	0
8	Sn-MCM-41	6	5	1	20
9	Zr-MCM-41	6	4	0	0
10	Sn-MFI	6	9	0	0
11	Zr-MFI	2	11	0	0
12	Sn-SiO_2 (amorphous)	6	16	2	13
13	H-Al-Beta	6	100	2	2

The feed solution and product solution ^{1}H NMR spectra for the experiments in entries 3-4 of Table 5.3 are given in Fig. 5.6-5.9. The MMFC and

MMBC peaks are clearly shown, along with the large dioxane peak (~3.6 ppm), DMSO peak (~2.5 ppm, NMR solvent residual signal), and tetraethylsilane (TES) peaks (~0.5 and ~0.9 ppm, external standard). Dissolved ethylene was also observed in the ^{1}H NMR spectrum when the analysis was performed soon after reaction. Note also there is a side band feature from the large dioxane peak at ~8.4 ppm that was observed in most of the spectra. The verification of MMBC formation was also made using GC/MS and comparing the mass spectrum of the product to the known standard (Fig 5.1-A in appendix).

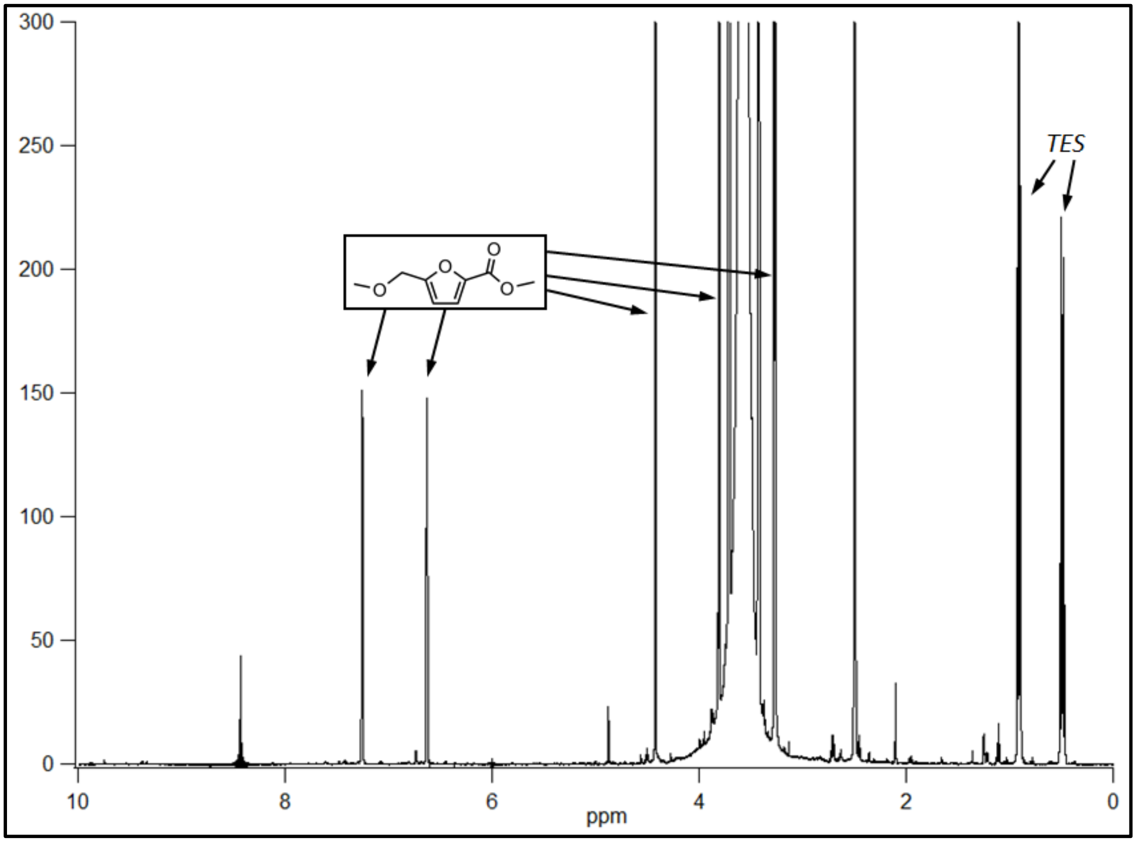

Fig. 5.6 ^{1}H NMR (in DMSO-d_6) of feed solution for experiment in Entry 4, Table 5.3.

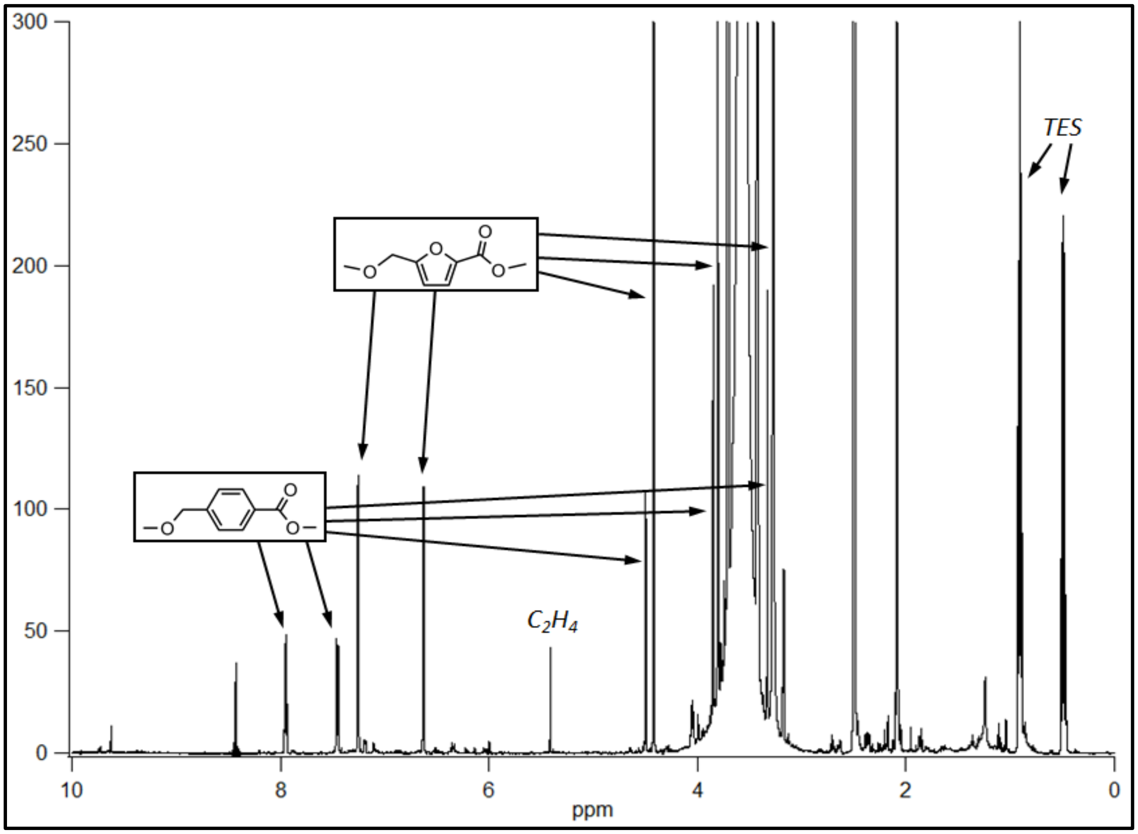

Fig. 5.7 ^{1}H NMR (in DMSO-d_6) of product solution for experiment in Entry 4, Table 5.3.

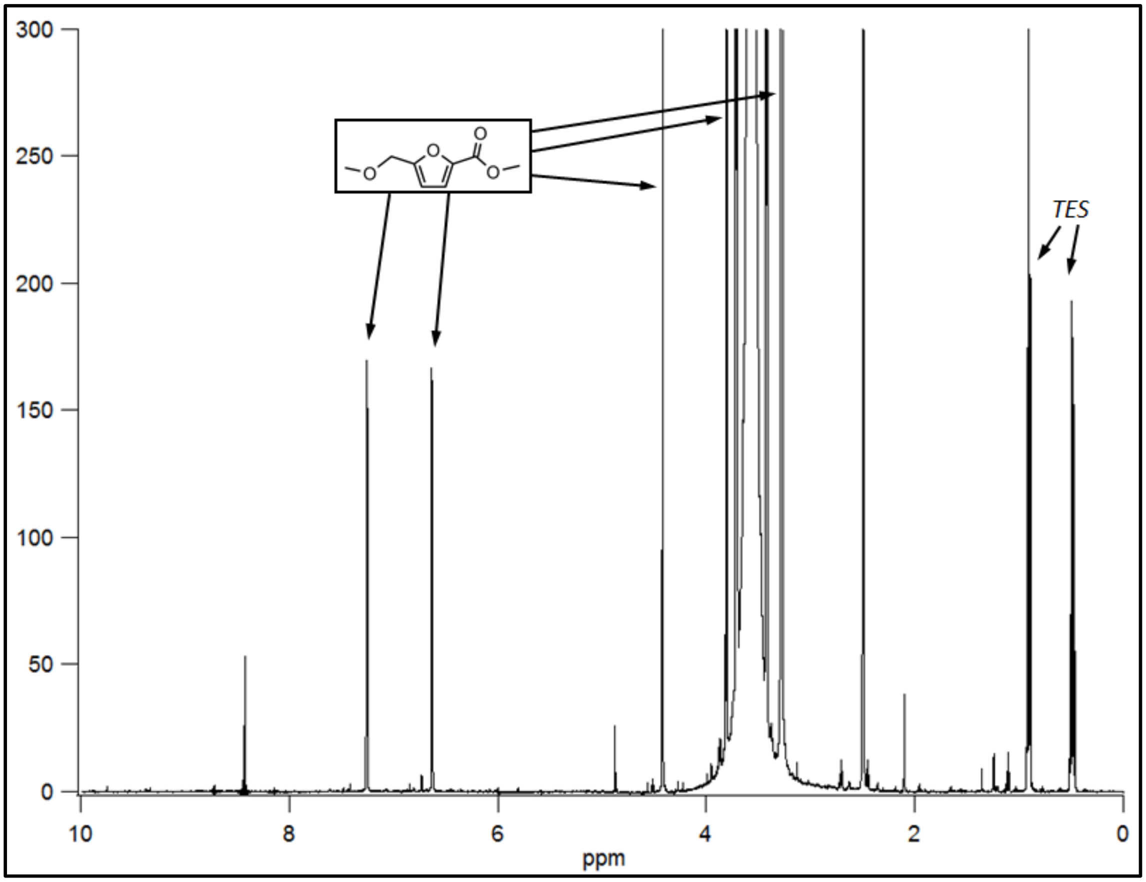

Fig. 5.8 ^{1}H NMR (in DMSO-d_6) of feed solution for experiment in Entry 3, Table 5.3.

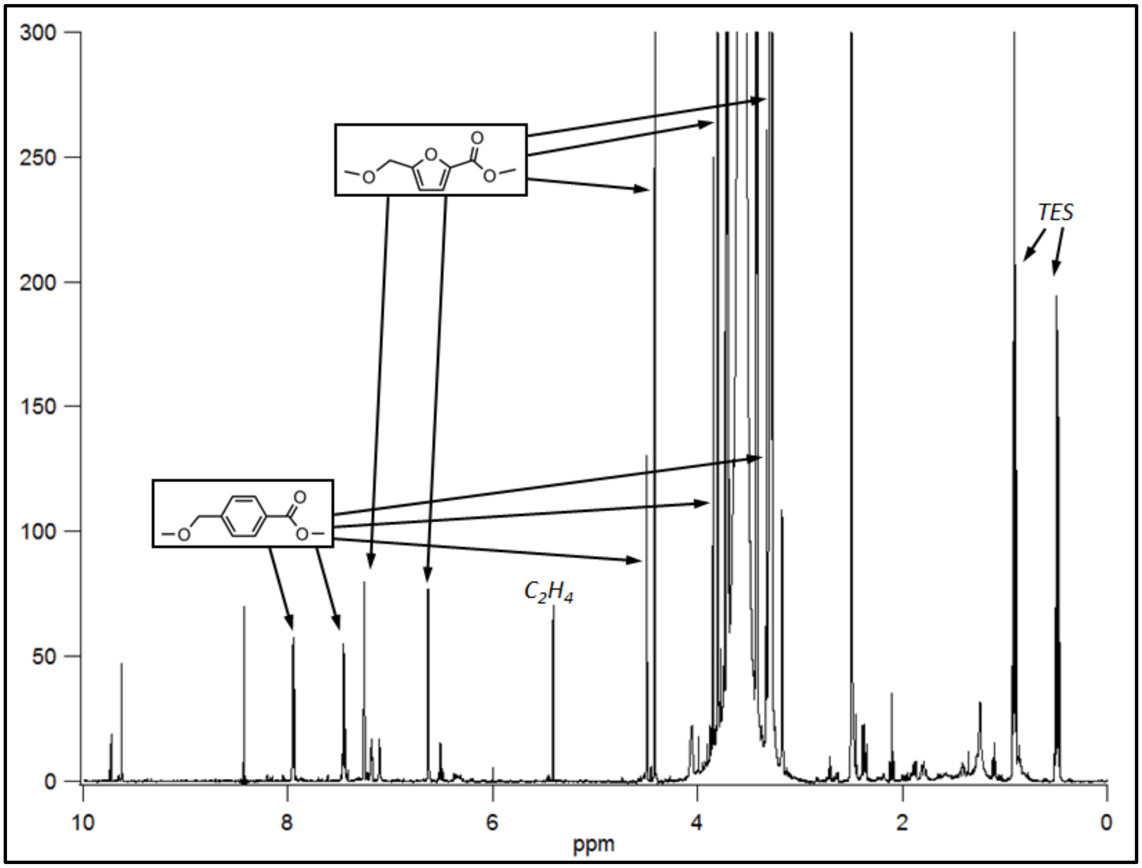

Fig. 5.9 ^{1}H NMR (in DMSO-d_6) of product solution for experiment in Entry 3, Table 5.3.

The product spectra for both the Zr-Beta and Sn-Beta systems look very similar and clearly there are some side products being formed that appear to be the same in both systems. The most significant peaks corresponding to these side products appear in the ^{1}H NMR spectra at 6.51, 7.11, 7.18, 9.62, and 9.73 ppm. The Sn-Beta catalyst produces a higher amount of these side products compared to Zr-Beta. There appears to be aldehyde groups being produced since two of these peaks are in the 9-10 ppm range.

The product solutions from the Sn-Beta and Zr-Beta systems were analyzed by GC/FID to determine the number of side products in addition to

MMBC (Fig. 5.10). The MMFC and MMBC peaks are indicated on the figure and appear at elution times of ~5.1 and ~6.8 minutes, respectively. As expected from the measured selectivities and NMR results, the chromatogram from the Zr-Beta system clearly indicates less side products than the Sn-Beta system.

There are three main side product peaks in the Zr-Beta chromatogram that elute at ~6.6, ~6.9 and ~7.9 minutes in Fig. 5.10. Interestingly, the two products that elute at ~6.6 and ~6.9 minutes in the Zr-Beta system are not only present in the Sn-Beta system as well, but are produced in significantly larger quantities. Chapter 6 provides detailed analysis and discussion of the identification of these main side products.

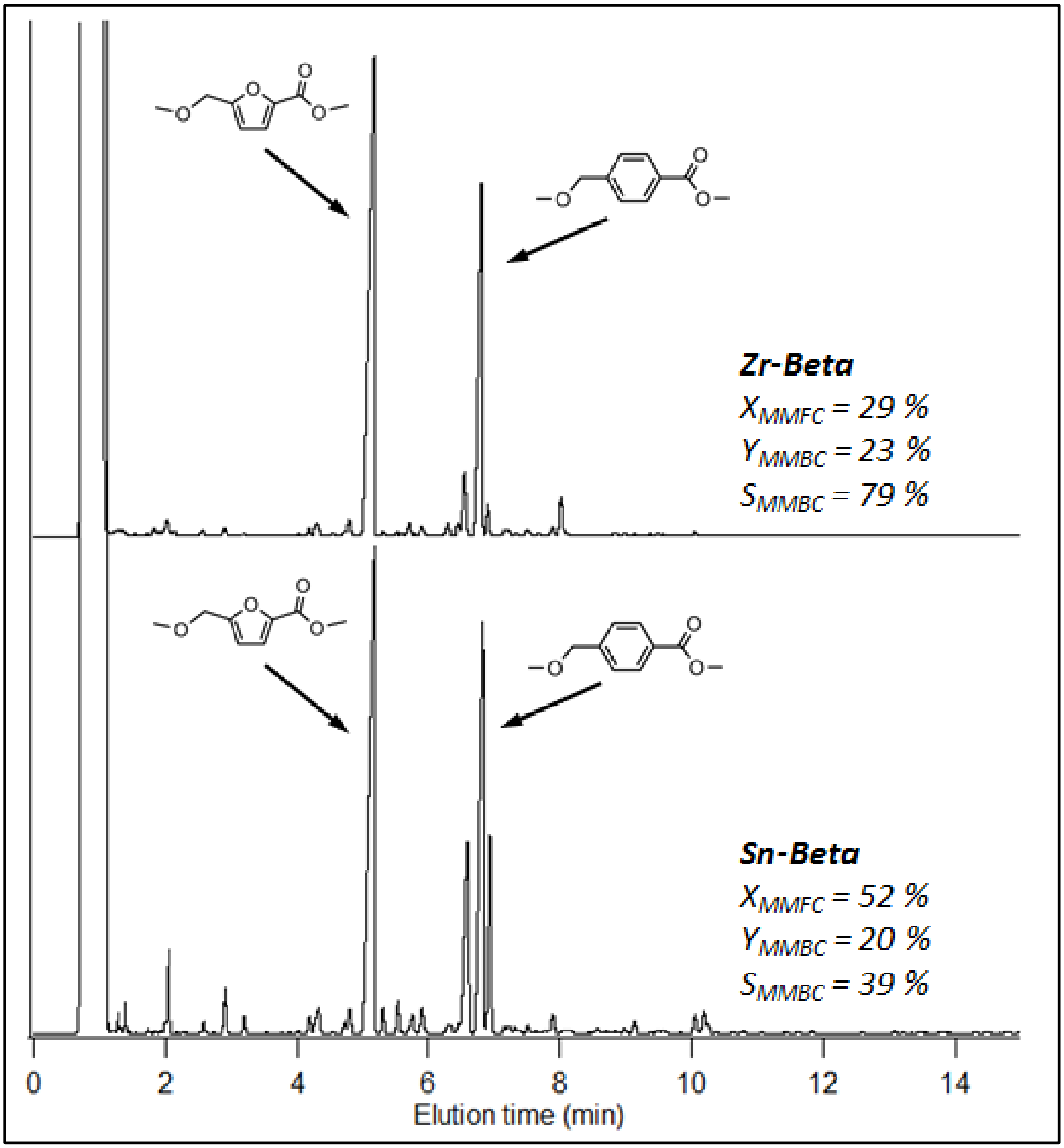

Fig. 5.10 GC-FID chromatograms of product solutions in the Diels-Alder-dehydration reaction of MMFC and ethylene using Zr-Beta and Sn-Beta catalysts. Reaction conditions: 0.1 M MMFC in dioxane, 100 mg catalyst, 190°C, 1000 psig C_2H_4, 6 hrs. Conversions and yields determined by ^{1}H NMR.

The MMFC conversion, MMBC yield, and MMBC selectivity using the Sn-Beta and Zr-Beta catalysts were measured over time (Fig 5.11). The Sn-Beta catalyst produces MMBC at 40-50 % selectivity for the first 6 hours. The yield of MMBC reaches a maximum at ~24 % while the MMFC continues to react to >70% conversion after 12 hours of reaction. The Zr-Beta catalyst is more selective with ~70-80% MMBC selectivities for the entire 12 hour reaction, and appears to remain active after 12 hours.

Further reaction testing was performed by changing various system parameters, such as reaction temperature, solvent, catalyst loading amount, and addition of water (Table 5.4). Comparison of entries 2 and 3 indicate that when using Sn-Beta an increase in temperature from 190^oC to 210^oC results in a decrease in MMBC selectivity as the conversion increases without any improvement in MMBC yield. When an aliphatic solvent (hexane) was added to the dioxane in a 1:1 v/v ratio, the selectivity decreased slightly (entries 2 and 4). The Zr-Beta catalyst loading was increased from the typical 100 mg to 300 mg in entry 6, and after 6 hours of reaction the selectivity dropped significantly from 85% to 63% while the MMBC yield only increased by 3%. Another ether solvent, triglyme, was tested in entry 7 and very similar performance as dioxane was observed, that is high selectivity and ~30% yield.

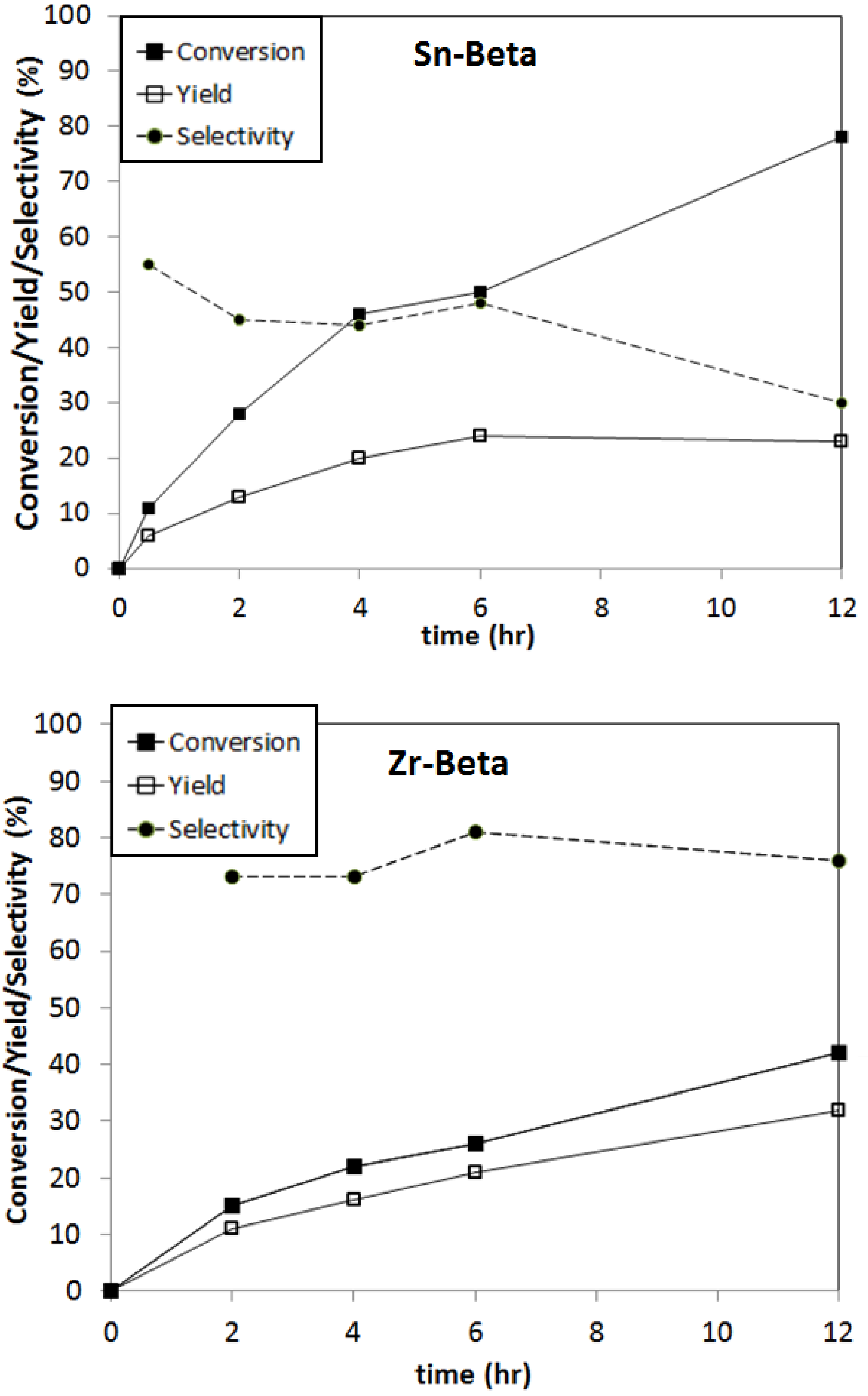

Fig. 5.11 Reaction profiles for the Diels-Alder-dehydration reaction of MMFC and ethylene using Zr-Beta (bottom) and Sn-Beta (top). Reaction conditions: 0.1 M MMFC in dioxane, 100 mg catalyst, 190°C, 1000 psig C_2H_4. Results determined by ^{1}H NMR.

Table 5.4 Additional reaction results for ethylene Diels-Alder dehydration of MMFC to MMBC. Reaction conditions: 0.1 M MMFC in solvent, 100 mg catalyst, 1000 psig C_2H_4. Results determined by ^{1}H NMR. *300 mg catalyst used.

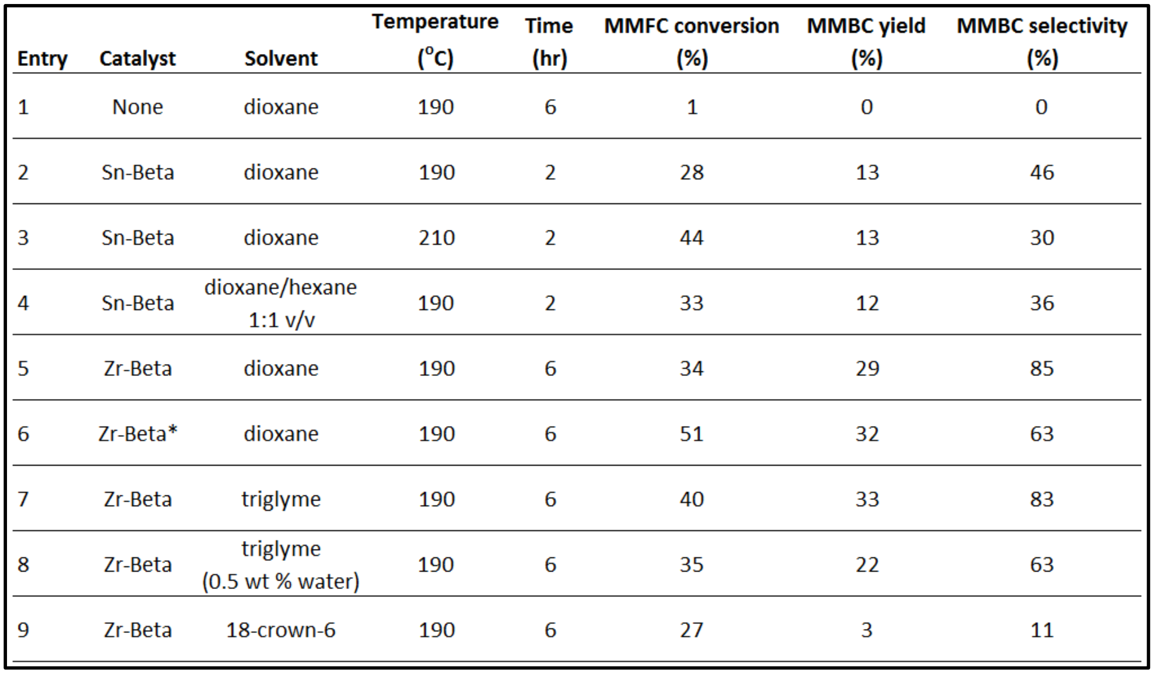

Entry	Catalyst	Solvent	Temperature (°C)	Time (hr)	MMFC conversion (%)	MMBC yield (%)	MMBC selectivity (%)
1	None	dioxane	190	6	1	0	0
2	Sn-Beta	dioxane	190	2	28	13	46
3	Sn-Beta	dioxane	210	2	44	13	30
4	Sn-Beta	dioxane/hexane 1:1 v/v	190	2	33	12	36
5	Zr-Beta	dioxane	190	6	34	29	85
6	Zr-Beta*	dioxane	190	6	51	32	63
7	Zr-Beta	triglyme	190	6	40	33	83
8	Zr-Beta	triglyme (0.5 wt % water)	190	6	35	22	63
9	Zr-Beta	18-crown-6	190	6	27	3	11

To probe the effect of the water being produced by the Diels-Alder-dehydration reaction, a small amount of water was added to the reaction in entry 8. Both the yield and selectivity drop significantly with just a small addition of water (0.5 wt % water added to triglyme). Since there was a small amount of water present in the dioxane and triglyme solvents used for these reactions, this result suggests that if the initial water were removed then selectivities closer to 100% and higher yields may be achieved. Since these experiments were not carried out in a dry glove box, controlling the exact amount of water, and removing the small amount of water from the feed solutions, while loading the Parr batch reactor was difficult.

An experiment using a large crown ether, 18-crown-6, as solvent was also performed (entry 9) and very low yields/selectivities were observed. This result may be explained by the large amount of water introduced into the system from using the very hydrophilic 18-crown-6.

Another example of the ^{1}H NMR spectra collected for a Zr-Beta catalyzed reaction between MMFC and ethylene is given in Fig. 5.12-5.13, correspond to the experiment reported in entry 5 of Table 5.4. The MMBC yield and selectivity was measured to be 29% and 85%, respectively, when using the TES external standard method. When the quantification was made using the dioxane solvent peak as an internal standard reference (method described in Chapter 2), a MMBC yield and selectivity of 30% and 93%, respectively, was measured. These results were some of the best obtained using any catalyst and reaction condition. The Zr-Beta sample (JP 4-89) used to generate the data in Table 5.4 showed higher activity and selectivity (in dioxane or triglyme) than other Zr-Beta samples prepared using the same or similar synthesis procedures. In an effort to understand how this sample was unique, further investigation was carried out to help elucidate what synthesis parameters are most important for making Zr-Beta catalysts with higher activities and selectivities.

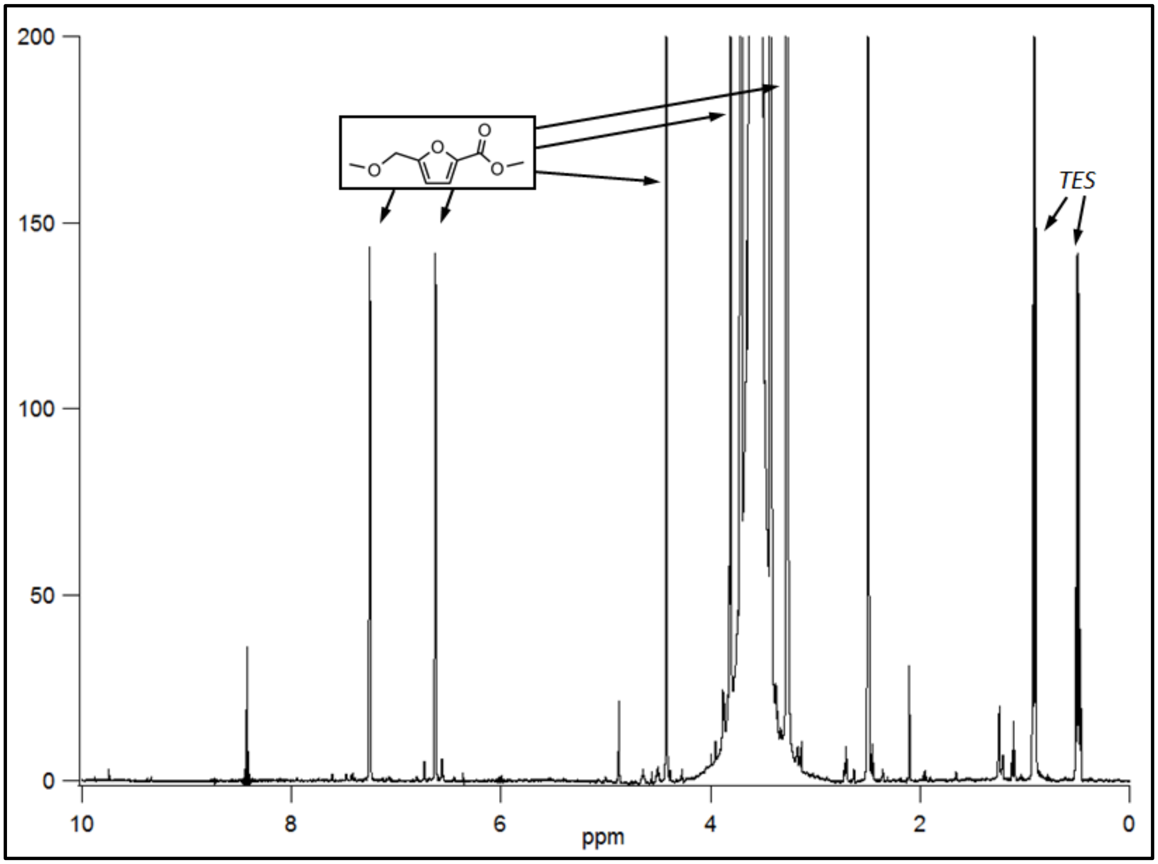

Fig. 5.12 ^{1}H NMR (in DMSO-d_6) of feed solution for experiment in Entry 5, Table 5.4.

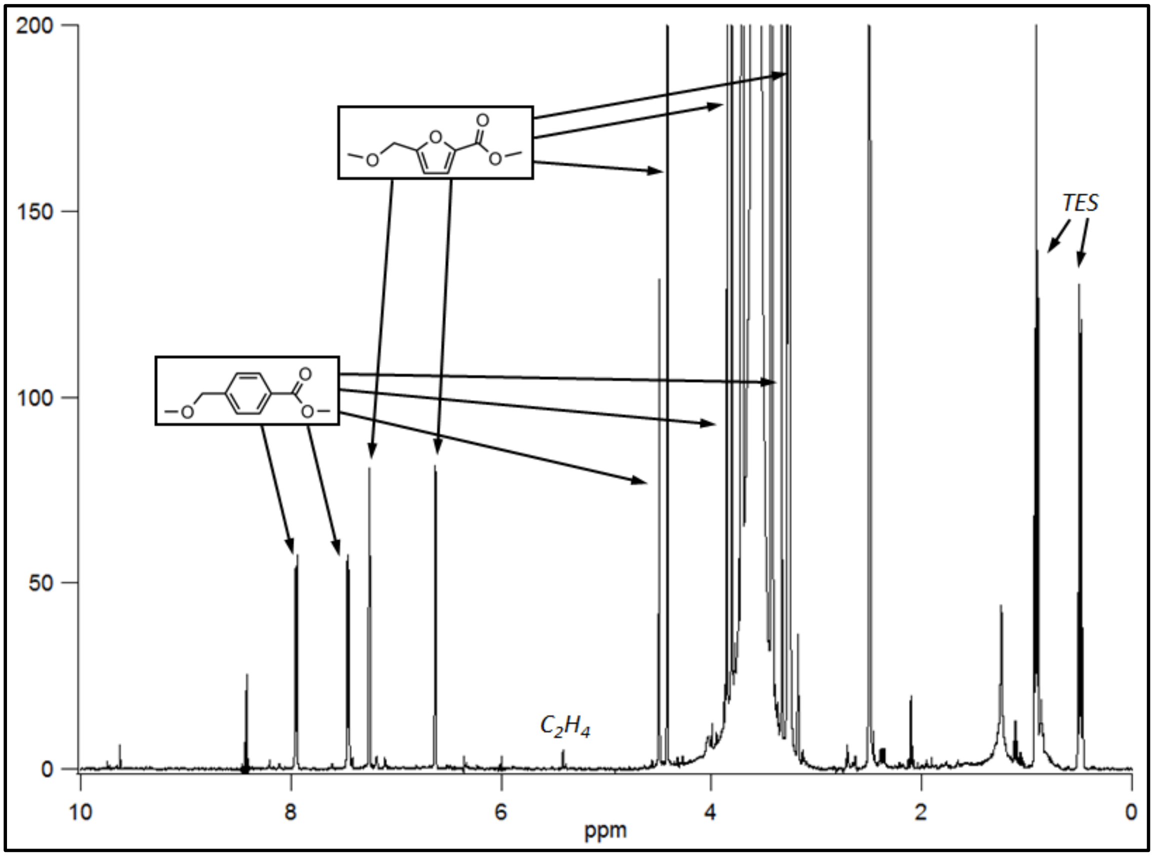

Fig. 5.13 ^{1}H NMR (in DMSO-d_6) of product solution for experiment in Entry 5, Table 5.4.

Reaction results using seven different Zr-Beta catalyst samples are summarized (entries 1-7, Table 5.5). Synthesis details of the samples are listed, including Zr source, gel stir time before addition of Zr source, gel Si/Zr ratio, and final Si/Zr ratio of the catalysts. Two different Zr sources were used – zirconyl chloride ($ZrOCl_2$) and Zr(IV) propoxide. The gel stir time is the time allowed for TEOS hydrolysis in the aqueous TEAOH solution before the addition of the zirconium source (see Chapter 2). “Short” stir times of 37-56 minutes (entries 1-3) are compared to “long” stir times of 94-123 minutes (entries 4-7). The Si/Zr ratio in the synthesis gel was varied between 63 and 400, resulting in final catalyst Si/Zr ratios between 92 and 492. Also included for comparison, is a result using ZrO_2 as catalyst (entry 8).

The result using the JP 4-89 sample with high activity and selectivity is given in entry 1. The Zr source for this catalyst was $ZrOCl_2$ with a high loading of Zr in the gel (Si/Zr = 63). Also, a “short” stir time of 56 minutes was used. After 6 hours of reaction under the typical conditions, the MMBC yield and selectivity was 30% and 93.2%, respectively. When a Zr-Beta sample prepared using the same synthesis method (entry 2) was prepared, only 13.6 % MMBC yield was made at 75.2 % selectivity. The sample in entry 3 was another attempt to replicate entry 1 while using a shorter stir time (37 min), but this catalyst produced another poor reaction result. The exact synthesis and reaction performance observed for the JP 4-89 sample was unable to be reproduced.

Table 5.5 Reaction results for Zr-Beta catalyzed synthesis of MMBC by Diels-Alder-dehydration reaction.

Reaction conditions: 0.1 M MMFC in dioxane, 190°C, 6 hours, 1000 psig C_2H_4. Conversions and yields determined by ^{1}H NMR.

Entry	Catalyst	Zr source in catal. synth.	Gel stir time before addition of Zr source (min)	Gel Si:Zr	Catalyst Si:Zr †	MMFC:Zr molar ratio	MMFC conversion (%)	MMBC yield (%)	MMBC selectivity (%)
1	Zr-Beta-1	$ZrOCl_2$	56	63	116	70	32.2	30.0	93.2
2	Zr-Beta-2	$ZrOCl_2$	56	63	130	78	18.1	13.6	75.2
3	Zr-Beta-3	$ZrOCl_2$	37	63	137	82	13.0	9.5	73.1
4	Zr-Beta-4	$ZrOCl_2$	98	63	123	74	25.4	21.8	86.0
5	Zr-Beta-5	Zr(IV) propoxide	108	63	92	55	29.1	22.7	78.2
6	Zr-Beta-6	Zr(IV) propoxide	123	125	155	58	33.2	25.4	76.6
7	Zr-Beta-7	Zr(IV) propoxide	94	400	492	74	42.5	26.4	62.2
8*	ZrO_2	-	-	-	-	-	-2.0	0	0

* 12 mg ZrO_2 used in reaction; Reaction time: 2 hours.

† Entries 1-4 determined by energy-dispersive x-ray spectroscopy (EDS). Entries 5-7 by Galbraith Laboratories (GLI procedure ME-70).

From the visual appearance of the synthesis gel for the catalysts in entries 2 and 3 it was apparent that at the time the Zr source was added to the gel (after the stir times listed), the gel was not completely homogeneous. That is, the organic TEOS was not hydrolyzed enough to dissolve into the aqueous TEAOH phase to form one homogeneous gel phase. Also, after the addition of the $ZrOCl_2$, white precipitate formed in the gel that was presumably ZrO_2 via TEAOH-catalyzed hydrolysis/condensation of $ZrOCl_2$. The formation of ZrO_2 at this point in the synthesis may result in less incorporation of the Zr into the zeolite framework of the final catalyst and fewer active sites. The time required for the TEOS to fully dissolve in the aqueous TEAOH solution varies and was noticed to depend on the stirring speed setting on the magnetic stir plate (e.g., faster stirring leads to shorter times to reach a homogeneous phase). It is still unclear as to why the JP 4-89 synthesis in entry 1 was not reproduced in entry 2 or 3, but the variable time required for the TEOS to form a single phase with the aqueous TEAOH phase may be an important factor.

Based on this assumption, additional Zr-Beta samples were prepared using “long” stir times (94-123 min) that allowed for a homogeneous phase to form prior to addition of the Zr source (entries 4-7). With the longer stir times the formation of white precipitates upon addition of the Zr source was significantly reduced, and the resulting Zr-Beta materials were more active catalysts with 21.8-26.4% MMBC yields after 6 hours of reaction. One explanation for this result is by allowing more time for the dissolution of the silica source (TEOS) into the aqueous TEAOH phase before introducing Zr into the gel, the Zr source is less likely to condense with itself to form ZrO_2 and more likely to incorporate into the silica networks being formed from the TEOS condensation reactions, and this may ultimately lead to more efficient Zr incorporation into the molecular sieve framework to generate more catalytically active Lewis acid centers.

The Zr source was also varied by using Zr(IV) propoxide and comparison of entries 4 and 5 show that while the MMBC yields are similar between Zr-Beta catalysts made using the different Zr sources (21.8 % vs. 22.7 %), the selectivity is higher for the catalyst made using the $ZrOCl_2$ (86.0 % vs. 78.2 %).

The Si/Zr ratio of the synthesis gel was increased in entries 6 and 7 to produce Zr-Beta with fewer Zr. The Diels-Alder-dehydration reactions were performed by keeping the number of Zr metal atoms (and therefore, the MMFC:Zr ratio) in the reactor relatively constant by using more catalyst (160 mg used in entry 6 and 400 mg used in entry 7). The MMBC yields for entries 5-7 are very similar and ranged between 22.7 %-26.4 %, while the selectivity dropped from 78.2 % to 62.2 % as the Si/Zr ratio in the catalyst was increased from 92 to 492. An explanation for the drop in selectivity with the higher Si/Zr ratio materials may be that as more catalyst was added to keep the number of Zr metal atoms in the system nearly constant, additional water was also introduced into the reactor (there is water adsorbed on the hydrophilic crystal surfaces). As was observed before, addition of water into the system can have a negative effect on MMBC selectivity.

To probe whether the selectivity was being affected by extraframework ZrO_2 on the Zr-Beta catalysts, a two hour reaction was performed using zirconia as catalyst (entry 8). No conversion or MMBC yield was observed. This result does not negate the notion that extraframework ZrO_2 nanoparticles within the molecular sieve pores are contributing to additional conversion of the MMFC to undesired side products, but indicates that bulk ZrO_2 particles are inactive in catalyzing side reactions of MMFC.

This investigation indicates that catalytic performance of Zr-Beta in the ethylene Diels-Alder-dehydration reaction to convert MMFC to MMBC depends significantly on how the catalyst is synthesized. The data suggest that higher MMBC selectivities may be achieved by using $ZrOCl_2$ as the Zr source (rather than Zr(IV) propoxide) and by allowing longer stir times of the TEOS/TEAOH/water mixture before addition of the Zr. Future research directions should be focused on Zr-Beta catalyst synthesis and characterization, and understanding the important characteristics of these materials for achieving high activity and selectivity towards MMBC.

Since a commercially viable process for the conversion of MMFC to MMBC in the liquid phase will likely require higher reaction concentrations than the 2 wt % MMFC concentration used here, an experiment using 10 wt % MMFC was performed to explore the feasibility of using higher MMFC concentrations (Table 5.6). A low loading of Zr-Beta (26 mg) was used since higher conversions were expected with the higher reactant concentrations. After the typical 6 hour reaction, only 4.8 % MMBC yield was produced with a selectivity of 16.4 %. No significant side products were detected by GC/FID (Fig 5.2-A), but the product solution and catalyst turned black. The MMFC had apparently polymerized/converted to insoluble products and had significantly coked/deposited onto the catalyst. This result indicates that the development of methods, reaction conditions, or catalysts that allow for higher MMFC concentrations while maintaining high MMBC selectivity is important for allowing this process to become more commercially viable.

Table 5.6 Ethylene Diels-Alder-dehydration of MMFC to MMBC using high MMFC concentrations. Reaction conditions: 10 wt % MMFC in dioxane, 190^oC, 6 hr, 1000 psig C_2H_4. Results determined by ^1H NMR.

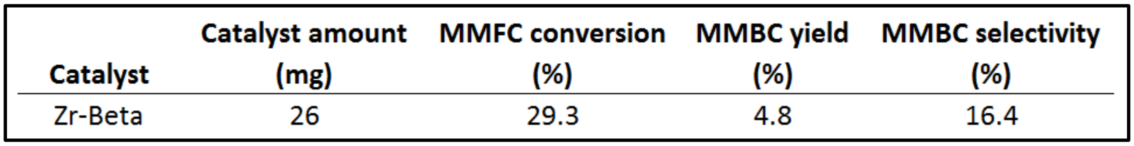

Catalyst	Catalyst amount (mg)	MMFC conversion (%)	MMBC yield (%)	MMBC selectivity (%)
Zr-Beta	26	29.3	4.8	16.4

To probe whether the MMBC product is participating in secondary reactions as it is being produced in the Diels-Alder-dehydration reaction between ethylene and MMFC, an experiment was performed using a feed solution containing only MMBC dissolved in dioxane. The reactor was charged with a 2 wt% MMBC solution and 100 mg of Zr-Beta, and a 2 hour reaction was performed under the typical reaction conditions (190^oC, 1000 psig C_2H_4). No measurable conversion of the MMBC was determined by ^1H NMR, suggesting that the MMBC is likely not participating in secondary reactions that would lead to lower selectivities. It is important to note that the Zr-Beta sample used for this experiment was one that was previously found to produce MMBC at lower selectivities (i.e., entry 2, Table 5.5), further suggesting that the MMBC product is not reacting over even the less selective Zr-Beta catalysts and that the loss in selectivity in those reactions are instead due to reactions of the MMFC reactant.

5.3 5-Hydroxymethyl-2-furoic acid (HMFA) as a diene in the ethylene Diels-Alder-dehydration reaction

The use of HMFA as a diene in the ethylene Diels-Alder-dehydration reaction to produce HMBA as a product was investigated (Fig. 5.14) and the reaction testing results will be summarized and discussed here. Reaction conditions that allowed for high selectivities to HMBA were significantly more challenging to find than in the MMFC/MMBC system, and this was clearly due to the higher reactivities of the alcohol and carboxylic acid functionalities.

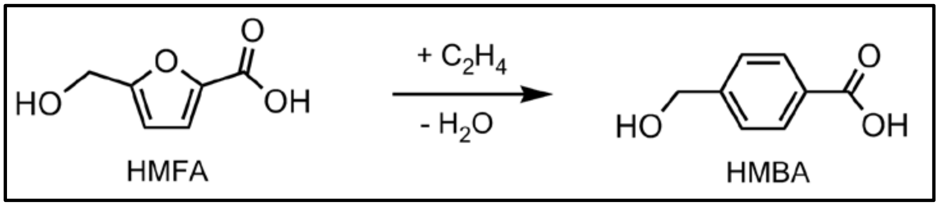

Fig. 5.14 Synthesis of HMBA by Diels-Alder-dehydration reaction of HMFA and ethylene.

Reaction screening results are shown in Table 5.7 for the conversion of HMFA to HMBA using different Lewis acid molecular sieve catalysts and two different HMFA suppliers - Matrix Scientific and Enamine. The Sn-Beta produces the highest yields of HMBA (19 %) at 31 % selectivity when using HMFA supplied by Matrix. The Zr-Beta, Ta-Beta, and Nb-Beta were also found to be active for catalyzing the formation of HMBA, but with less yield and selectivity.

The reactivity was found to also depend on the chosen HMFA supplier. The HMFA from Matrix was found to react more selectivity over Sn-Beta than the HMFA from Enamine. A similar result was found when using the Zr-Beta catalyst, although the effect was less significant. Interestingly, when the control experiments were performed without the addition of catalyst, the Matrix HMFA converted significantly (17 %) over the six hour reaction period while no conversion was measured with the Enamine HMFA. Clearly, there are unknown impurities in the supplied HMFA that are contributing to the observed reactivity.

Table 5.7 Results for ethylene Diels-Alder-dehydration of HMFA to HMBA using Lewis acid molecular sieve catalysts. Reaction conditions: 0.1 M HMFA in dioxane, 190^{o}C, 6 hr, 1000 psig C_2H_4, 100 mg catalyst. Results determined by ^{1}H NMR.

Entry	Catalyst	HMFA supplier	HMFA conversion (%)	HMBA yield (%)	HMBA selectivity (%)
1	Sn-Beta	Matrix Scientific	61	19	31
2	Zr-Beta	Matrix Scientific	87	9	10
3	Sn-Beta	Enamine	70	12	17
4	Zr-Beta	Enamine	92	6	7
5	Ta-Beta	Enamine	61	6	10
6	Nb-Beta	Enamine	75	3	4
7	None	Matrix Scientific	17	0	0
8	None	Enamine	-1	0	0

An example ^{1}H NMR spectrum of a reaction product solution containing the HMFA diene and HMBA product is shown in Fig. 5.15, along with a spectrum of the same solution spiked with HMBA standard to clearly show which peaks correspond to the HMBA product.

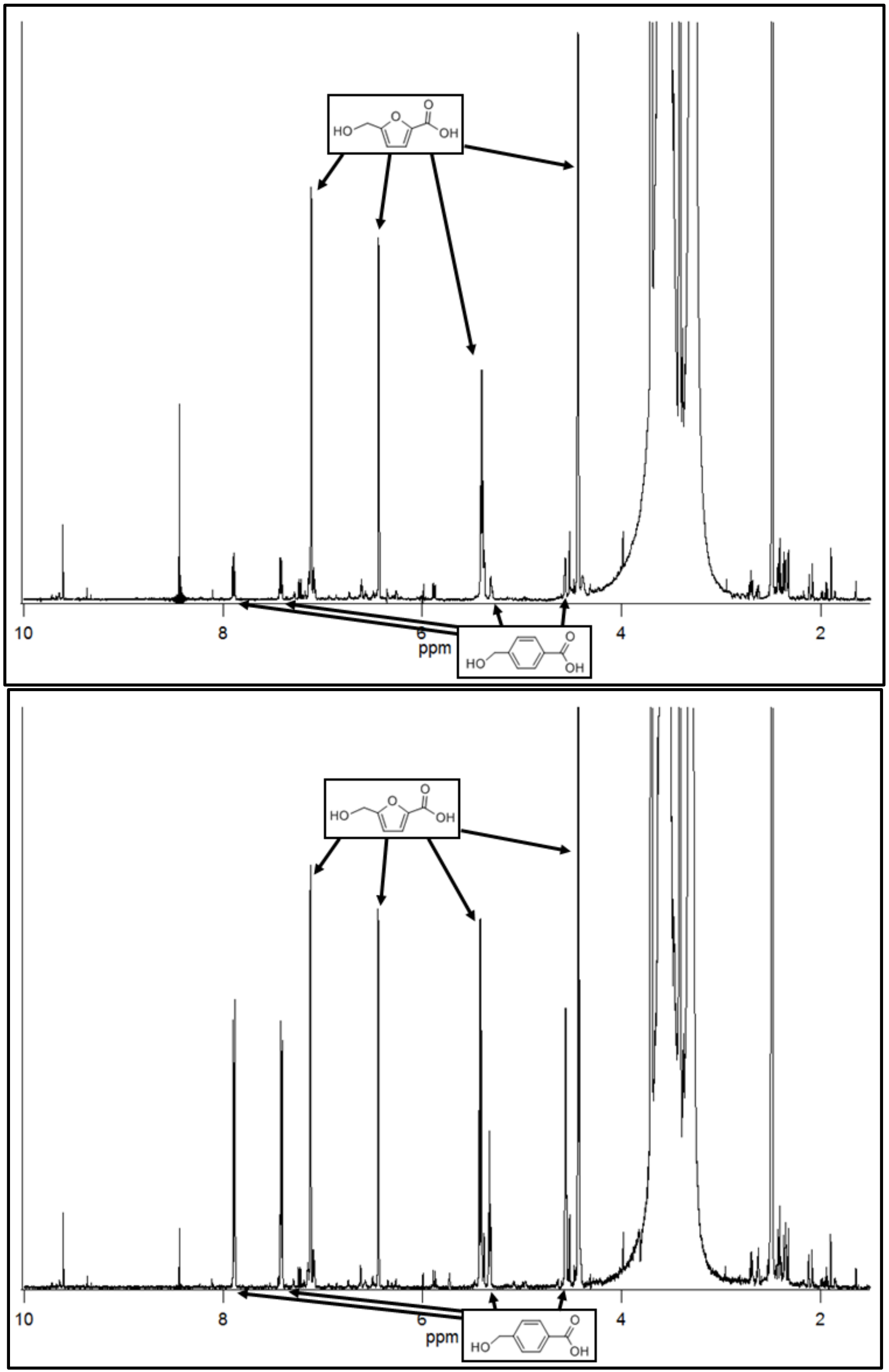

Fig. 5.15 ^{1}H NMR (in DMSO-d_6) of a product solution for the Diels-Alder-dehydration of HMFA and ethylene to form HMBA (top), and the same solution spiked with the HMBA standard (bottom).

Table 5.8 Results for control experiments for ethylene Diels-Alder-dehydration of HMFA. Reaction conditions: 1000 psig C_2H_4, 190°C, 0.1 M HMFA in dioxane, 100 mg catalyst. Results determined by ^{1}H NMR.

Entry	Catalyst	HMFA supplier	Other exp. conditions	Time (hr)	HMFA conversion (%)	HMBA yield (%)	HMBA selectivity (%)
1	None	Matrix Sci.		2	5	0	0
2	None	Matrix Sci.		6	17	0	0
3	None	Matrix Sci.	glass liner in reactor	6	15	0	0
4	None	Matrix Sci.	100 mg $MgSO_4$	2	5	0	0
5	None	Matrix Sci.	100 mg $MgSO_4$	6	12	0	0
6	None	Matrix Sci.	200 mg $MgSO_4$	6	12	0	0
7	None	Enamine		6	-1	0	0
8	Si-Beta	Matrix Sci.		2	20	0	0
9	Si-Beta	Matrix Sci.		6	56	0	0
10	Si-Beta	Enamine		6	14	0	0

Several control experiments were performed to help provide understanding for the reason for the low HMBA selectivities and high conversion of HMFA in the absence of any catalyst (Table 5.8). To test whether side reactions resulting from contact with the steel walls of the Parr reactor were the reason for the high HMFA conversion s in the absence of any catalyst (entries 1 & 2), a glass liner for the Parr reactor was used (entry 3) but the conversion still remained significant. A desiccant, magnesium sulfate, was tested (entries 4-6) to determine if by removing water from solution the HMFA conversion could be slowed, but only a small decrease in HMFA conversion compared to that in entries 1-2 was measured after six hours at reaction conditions. Entry 7 shows that HMFA conversion in the no catalyst control experiment can be avoided by using the Enamine-supplied HMFA. Other control experiments in which Si-Beta was tested (entries 8-10) showed that the pure silica material contributes to

HMFA conversion. Over half of the Matrix HMFA reacted and 14 % of the Enamine HMFA reacted after six hours in the presence of Si-Beta.

These findings suggest that future research directions should focus on understanding the impurities, and the side reactions that these impurities cause, in the HMFA supply. Additionally, the development of methods, reaction conditions, and catalyst modifications that reduce the side reactions and deposition of HMFA onto the silica catalyst surface will be crucial for improving the selectivity to the desired HMBA product.

5.4 5-Methoxymethyl-2-furoic acid (MMFA) and methyl 5-hydroxymethyl furan-2-carboxylate (HMFC) as dienes in the ethylene Diels-Alder-dehydration reaction.

Clearly, the selectivity to the 1,4-substituted aromatic product can be improved substantially by adding methanol to the alcohol and carboxylic acid functions of HMFA before performing the ethylene Diels-Alder-dehydration reaction with the Lewis acid molecular sieve catalyst. This section summarizes experiments that were performed using the dienes shown in Fig. 5.16 that have either the ether *or* the ester function. These dienes are 5-methoxymethyl-2-furoic acid (MMFA) and methyl 5-hydroxymethyl furan-2-carboxylate (HMFC), and the products are 4-methoxymethyl benzoic acid (MMBA) and methyl 4-hydroxymethyl benzene carboxylate (HMBC), respectively.

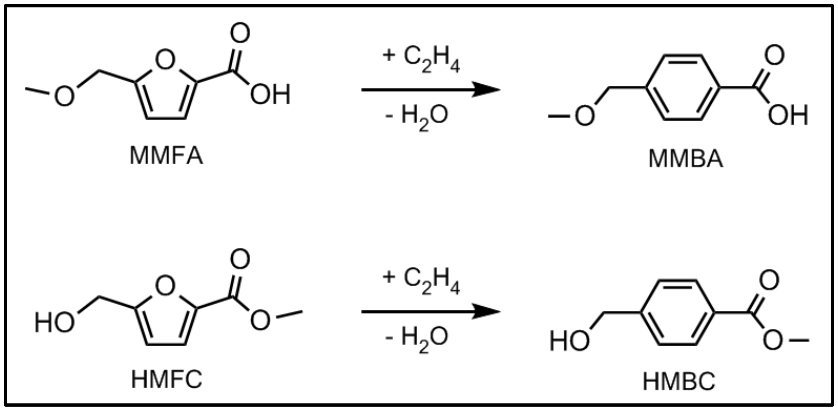

Fig. 5.16 Synthesis of HMBA by Diels-Alder-dehydration reaction of HMFA and ethylene.

Table 5.9 shows reaction results obtained using Sn-Beta as catalyst and compares the reactivity of the four HMFA-derived dienes – HMFA, MMFC, MMFA, and HMFC. Entries 1 and 2 show that the selectivity for the conversion of MMFA to the MMBA product is low (17 %) after two and six hours of reaction, and entry 3 shows that a higher selectivity (42%) is achieved when using the HMFC diene. The yields of the MMBA and HMBC are lower than the yields reported earlier for the conversions of both HMFA to HMBA (entry 4) and MMFC to MMBC (entry 5). It is clear that the highest yields and selectivities are achieved by protecting both the alcohol and acid functions of HMFA (i.e., MMFC).

Table 5.9 Results for ethylene Diels-Alder-dehydration reactions using MMFA, HMFC, HMFA, and MMFC with Sn-Beta. Reaction conditions: 1000 psig C_2H_4, 190^{o}C, 0.1 M diene in dioxane, 100 mg Sn-Beta. Results determined by ^{1}H NMR.

Entry	Diene	Time (hr)	Conversion (%)	Yield (%)	Selectivity (%)
1	MMFA	2	36	6	17
2	MMFA	6	52	9	17
3	HMFC	6	12	5	42
4	HMFA	6	61	19	31
5	MMFC	6	50	24	48

5.5 References

[1] Casanova, O.; Iborra, S.; Corma, A.; *ChemSusChem* **2009** *2*(12), 1138 – 1144.

CHAPTER 6

IDENTIFICATION OF SIDE PRODUCTS IN THE PRODUCTION OF METHYL 4-(METHOXYMETHYL) BENZENE CARBOXYLATE (MMBC) FROM METHYL 5-(METHOXYMETHYL)-FURAN-2-CARBOXYLATE (MMFC) AND ETHYLENE

6.1 Identification of side products in the synthesis of MMBC

As shown in the previous chapter, MMBC can be produced with high selectivity (70-80+ %) from MMFC under high ethylene pressures using Zr-Beta. This chapter summarizes the main side products that have been identified in the reaction system. These findings may help in future investigations for improving catalyst selectivity or for discovering more selective (and active) catalytic materials for the ethylene Diels-Alder-dehydration reaction of HMFA-derived dienes. The methods used to elucidate these side products include GC/FID, GC/MS, prep-thin layer chromatography (prep-TLC), and ^{1}H NMR.

GC/FID was used to analyze the reaction product mixtures to determine the number of side products being produced in the MMFC/MMBC system using the Zr-Beta and Sn-Beta catalysts. Typical chromatograms of product solutions, along with the reaction results (conversion, yield, selectivity), are shown in Fig. 6.1. A chromatogram from an Al-Beta (Bronsted acid zeolite) catalyzed reaction is included for comparison.

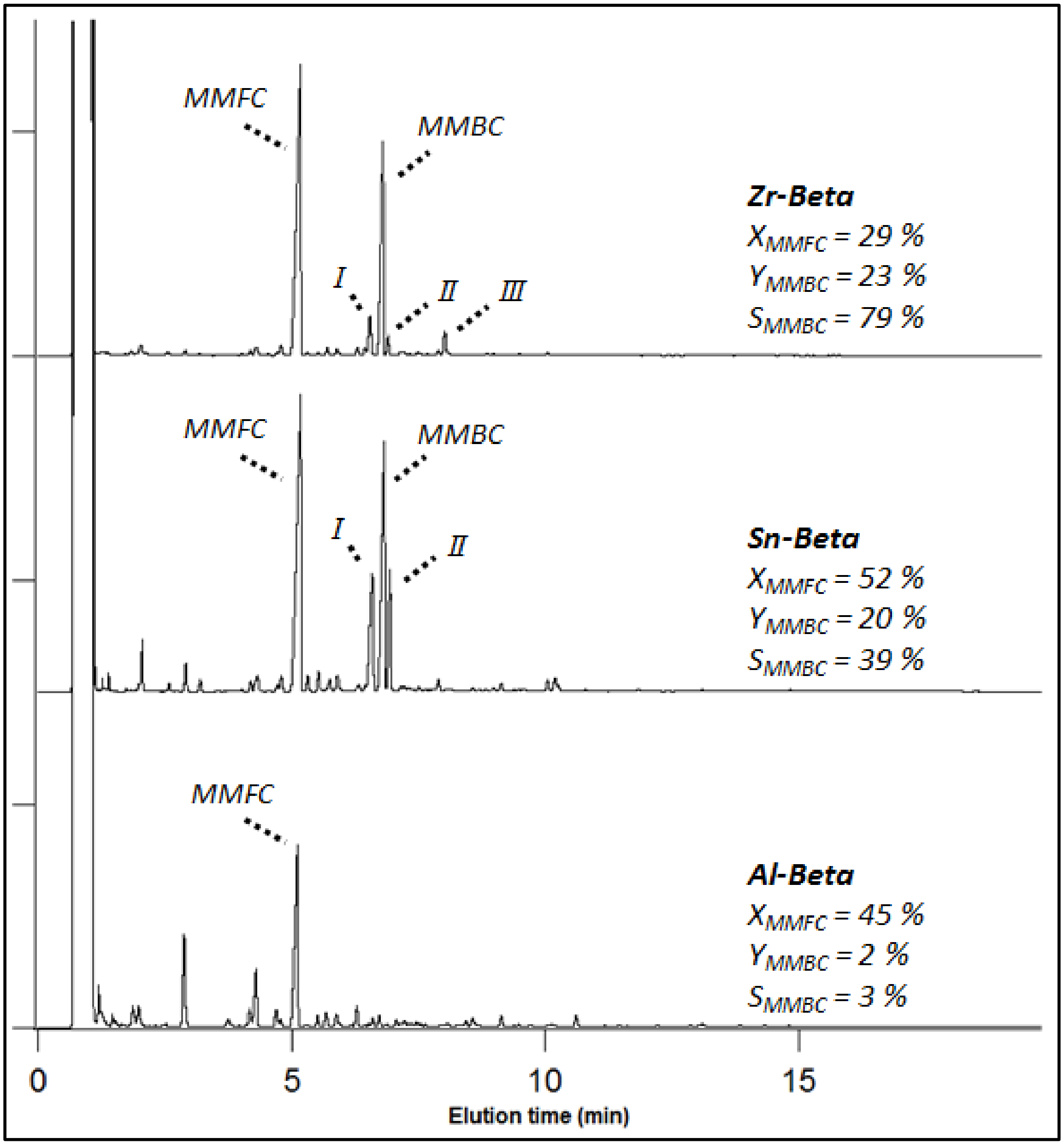

Fig. 6.1 GC-FID chromatograms of product solutions in the Diels-Alder-dehydration reaction of MMFC and ethylene using Zr-Beta, Sn-Beta, and Al-Beta catalysts. Reaction conditions: 0.1 M MMFC in dioxane, 100 mg catalyst, 190°C, 1000 psig C_2H_4, 6 hrs. Al-Beta reaction time was 3 hr. Conversions and yields determined by ^{1}H NMR.

As shown in the previous chapter only the Zr-Beta and Sn-Beta molecular sieves were found to produce the Diels-Alder-dehydration product, MMBC, with reasonable yield and selectivity, and the Bronsted acid zeolite produces only small amounts of the desired product with very low selectivity. The largest side product peaks in the Zr-Beta chromatogram are identified as products I, II, and III. In the Sn-Beta system, these same products also appear along with many additional side products. Interestingly, the products I and II in the Zr-Beta system are produced in a significantly higher amount by the Sn-Beta. Further investigation was mainly focused on identifying side products I and II.

The Sn-Beta and Zr-Beta product solutions were analyzed by GC/MS to obtain EI mass spectra of the side products. The mass spectra of the three main side products in the Zr-Beta system (I, II, and III) are shown in Fig. 6.2-6.4. Compounds I, II, and III have molecular weights of 166, 194, and 194, respectively. MS libraries of known compounds were screened and no match was found for any of these three spectra.

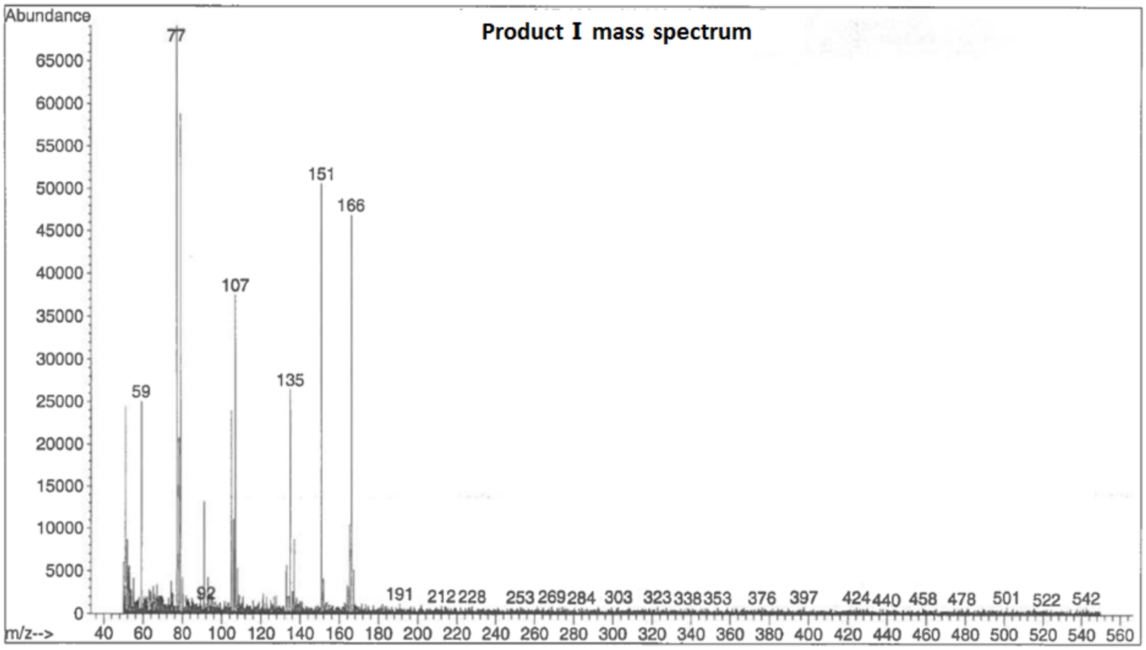

Fig. 6.2 EI mass spectrum of Product I.

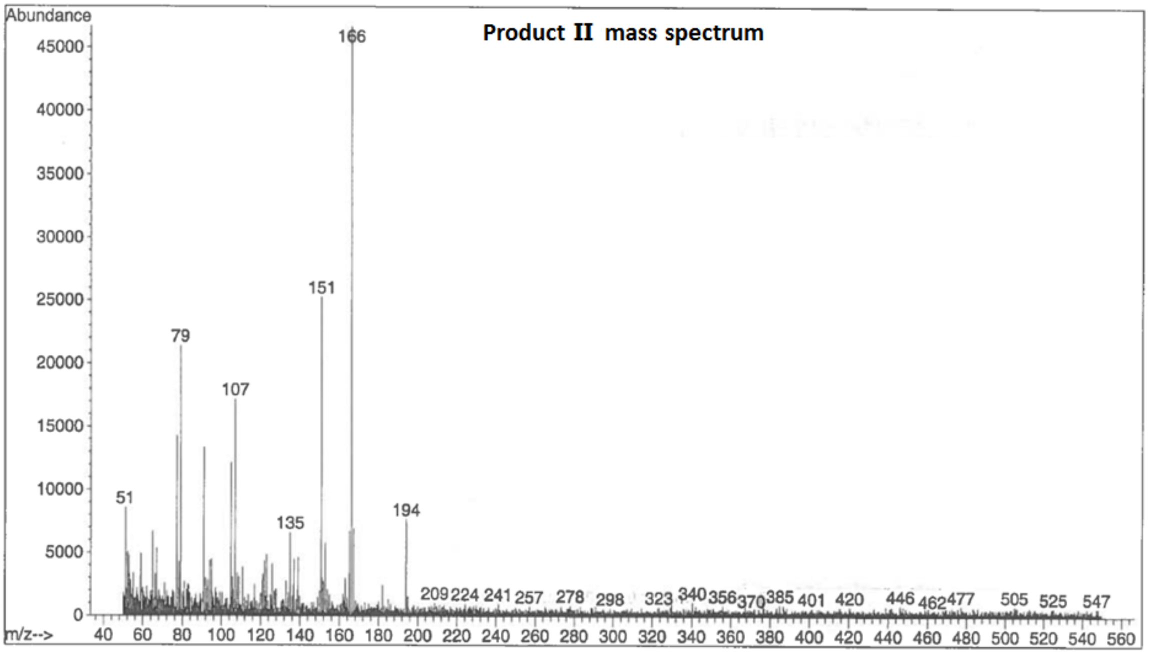

Fig. 6.3 EI mass spectrum of Product II.

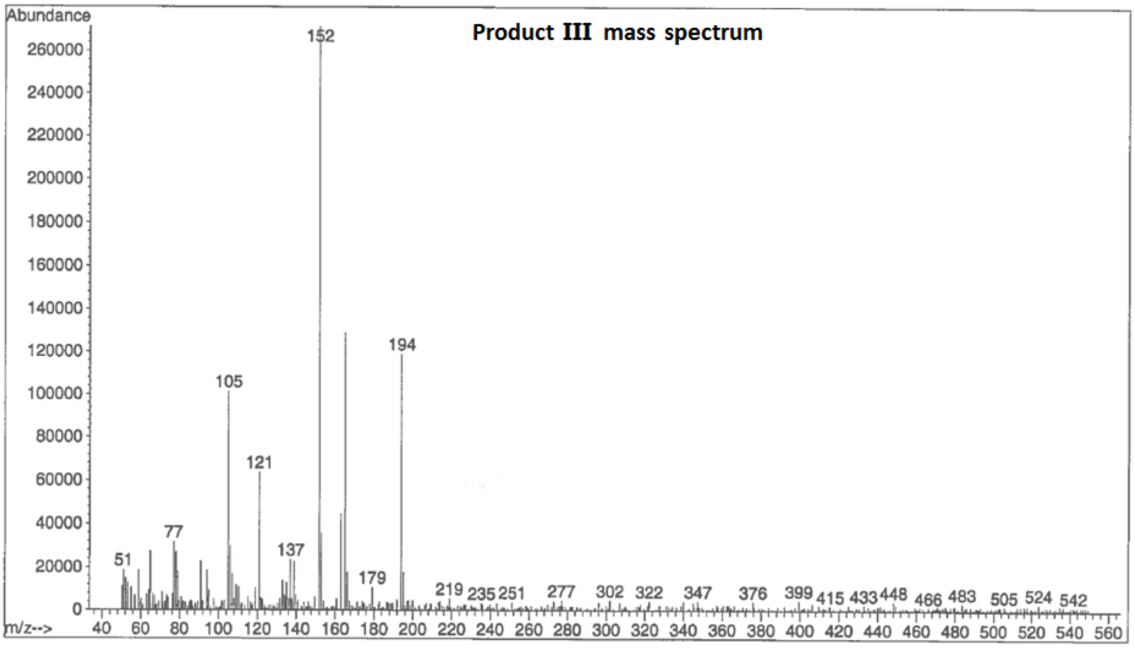

Fig. 6.4 EI mass spectrum of Product III.

To provide additional information that would be helpful for determining the identity of these compounds, more accurate fragment masses and chemical formula predictions were obtained by collecting time of flight mass spectra (TOF-MS). The EI mass spectra and predicted chemical formulas were obtained for products I and II (Fig. 6.5). The masses of products I and II are 166.063 and 194.094, respectively, and based on the fragment weights the predicted chemical formulas were determined as $C_9H_{10}O_3$ and $C_{11}H_{14}O_3$.

When comparing the spectra in Fig. 6.5, it is clear that the masses of all the fragments in the two spectra are very similar, if not identical. Additionally, the difference in the predicted chemical formulas is one ethylene molecule (C_2H_4) and the mass of the first molecular ion fragment peak (166.063) in the product II mass spectrum corresponds to a loss of one ethylene molecule. This information suggests that a close relationship between the two compounds exist and that an ethylene molecule is reacting in some way with I to form II.

As mentioned, mass spectra libraries have been searched to find a match to either of these spectra but no match was found. Therefore, to provide further information to identity of these compounds, efforts were made to separate the product mixture and isolate the unknowns for NMR analysis.

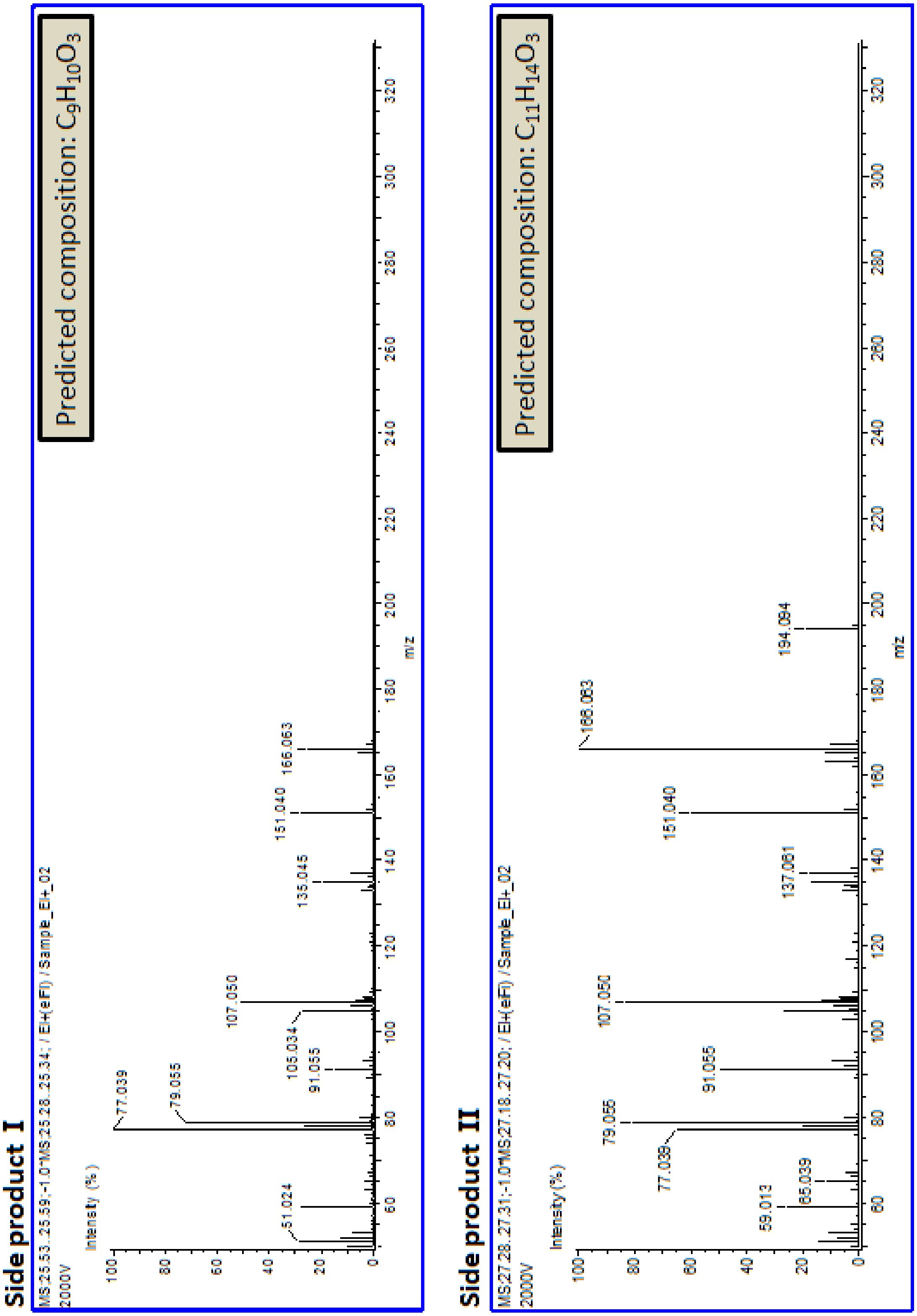

Fig. 6.5 TOF EI mass spectra and predicted chemical formulas of side products I and II.

To isolate the unknown side products, thin layer chromatography (TLC) was used as a method to separate the reaction product mixtures. Since larger amounts of products I and II are produced using Sn-Beta as catalyst, the product solutions made from the Sn-Beta catalyzed reactions were used in the TLC experiments. The product mixture was filtered to remove catalyst and deposited onto silica plates using a needle syringe. Using a 1 ethyl acetate:3 hexanes v/v mobile phase, the product mixture was separated into multiple bands (visible under UV light) on the silica plates. The organics in each of the bands were collected by scratching away the silica from the plates and collecting into separate vials. The silica was contacted in dichloromethane (DCM) and the DCM was then collected, filtered, and analyzed by GC/FID.

Contained in one of the TLC bands was both MMFC and the side product I. The gas chromatogram of the DCM solution containing the compounds in the TLC band is shown in Fig. 6.6, and essentially only MMFC and side product I are present. Several TLC plates were prepared, and enough of the separated band was collected and redissolved in $CDCl_3$ to obtain a ^1H NMR spectrum (Fig. 6.7). The MMFC peaks are indicated by "*", and six additional peaks are labeled corresponding to side product I.

The ^1H NMR spectrum supports the proposed cyclohexadiene molecular structure (Fig. 6.8), namely methyl 4-formylcyclohexa-1,3-diene-1-carboxylate. The relative areas and chemical shifts of the six numbered peaks in the NMR (Table 6.1) can be related to each of the protons in methyl 4-formylcyclohexa-1,3-diene-1-carboxylate. Additionally, this molecule has a chemical formula of

$C_9H_{10}O_3$ which is consistent with the predicted formula from the TOF/MS experiment, and the EI mass spectrum of side product I can be interpreted from this structure .

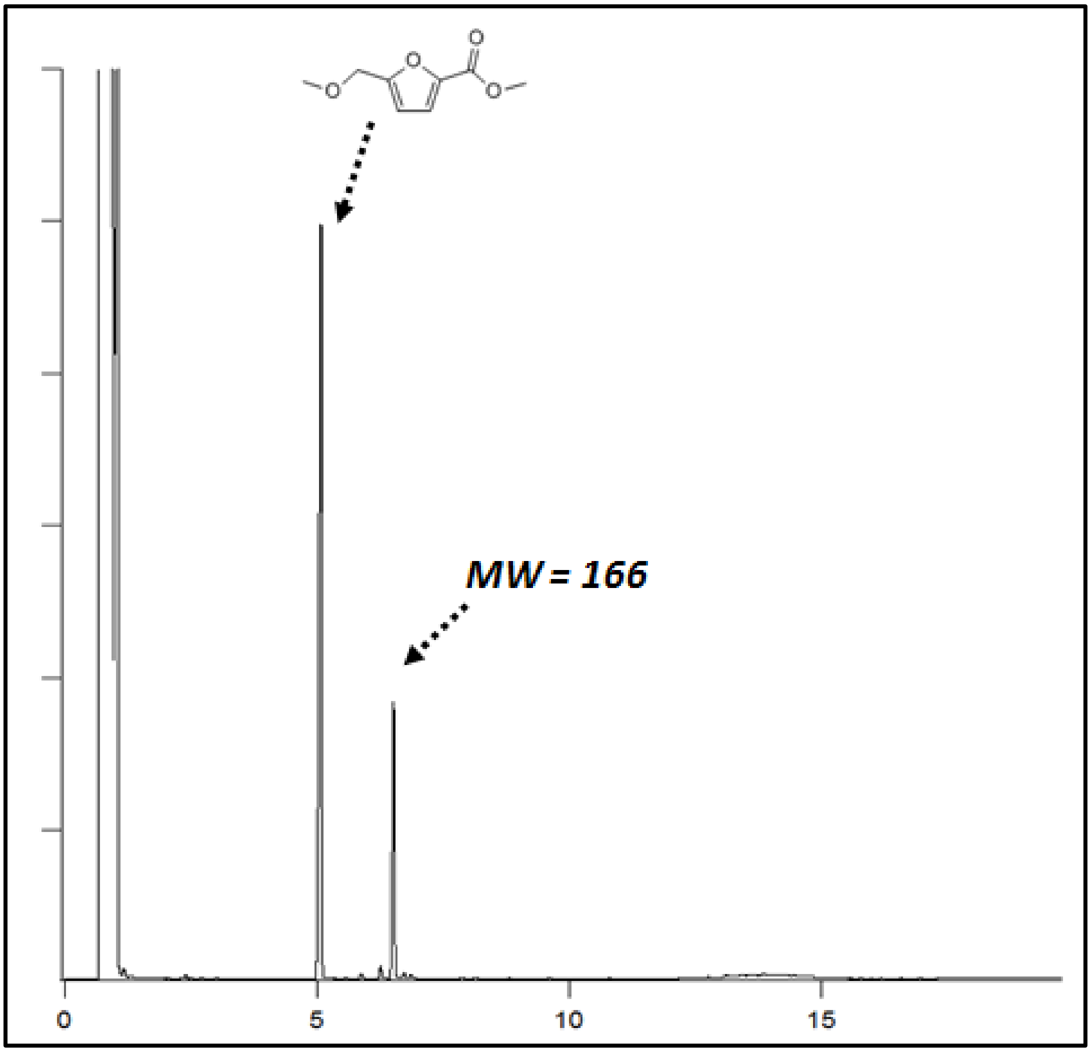

Fig. 6.6 GC-FID chromatogram of TLC fraction containing I (MW=166) and MMFC.

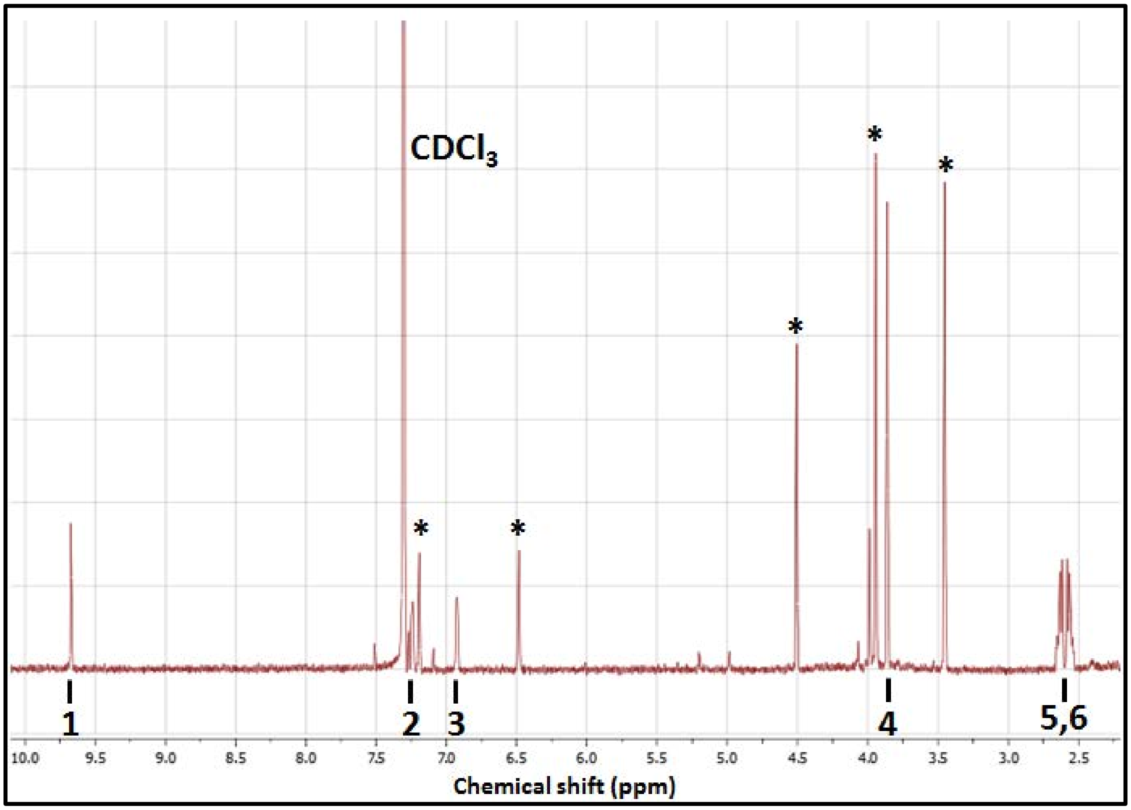

Fig. 6.7 ^{1}H NMR spectrum of TLC fraction containing product I and MMFC (∗).

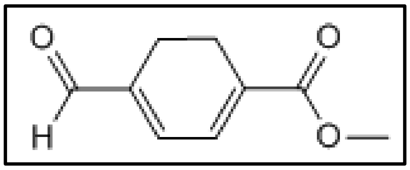

Fig. 6.8 Proposed molecular structure of product I (MW = 166), methyl 4-formylcyclohexa-1,3-diene-1-carboxylate.

Table 6.1 Relative areas of numbered peaks corresponding to I in Fig. 6.7.

Peak No.	Area
1	1
2	0.93
3	1.03
4	3.22
5	2.09
6	2.08

The TLC method was also able to isolate a fraction containing side product II by GC/FID and GC/MS, although several other compounds were also present in the fraction and very little material was collected on each plate which prevented a satisfactory ^{1}H NMR spectrum from being collected.

Since the mass spectrum of II is similar to I with the main difference being an additional ethylene fragment, and since the proposed structure of I has a cyclohexadiene functionality to it, there is a reasonable possibility that II is a Diels-Alder product between I and ethylene. One likely structure of II is methyl 4-formylbicyclo[2.2.2]oct-2-ene-1-carboxylate (Fig. 6.9). The thermally induced retro-Diels-Alder reaction to produce ethylene and I is probably the first dissociation reaction that occurs during ionization in the MS to produce a fragmentation pattern similar to I. Another example of the similarity in mass spectra between a cyclohexadiene and the Diels-Alder adduct of the diene with ethylene is seen when comparing the mass spectra of 1,3- cyclohexadiene and bicyclo[2.2.2]oct-2-ene (Mass spectra available on webbook.nist.gov). The formation of a bicyclo[2.2.2]oct-2-ene product from the Diels-Alder addition of ethylene to a cyclohexadiene side product was also observed by Do, et al. in the elucidation of the reaction network for the ethylene Diels-Alder-dehydration reaction of DMF and ethylene to PX (Fig. 6.10).[1]

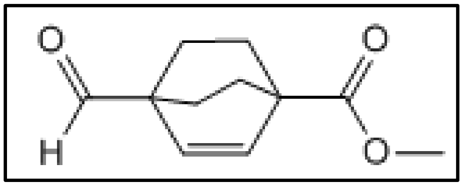

Fig. 6.9 Proposed molecular structure of product II (MW = 194), methyl 4-formylbicyclo[2.2.2]oct-2-ene-1-carboxylate.

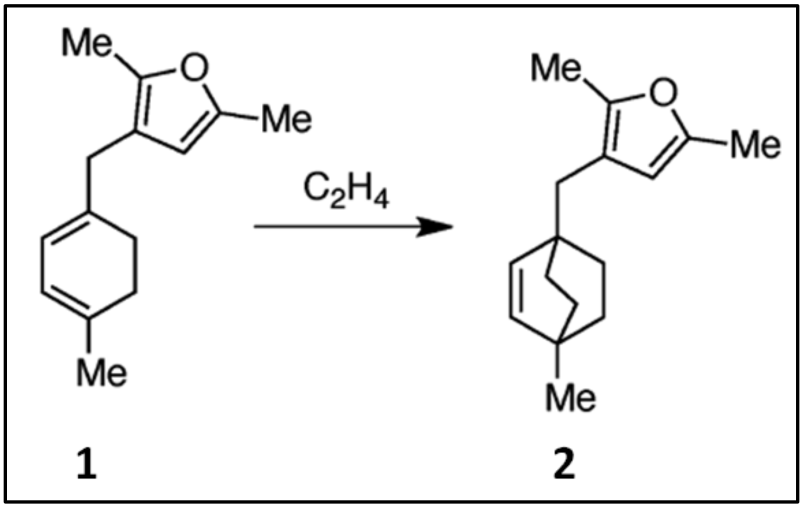

Fig. 6.10 Formation of a bicyclo[2.2.2]oct-2-ene product from the Diels-Alder addition of ethylene with a cyclohexadiene side product observed by Do, et al.[1]

After several weeks of storing in vials at ambient conditions, the Sn-Beta and Zr-Beta catalyzed product solutions were analyzed again and the formation of different side products were observed. In addition to MMFC and MMBC, methyl 4-formyl benzoate, dimethyl 2,5-furandicarboxylate, and dimethyl terephthalate were the main products, as shown in the GC/FID chromatogram in Fig. 6.11. The compounds were confirmed by comparing the GC elution times and mass spectra with known product standards (mass spectra in Fig. 6.1-6.3-A of appendix). Along with the formation of these new side products was the disappearance of the initially formed side products, methyl 4-formylcyclohexa-1,3-diene-1-carboxylate and methyl 4-formylbicyclo[2.2.2]oct-2-ene-1-carboxylate.

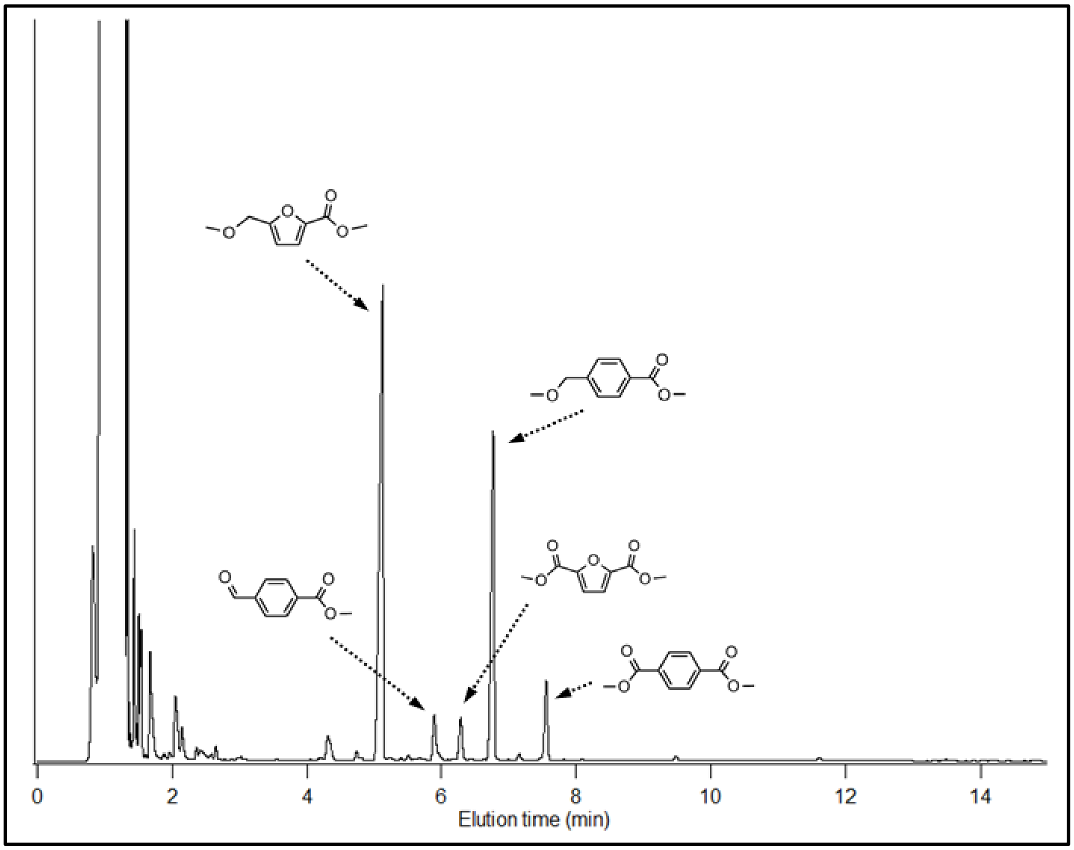

Fig. 6.11 Example of gas chromatogram of MMFC/ethylene Diels-Alder product solution after storing for several weeks at room temperature.

It is highly probable that methyl 4-formyl benzoate forms from the methyl 4-formylcyclohexa-1,3-diene-1-carboxylate side product by an air oxidation as shown in Fig. 6.12. Similar types of oxidations from cyclohexadiene side products to the aromatics were also reported by Do, et al.[1] Specifically, isolated samples of **1** and **3** converted to **2** and **4**, respectively, upon standing in air (Fig. 6.13). In another example, Mcgraw, et al. reported the thermally induced oxidation at 120 °C of α-terpinene to p-cymene, thymol, and carvacrol (Fig. 6.14).[2]

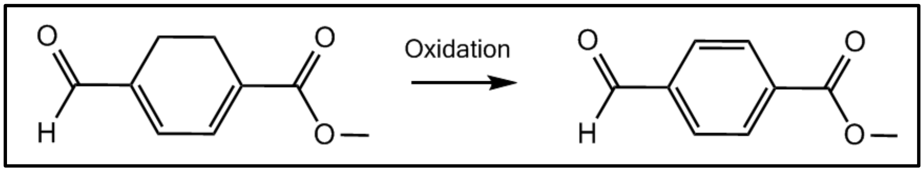

Fig. 6.12 Proposed oxidation of methyl 4-formylcyclohexa-1,3-diene-1-carboxylate to methyl 4-formyl benzoate at ambient conditions.

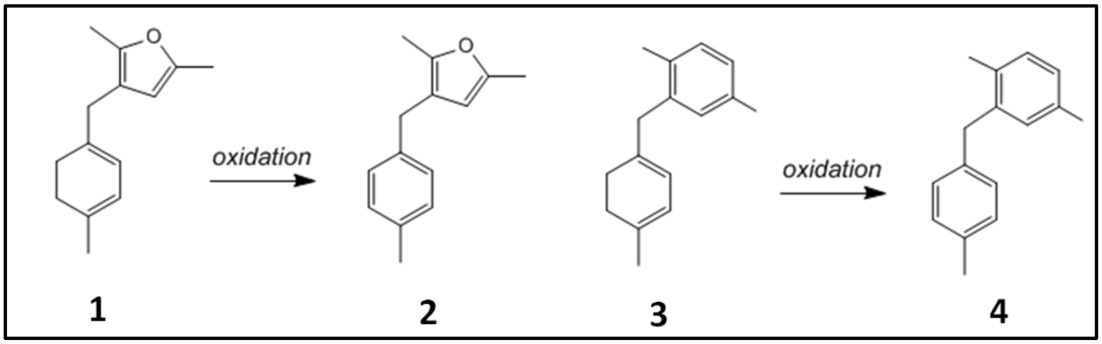

Fig. 6.13 Oxidation of cyclohexadiene side products to the corresponding aromatics observed by Do, et al.[1]

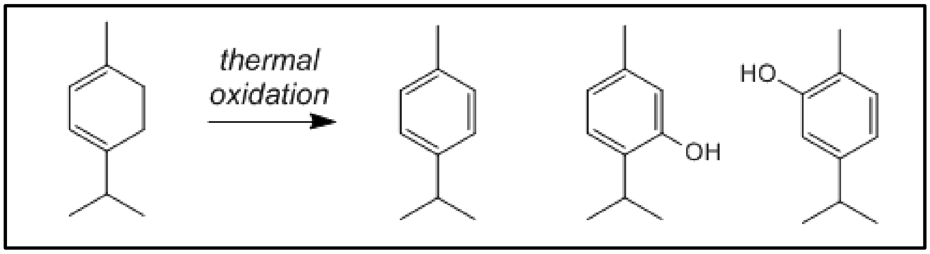

Fig. 6.14 Thermal oxidation of α-terpinene to p-cymene, thymol, and carvacrol reported by Mcgraw, et al.[2]

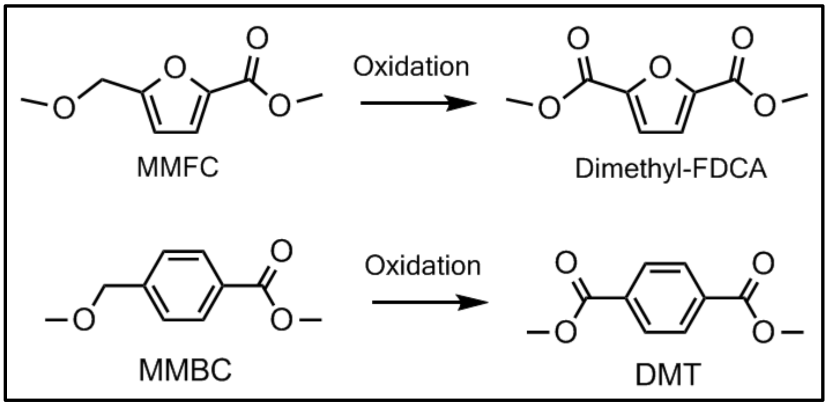

Fig. 6.15 Possible formation of dimethyl-FDCA and DMT from oxidation of MMFC and MMBC, respectively.

The dimethyl ester of FDCA (dimethyl-FDCA) and DMT are likely formed from MMFC and MMBC, respectively, by oxidation (Fig. 6.15).

The proposed overall reaction network for the system based on the findings of this investigation is shown in Fig. 6.16. The Lewis acid catalyst is involved in catalyzing the Diels-Alder-dehydration of MMFC (**1**) and ethylene to MMBC (**4**) under reaction conditions (190^{o}C, 1000 psig C_2H_4) via the ring-opened Diels-Alder adduct **3**. The formation of the side product methyl 4-formylcyclohexa-1,3-diene-1-carboxylate (**10**) could also be formed via a Lewis acid-catalyzed pathway. One possible mechanism for the formation of **10** involves an alternate ring-opened Diels-Alder adduct (**6**) and the formation of methanol. The product **10** then reacts with ethylene to form the product **12**. The conversion of **10** to **12** is expected to be reversible, therefore as **10** oxidizes to form **11**, both **10** and **12** are consumed. This would reasonably explain the formation of **11** at the expense of **10** and **12** in the GC chromatogram after the solutions are stored at long times. Dimethyl-FDCA (**13**) and DMT (**5**) are likely formed from the oxidation of MMFC (**1**) and MMBC (**4**), respectively, while being stored at room temperature.

Alternate acid-catalyzed pathways for the ring-opening of the Diels-Alder adduct between ethylene and DMF have also been proposed and observed in some recent investigations.[1,3] When the DMF/PX reaction is catalyzed by Bronsted acid zeolites, the different ring-opening pathways are shown in Fig. 6.17. The acidic proton attacks the oxygen atom to induce the breaking of a bridging C-O bond that forms a hydroxyl group and a cationic charge. The acid zeolite abstracts a proton from one of the saturated carbons adjacent to the cationic charge to produce two different PX precursors (**16** and **17**) that further dehydrate/isomerize to PX (**18**). Do, et al. observed experimentally the formation of **17**[1] which supports the proposed formation of intermediate **6** in the MMFC/MMBC system. Additionally, Bell et al. used computational methods to predict the formation of both **16** and **17** in the DMF/PX system[3] which provides further supporting evidence for the proposed ring-opening pathways for the MMFC/ethylene adduct (**2**).

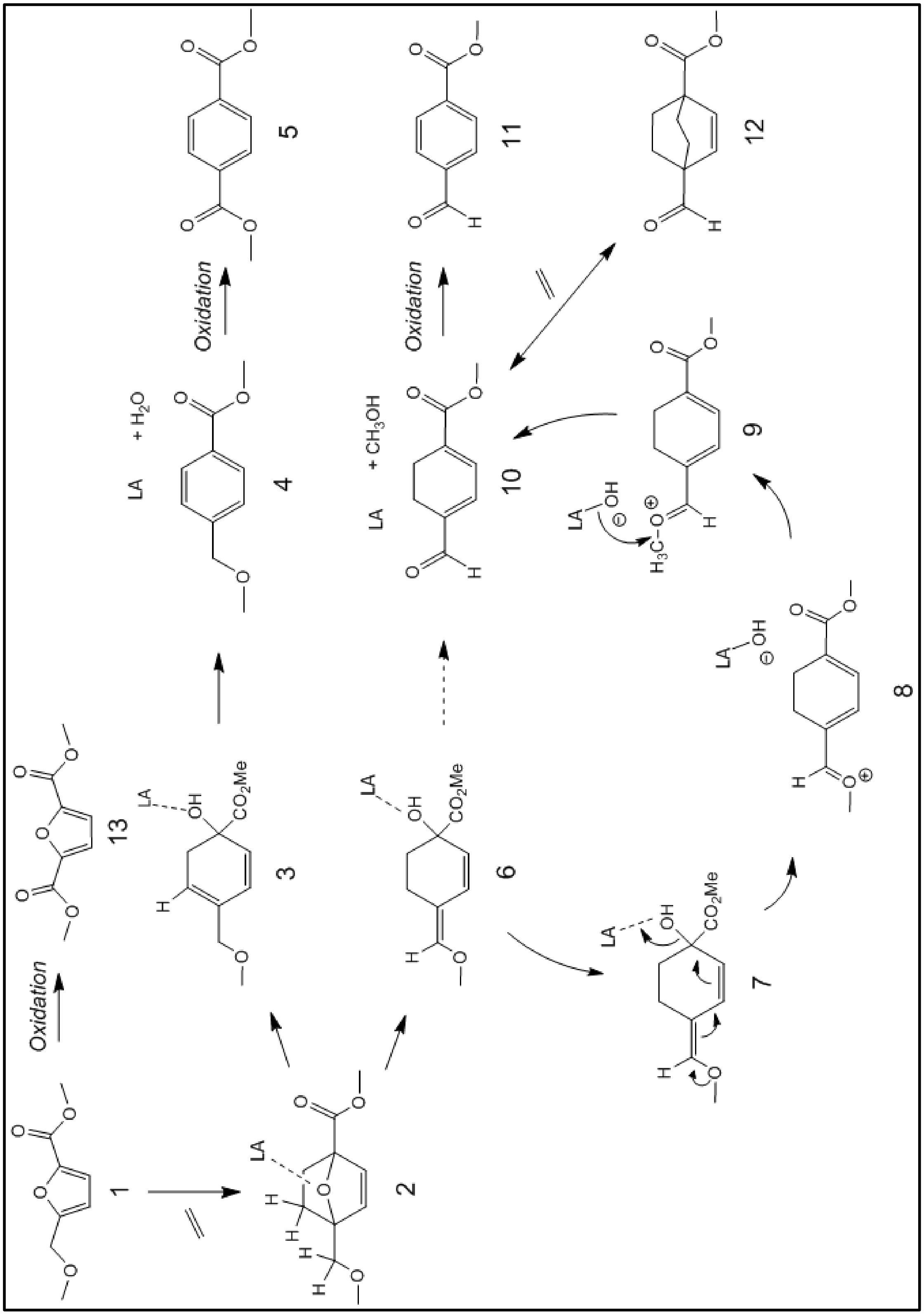

Fig. 6.16 Proposed reaction network for the Diels-Alder-dehydration of MMFC and ethylene to MMBC with Lewis acid Beta molecular sieve catalysts.

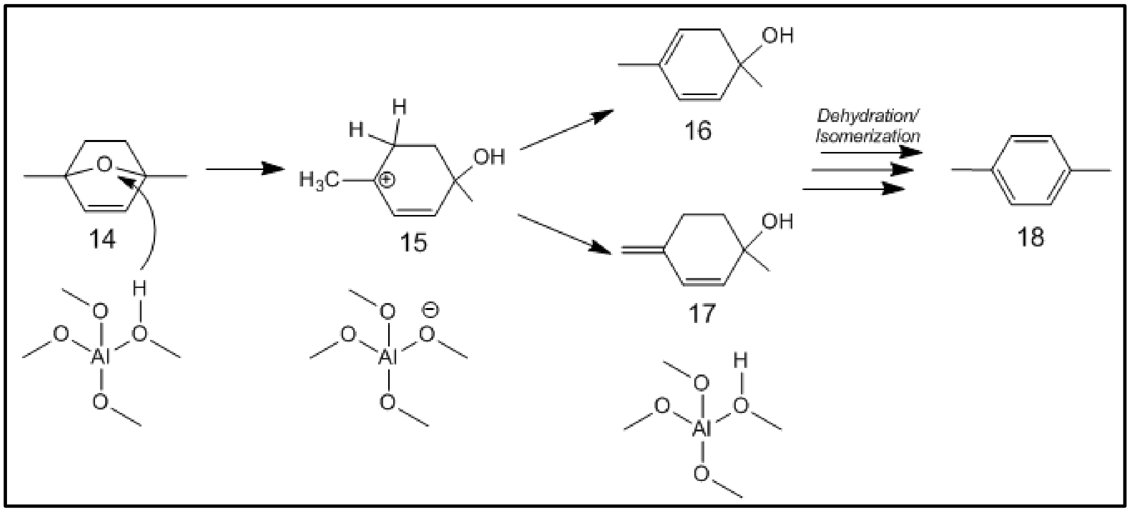

Fig. 6.17 Alternate acid-catalyzed pathways for the ring-opening of the Diels-Alder adduct between ethylene and the DMF.

6.2 References

[1] Do, P.T.M.; McAtee, J.R.; Watson, D.A.; Lobo, R.F.; *ACS Catal.* **2013**, *3*, 41 – 46.

[2] Mcgraw, W.B., et al.; *Environ.Sci. Technol.* **1999**, *33*, 4029.

[3] Li, Y-P.; Head-Gordon, M.; Bell, A.T.; *J. Phys. Chem. C* **2014**, *118*, 22090 – 22095.

CHAPTER 7

MEASUREMENT OF ACTIVATION ENERGIES FOR ETHYLENE DIELS-ALDER-DEHYDRATION REACTIONS

This chapter provides a summary and discussion of kinetic data obtained for two different Diels-Alder-dehydration reactions catalyzed by the Lewis acid molecular sieve, Zr-Beta: (1) the synthesis of PX from DMF and ethylene, and (2) the synthesis of MPT from MMF and ethylene (Fig. 7.1).

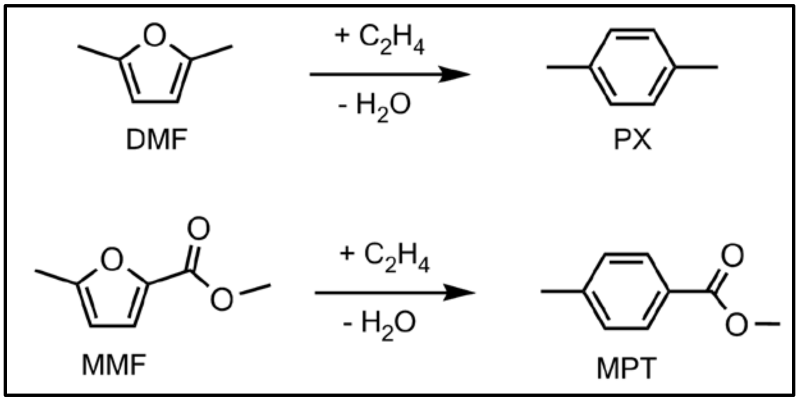

Fig. 7.1 Ethylene Diels-Alder-dehydration reactions of DMF to PX and MMF to MPT.

Each system was investigated by first determining whether the kinetics of the Diels-Alder-dehydration reactions were influenced by mass transfer limitations within the molecular sieve catalysts. This was determined by performing the Madon-Boudart test and plotting the initial rates of product formation versus varying active site content in the catalyst. The Madon-Boudart criterion states that if the initial rates are linear with the number of active sites in different crystalline microporous catalyst samples of constant crystal size, then the transport of the reactant molecule to the catalytic active site is not limiting the rate of reaction.[1] Here, the test is performed based on the assumption that all Zr metal atoms in the Zr-Beta catalysts are equally active and accessible active sites for the Diels-Alder-dehydration reaction. It is critical to determine if transport limitations are present before measuring any further kinetics of a reaction. If transport of the reactant to the active site is limiting, any measured activation energy will not be characteristic of the chemical reaction over the catalyst being studied. Therefore, this makes it impossible to compare the effect different catalysts have on the actual rate of chemical reaction.

After determining if measured reaction rates were influenced by transport limitations for both reactions, the initial rates of product formation using Zr-Beta were measured at different reaction temperatures to generate Arrhenius plots. Apparent activation energies of reaction using the Zr-Beta catalyst were then determined from the slopes of these plots. The results for the synthesis of PX from DMF and ethylene will be discussed first, followed by a discussion of the results for the production of MPT from MMF and ethylene.

7.1 Synthesis of PX from DMF and ethylene with Zr-Beta catalyst

A series of four Zr-Beta samples of varying Si/Zr atomic ratios were prepared by methods described in Chapter 2. The Zr source used in the syntheses was Zr(IV) propoxide. Table 7.1 summarizes the Si/Zr ratios and crystal size of each sample used in the investigation.

Table 7.1 Zr-Beta sample characterization. Each sample was highly crystalline as determined by XRD, and scanning electron microscopy (SEM) images indicated nearly constant crystal size among all samples (see appendix Fig. 7.1-8-A). Elemental composition was determined by Galbraith Laboratories (GLI procedure ME-70).

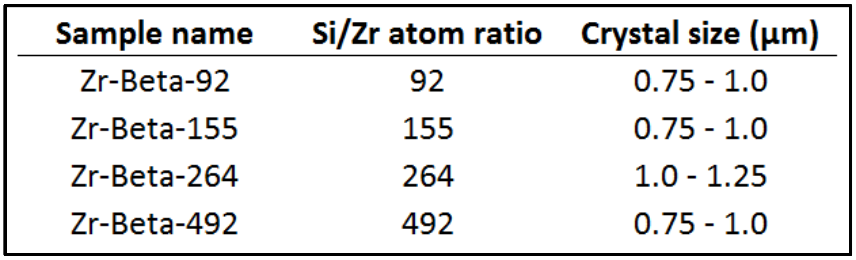

Sample name	Si/Zr atom ratio	Crystal size (µm)
Zr-Beta-92	92	0.75 - 1.0
Zr-Beta-155	155	0.75 - 1.0
Zr-Beta-264	264	1.0 - 1.25
Zr-Beta-492	492	0.75 - 1.0

To determine whether transport limitations within the microporous Zr-Beta catalysts were influencing the measured rates of PX production from DMF and ethylene in dioxane solvent, the initial rates of PX production were measured as function of Zr content in the catalyst. The PX yield profiles using the four Zr-Beta catalysts were collected at 230^{o}C (Fig. 7.2) and initial rates (t = 0) were determined (Table 7.2).

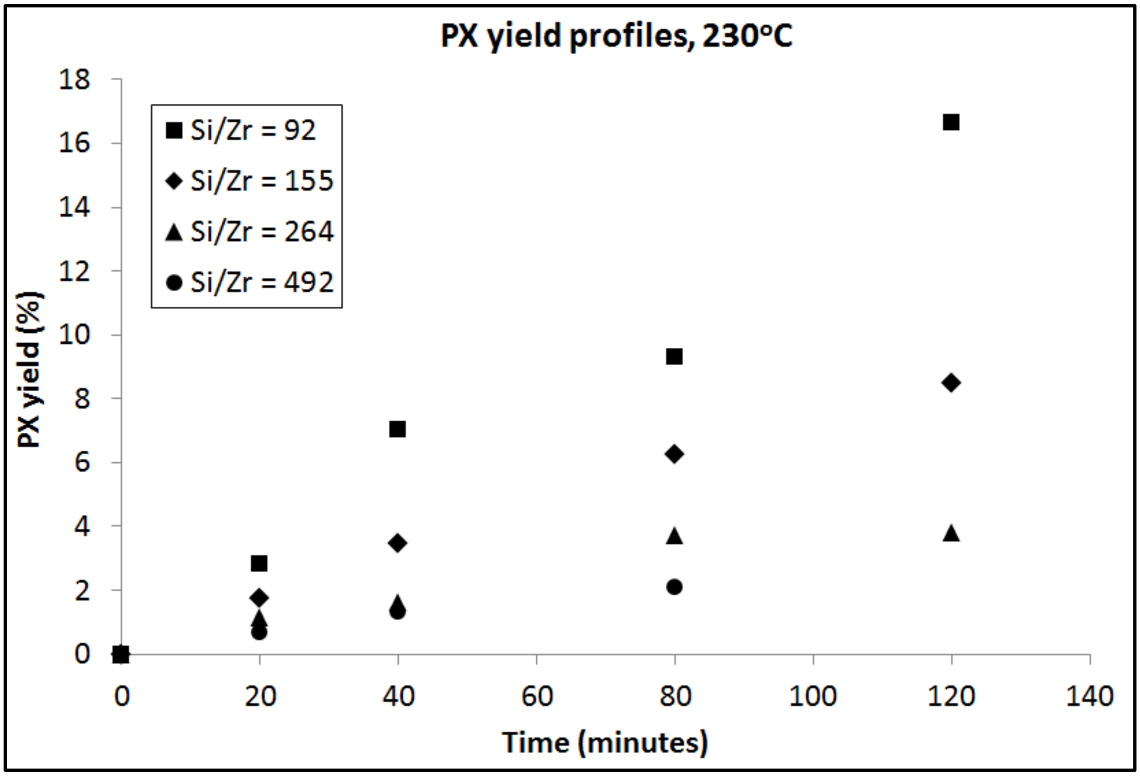

Fig. 7.2 PX yield profiles for Diels-Alder-dehydration of DMF and ethylene using Zr-Beta catalysts with varying Si/Zr molar ratios. Reaction conditions: 0.1 M DMF in dioxane, 0.1 M triglyme (internal standard), 30 mg catalyst, 230°C, 35 bar C_2H_4 (room temperature).

Table 7.2 Initial rates of PX formation for profiles in Fig. 7.2.

		Initial rate (mM PX/hr)		
Si/Zr	**Zr (mmol)**	Min	Max	Average
92	0.0054	8.40	10.68	9.54
155	0.0032	5.16	5.22	5.19
264	0.0019	2.40	3.30	2.85
492	0.0010	1.86	1.98	1.92

The initial rates were determined by simply estimating the slope of the profiles at initial time (t=0 min). The data displayed a small amount of scatter that can be attributed to the separate batch reaction experiments required to collect each individual data point. To account for the scatter in estimating the initial rates, a “maximum” and “minimum” slope was drawn for each profile and the “average” initial rate was the average of these two slopes. See the methods section in this chapter for experimental details.

The measured initial PX production rates (in mM PX/hr) are plotted against the Zr content in the catalyst (using 30 mg of catalyst loading) in Fig. 7.3. The initial rate of PX production is clearly linear with the amount of Zr in the catalyst for the four Zr-Beta materials tested. If the assumption holds true that each Zr atom is equal, active, and accessible, then the possibility of a transport limitation influencing the measured kinetics at temperatures up to 230^{o}C may now be neglected.

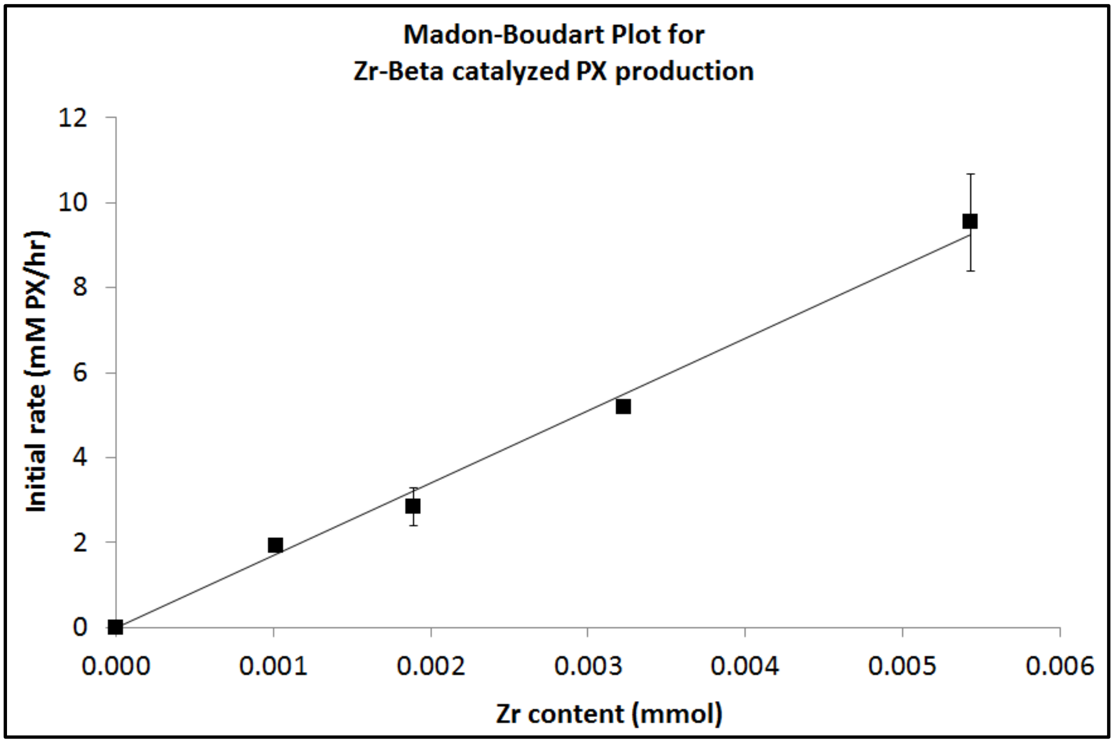

Fig. 7.3 Madon-Boudart plot for Zr-Beta catalyzed PX production at 230^{o}C. The error bars are the max/min slopes of the PX yield profiles (see Chap. 7 methods section).

Next, an apparent activation energy (E_a) for the conversion of DMF and ethylene to PX using Zr-Beta was measured. The PX yield profiles were collected at four different temperatures (170, 190, 210, and 230 ^oC) using the sample Zr-Beta-155 (Fig. 7.4.). The same procedure was applied to measure the initial rates (Table 7.3).

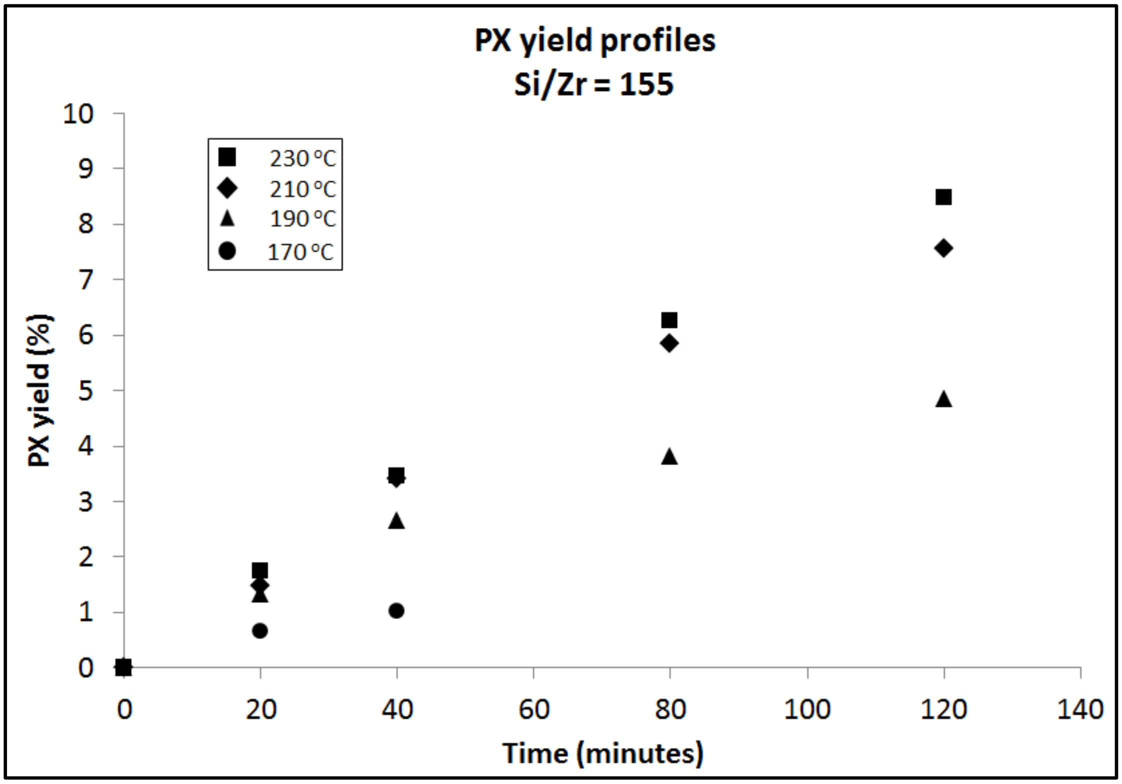

Fig. 7.4 PX yield profiles for Diels-Alder-dehydration of DMF and ethylene using Zr-Beta-155 with varying reaction temperature. Reaction conditions: 0.1 M MMF in dioxane, 0.1 M triglyme (internal standard), 30 mg Zr-Beta-155, 35 bar C_2H_4 (room temperature).

Table 7.3 Initial rates of PX formation for profiles in Fig. 7.4.

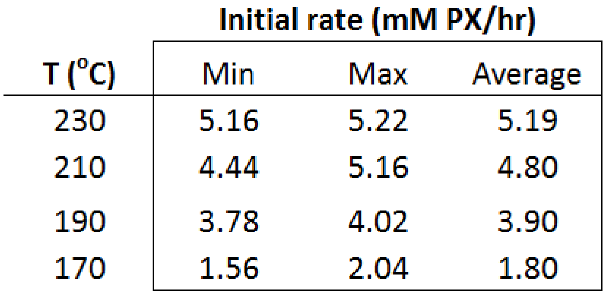

	Initial rate (mM PX/hr)		
T (^{o}C)	Min	Max	Average
230	5.16	5.22	5.19
210	4.44	5.16	4.80
190	3.78	4.02	3.90
170	1.56	2.04	1.80

An Arrhenius plot was generated from the data (Fig. 7.5) and the apparent E_a determined by the slope of a fitted line through the four points is 8.2 kcal/mol. Since it appears that the slope of the plot may be different at the low and high temperature ranges, apparent E_a's corresponding to the different slopes were also measured (Fig. 7.6 and Fig. 7.7). In the 170-210 ^{o}C range the apparent E_a is 10.5 kcal/mol and in the 210-230 ^{o}C range an apparent E_a of only 1.9 kcal/mol is measured.

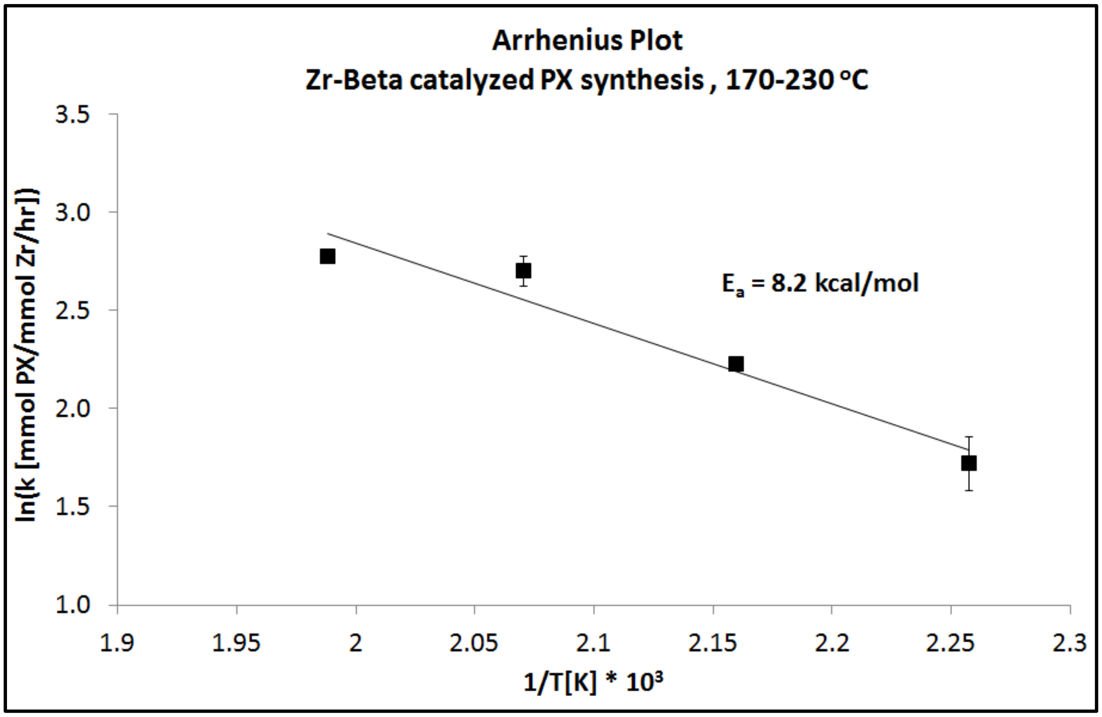

Fig. 7.5 Arrhenius Plot for Zr-Beta catalyzed PX synthesis for 170-230°C.

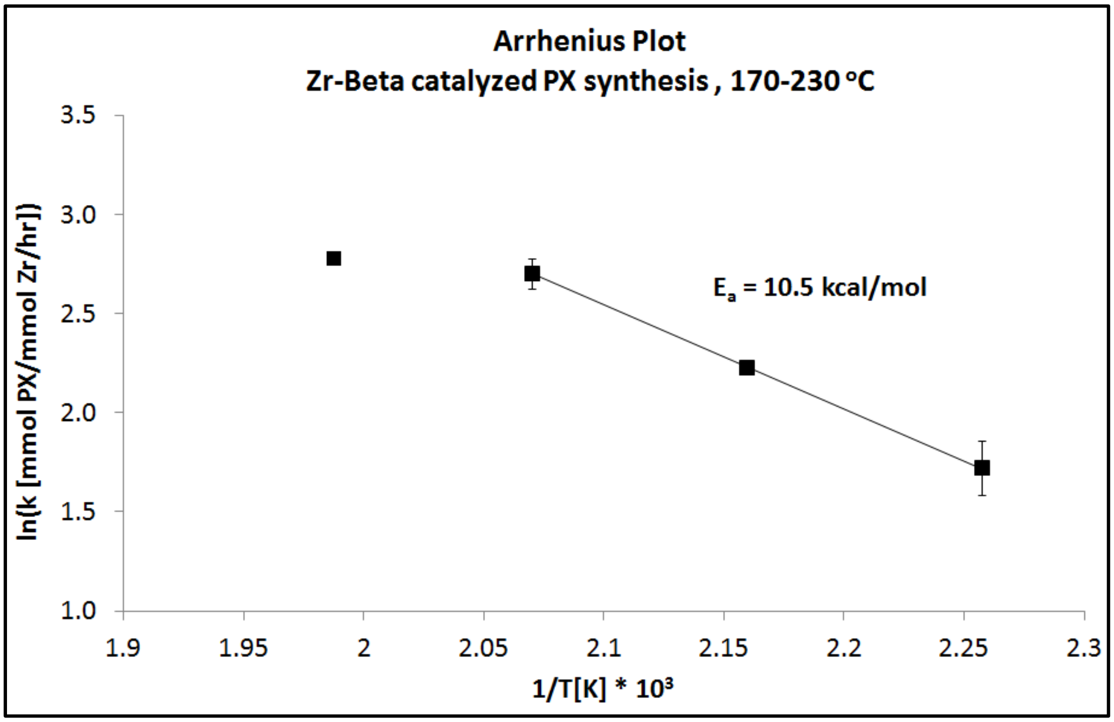

Fig. 7.6 Arrhenius Plot for Zr-Beta catalyzed PX synthesis for 170-230 °C. Apparent E_a = 10.5 kcal/mol reported for low temperature range (170-210 °C).

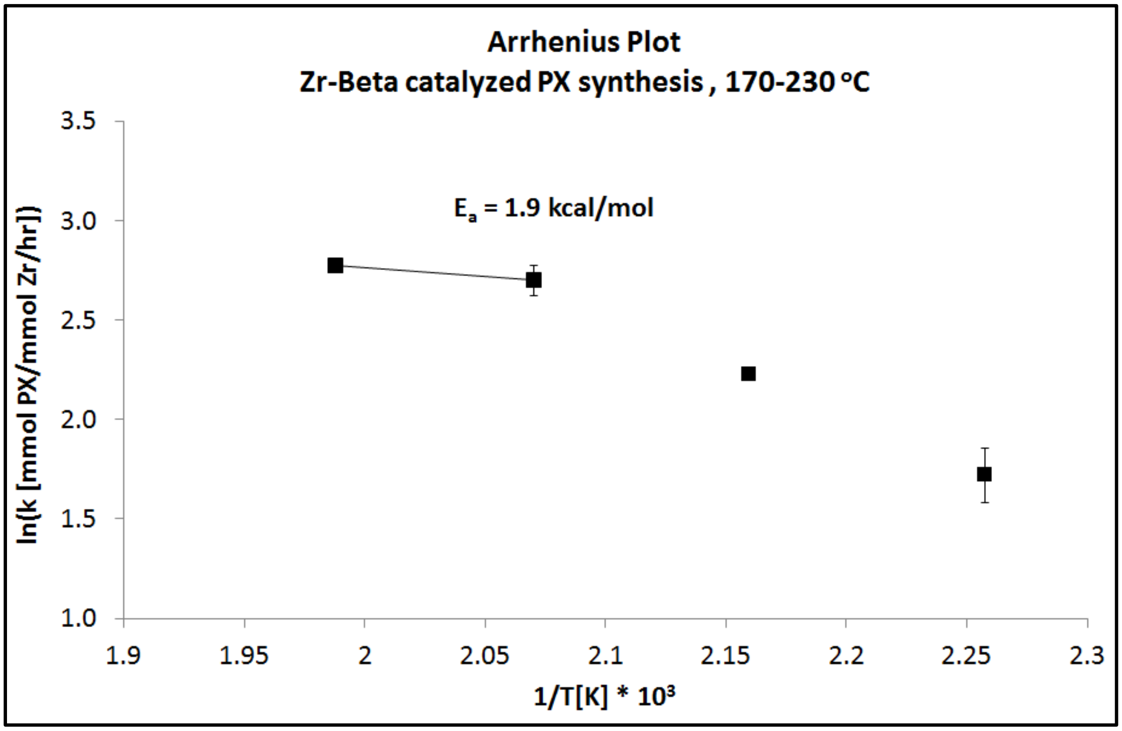

Fig. 7.7 Arrhenius Plot for Zr-Beta catalyzed PX synthesis for 170-230 °C. Apparent E_a = 1.9 kcal/mol reported for high temperature range (210-230 °C).

7.2 Synthesis of MPT from MMF and ethylene with Zr-Beta catalyst

To compare with the DMF/PX system, a nearly identical analysis was performed for the Zr-Beta catalyzed Diels-Alder-dehydration reaction of MMF and ethylene to MPT. Refer to the methods section in this chapter for experimental details.

MPT yield profiles were collected using the four Zr-Beta samples at 230°C (Fig. 7.8) and initial rates were estimated (Table 7.4). The initial rates using each sample are plotted against the Zr content in the catalyst to generate a Madon-Boudart plot (Fig. 7.9). The Madon-Boudart plot appears to be non-linear, especially with the highest Zr content catalyst (Zr-Beta-92), indicating a possible diffusion limitation. Since the lowest Zr content catalyst (Zr-Beta-492) has a large uncertainty (larger error bars) and the middle two catalysts (Zr-Beta-264, Zr-Beta-155) look to be linear with (0,0), the first three catalysts (Zr-Beta-492, Zr-Beta-264, and Zr-Beta-155) may not be diffusion limited. The line on the plot is the trendline for the first three points passing through (0,0). Additional experiments are required to know the true shape of the plot and to have more confidence in knowing whether a diffusion limitation exists.

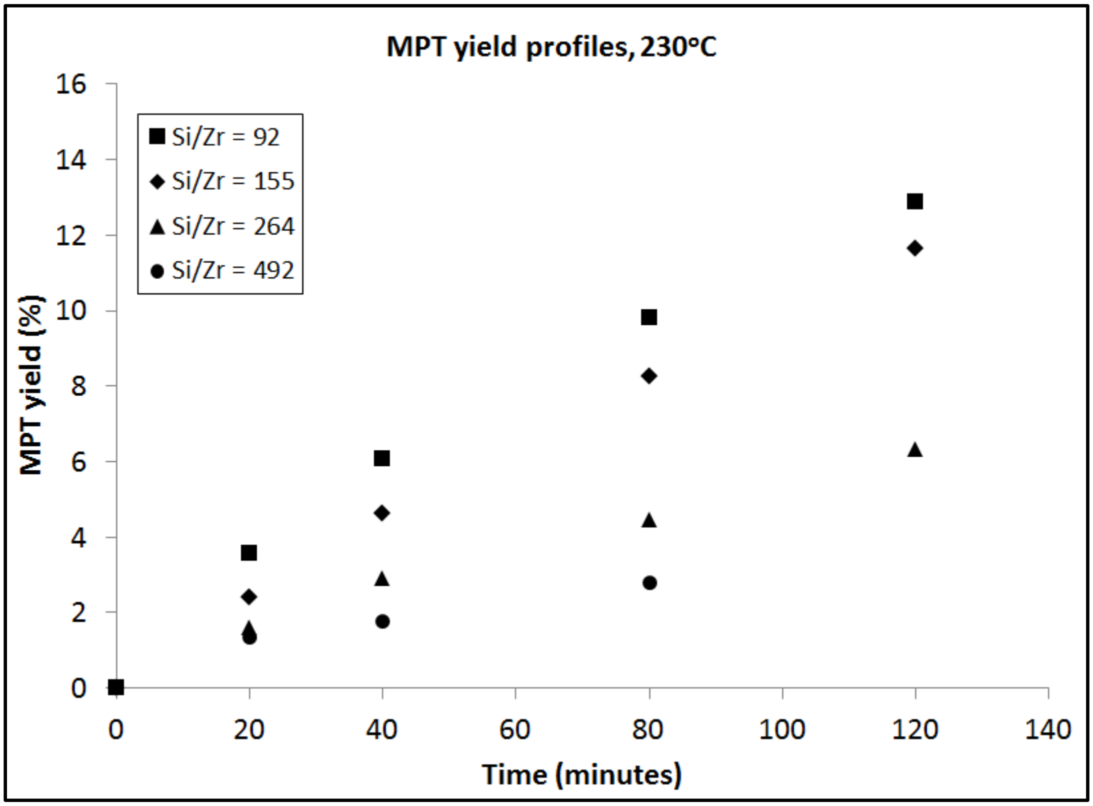

Fig. 7.8 MPT yield profiles for Diels-Alder-dehydration of MMF and ethylene using Zr-Beta catalysts with varying Si/Zr molar ratios. Reaction conditions: 0.1 M MMF in dioxane, 0.1 M triglyme (internal standard), 100 mg catalyst, 230^{o}C, 35 bar C_2H_4 (room temperature).

Table 7.4 Initial rates of MPT formation for profiles in Fig. 7.8.

		Initial rate (mM MPT/hr)		
Si/Zr	**Zr (mmol)**	Min	Max	Average
92	0.018	9.00	10.62	10.35
155	0.011	6.84	7.20	7.02
264	0.006	4.32	4.86	4.59
492	0.003	2.70	3.96	3.33

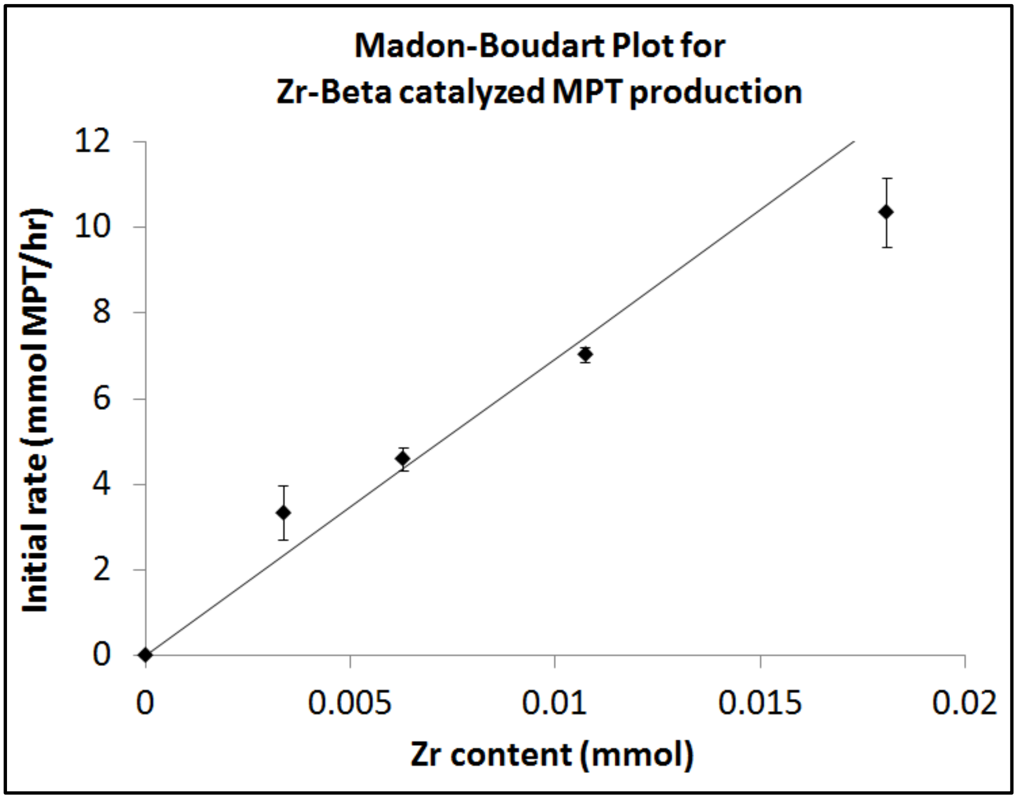

Fig. 7.9 Madon-Boudart plot for Zr-Beta catalyzed MPT production at 230^{o}C. The error bars are the max/min slopes of the MPT yield profiles (see Chap. 7 methods section).

The MPT yield profiles were collected at five different temperatures (170, 190, 210, 220, and 230 ^{o}C) using the sample Zr-Beta-155 (Fig. 7.10) and the initial rates were estimated (Table 7.5). An Arrhenius plot was generated from the data (Fig. 7.11) and the apparent E_a determined by the slope of a fitted line through the five points is 6.4 kcal/mol.

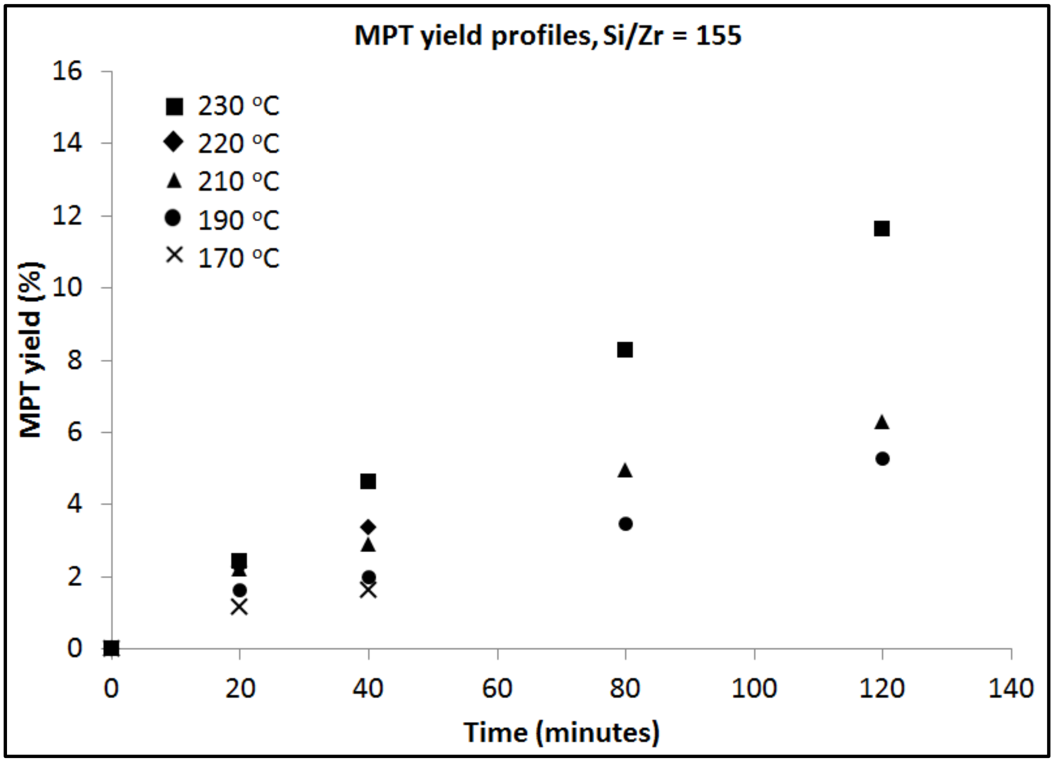

Fig. 7.10 MPT yield profiles for Diels-Alder-dehydration of MMF and ethylene using Zr-Beta-155 with varying reaction temperature. Reaction conditions: 0.1 M MMF in dioxane, 0.1 M triglyme (internal standard), 100 mg Zr-Beta-155, 35 bar C_2H_4 (room temperature).

Table 7.5 Initial rates of MPT formation for profiles in Fig. 7.10.

	Initial rate (mM MPT/hr)		
T (°C)	Min	Max	Average
230	6.84	7.38	7.11
220	5.04	6.84	5.94
210	4.32	6.48	5.40
190	2.88	5.04	3.96
170	2.52	3.42	2.97

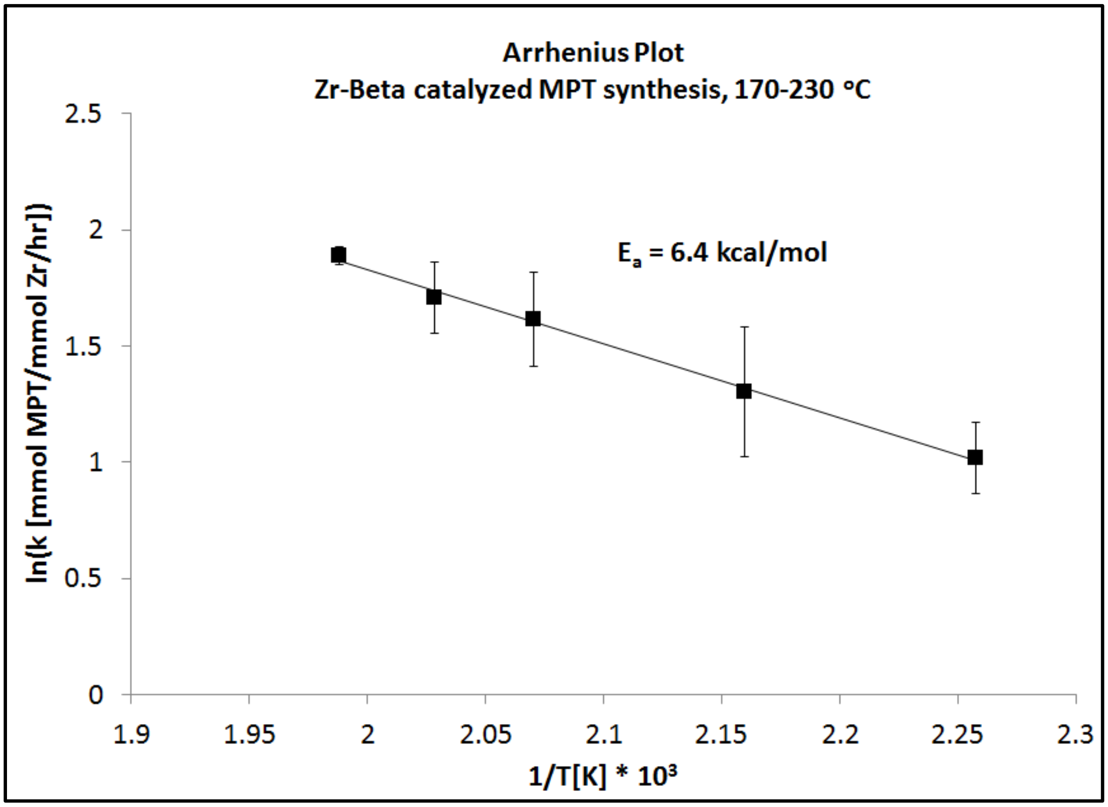

Fig. 7.11 Arrhenius Plot for Zr-Beta catalyzed MPT synthesis for 170-230°C.

Table 7.6 Summary of measured apparent E_a's for PX and MPT synthesis using Zr-Beta catalyst.

Reaction	T (°C)	E_a (kcal/mol)
DMF-PX	170-230	8.2 (avg)
	170-210	10.5
	210-230	1.9
MMF-MPT	170-230	6.4

7.3 Discussion of apparent E_a measurements for DMF/PX and MMF/MPT reactions using Zr-Beta.

All the apparent E_a measurements are summarized in Table 7.6. Since all four of these apparent E_a's are likely too low to be the true activation energy of a single chemical step, these data suggest the apparent E_a for the two processes may include a collection of terms that could result in low overall values. Since two chemical reactions are occurring in tandem (Diels-Alder cycloaddition and dehydrative aromatization) with the first reaction (Diels-Alder cycloaddition) possibly in thermodynamic equilibrium, it is reasonable to propose that the measured apparent E_a's are a combination of terms that may include, for example, the ΔH_{rxn} for the reversible Diels-Alder reaction, the true E_a for the dehydrative aromatization of the Diels-Alder adduct, and others. Additionally, ΔH_{ads} terms for adsorption steps in equilibrium (reactants or intermediates adsorbing reversibly onto the catalyst surface or active site) may be part of the apparent E_a's and could contribute to an overall low E_a value.

For example, a recent investigation by Patet, et al. on the Diels-Alder-dehydration of DMF and ethylene to produce PX using a Bronsted acid H-Y zeolite catalyst in heptane solvent showed a reaction regime in which the effective rate constant for the production of PX included multiple terms.[2] A simplified kinetic model for the H-Y catalyzed production of PX was proposed (Table 7.7) and the model was solved for a rate equation (Fig. 7.12). At low Bronsted acid active site concentrations this rate equation simplifies (Fig. 7.13), showing that under these conditions the effect rate constant for PX production may include a collection of terms (k_2, K_1, K_4, K_6, etc.).

Table 7.7 Simplified kinetic model for the Diels-Alder-dehydration of DMF and ethylene to PX from Patet, et al. (2015).[2] Labels: DMF = dimethylfuran, E = ethylene, CA = Diels-Alder cycloadduct between DMF and E, PX = p-xylene, W = water, HDI = 2,5-hexanedione, * = Vacant strong acid H-Y site.

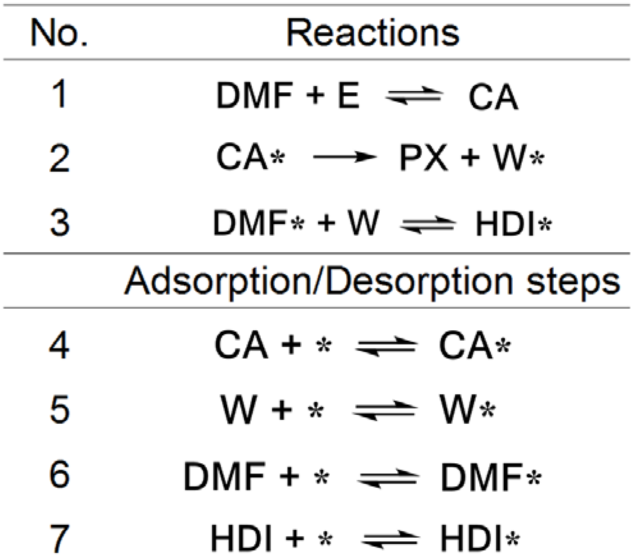

No.	Reactions
1	$DMF + E \rightleftharpoons CA$
2	$CA* \rightarrow PX + W*$
3	$DMF* + W \rightleftharpoons HDI*$
	Adsorption/Desorption steps
4	$CA + * \rightleftharpoons CA*$
5	$W + * \rightleftharpoons W*$
6	$DMF + * \rightleftharpoons DMF*$
7	$HDI + * \rightleftharpoons HDI*$

$$\boxed{r_{PX} = \frac{k_2 K_1 K_4 [DMF][E][*]}{K_6(1 + K_3[W])[DMF] + \left(\frac{k_2}{k_{-1}}\right) K_4[*]}}$$

Fig. 7.12 Rate of PX production using the simplified kinetic model in Table 7.7, reported in Patet, et al. (2015).[2] The parameters k_i and K_i are the reaction rate and equilibrium constants for reaction *i*, [i] is the concentration of component *i*, and [*] is the total Bronsted acid active site concentration.

$$\boxed{r_{PX} = \left(\frac{k_2 K_1 K_4}{K_6(1 + K_3[W])}\right)[E][*]}$$

Fig. 7.13 Reduced form of the PX production rate equation from Fig. 7.12 at low Bronsted acid active site concentrations, as reported in Patet, et al. (2015).[2]

Clearly, the conversions of DMF and MMF to PX and MPT with ethylene Diels-Alder-dehydration reactions are complex systems and additional investigation is required to provide deeper insight into the reaction mechanism.

7.4 Methods for determining initial rates

The measurement of PX yield was performed by GC/FID using triglyme as internal standard in dioxane solvent. Due to the similarity in boiling points, the DMF reactant elutes at the same time as dioxane in the GC. Therefore, DMF conversion (and PX selectivity) was unable to be determined by GC-FID. Quantitative ^{1}H NMR analysis was used to measure DMF conversion, and it was found that PX selectivities were ~40%. This is in agreement with previous reports of PX selectivity at low PX yields.[2] Due to the low PX selectivities at low yields, the PX yields were used (rather than DMF conversion) for determining the apparent E_a.

The MMF conversion and MPT yield was measured by GC/FID using triglyme as internal standard in dioxane solvent. The MMF conversion profiles at low conversion were unreliable and exhibited a larger amount of error. This was due to irreproducibility in the area ratio of the MMF/triglyme peaks in the gas chromatogram from injection to injection, and the source of the irreproducibility was unresolved. The area ratios of the MPT/triglyme peaks were very reliable from injection to injection and, therefore, the MPT yield profiles were used for determining the apparent E_a.

The plots in Fig. 7.14-15 show how initial rates were estimated using the collected PX and MPT yield profiles, including the maximum and minimum slopes used for reporting the error bars in Fig. 7.3, Fig. 7.5, Fig. 9, and Fig. 7.11.

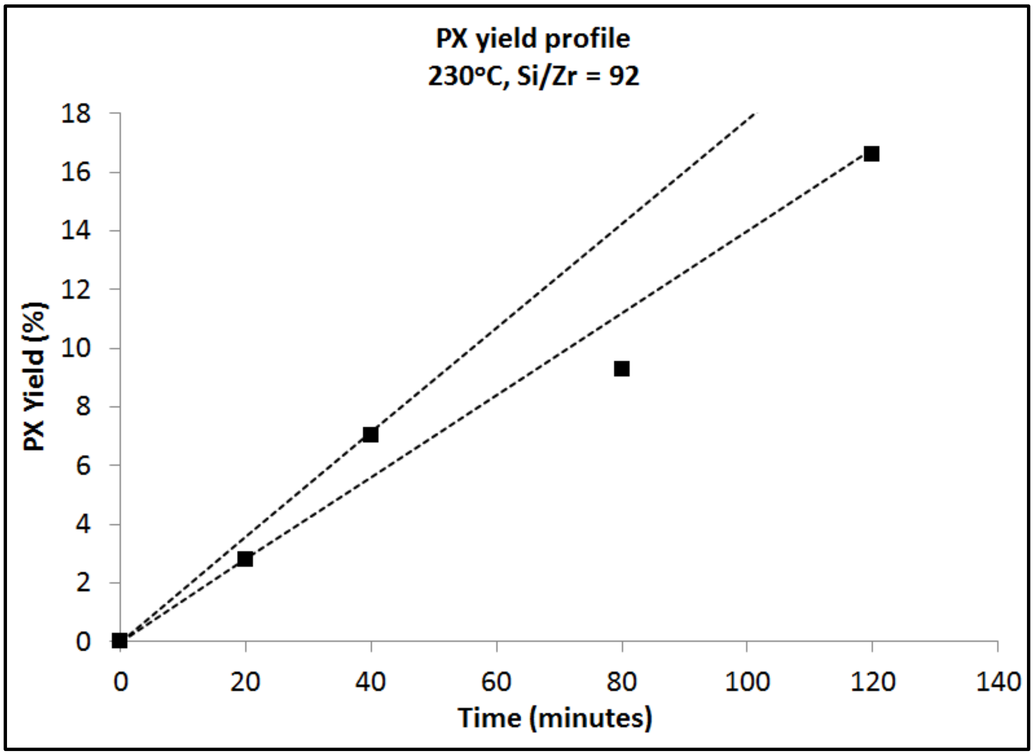

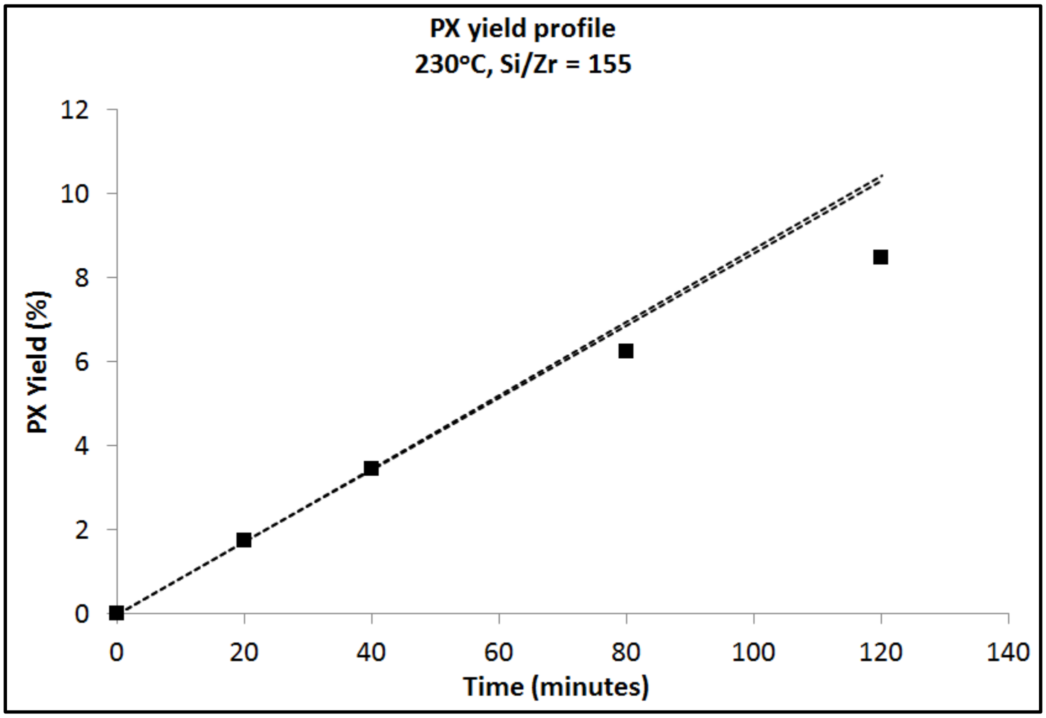

Fig. 7.14 Plots used for measuring the initial rates from the collected PX yield profiles.

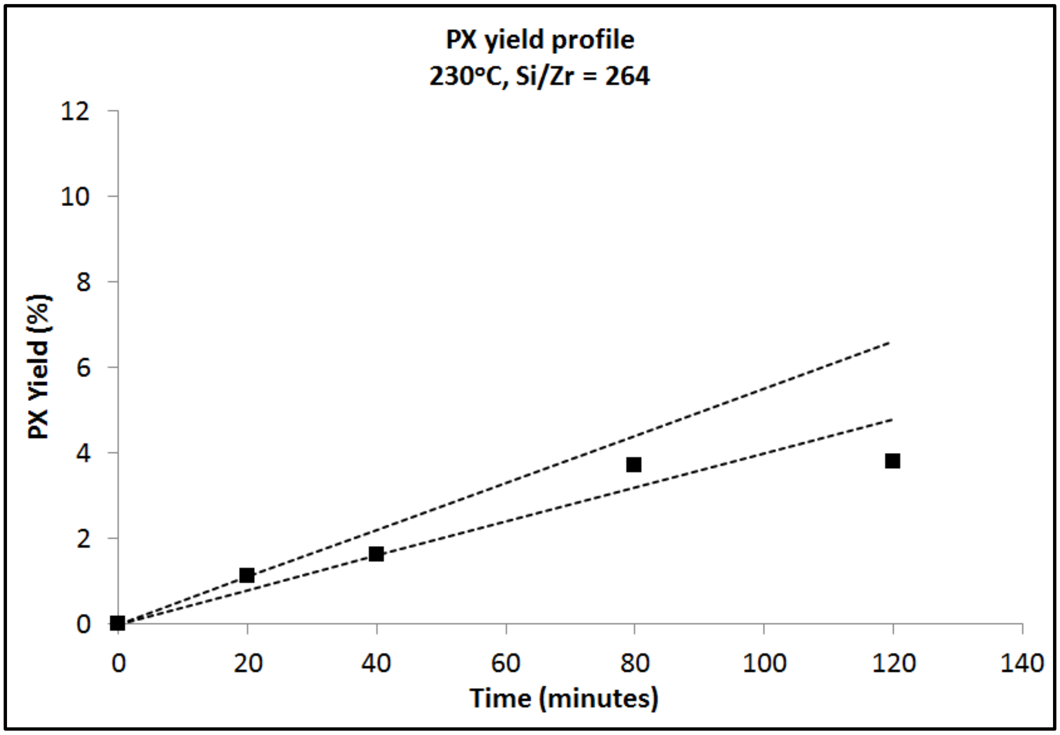

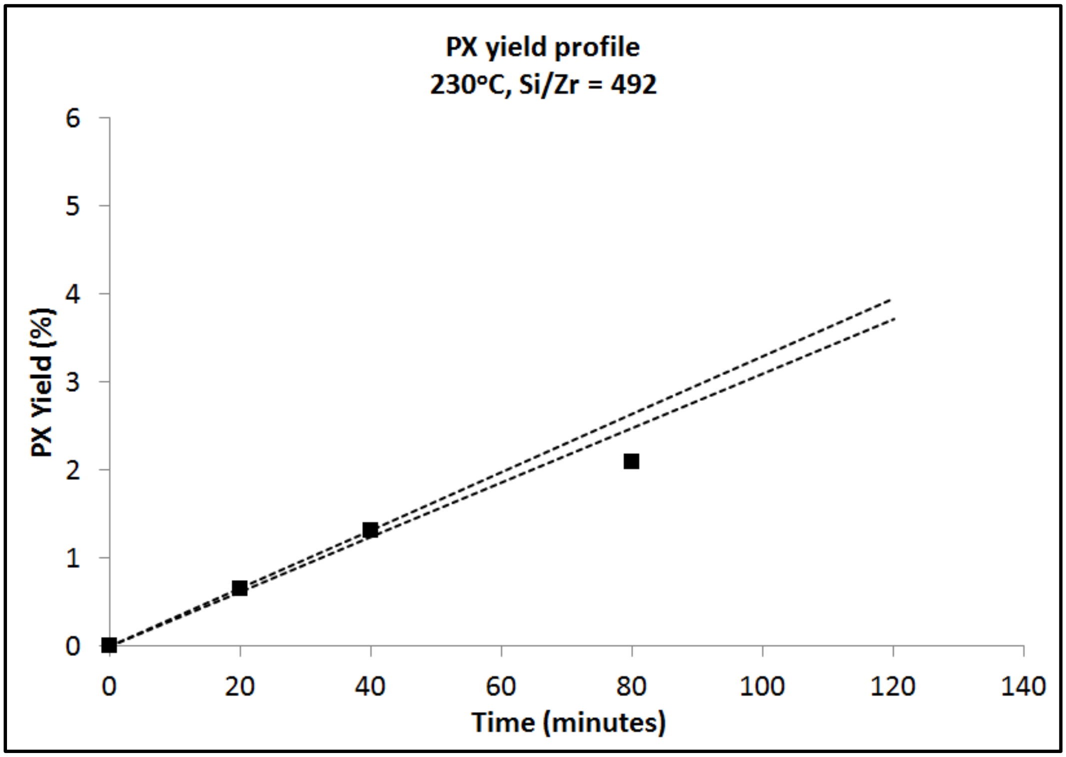

Fig. 7.14 continued. Plots used for measuring the initial rates from the collected PX yield profiles.

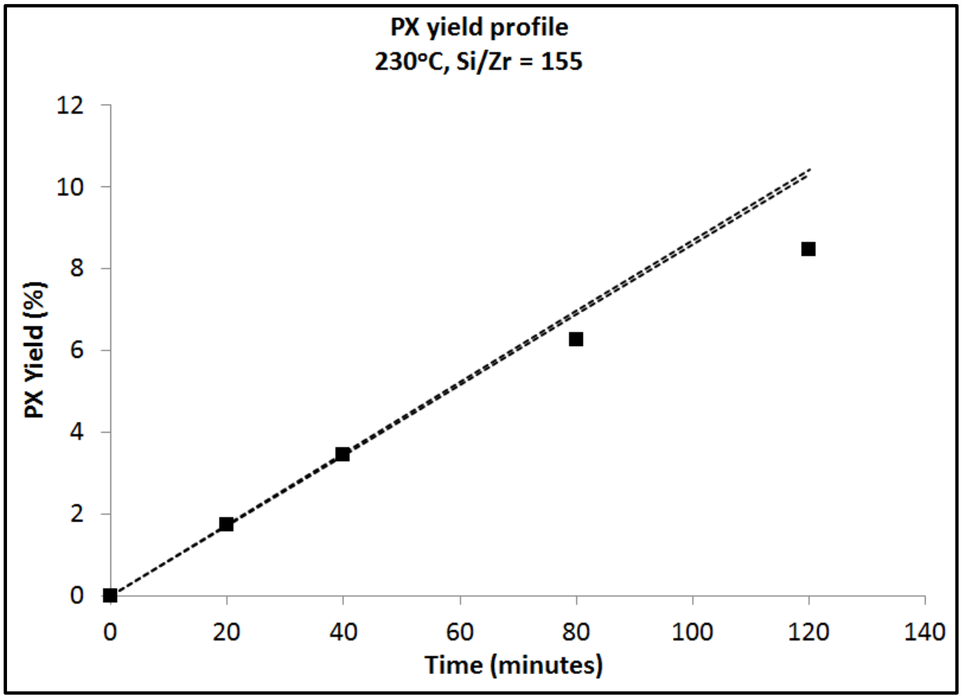

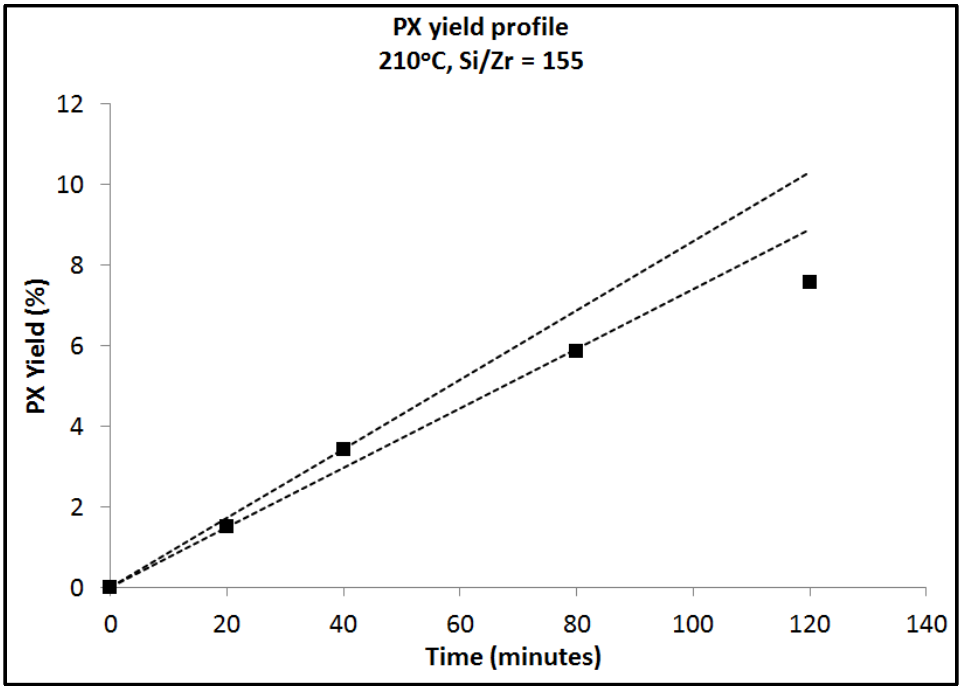

Fig. 7.14 continued. Plots used for measuring the initial rates from the collected PX yield profiles.

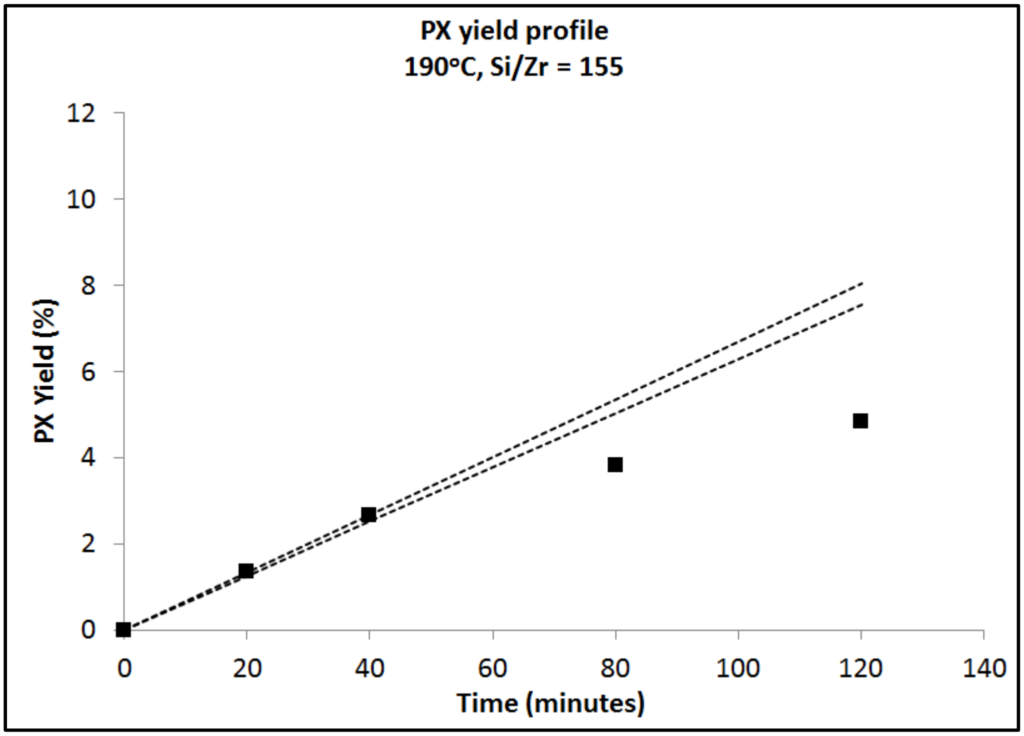

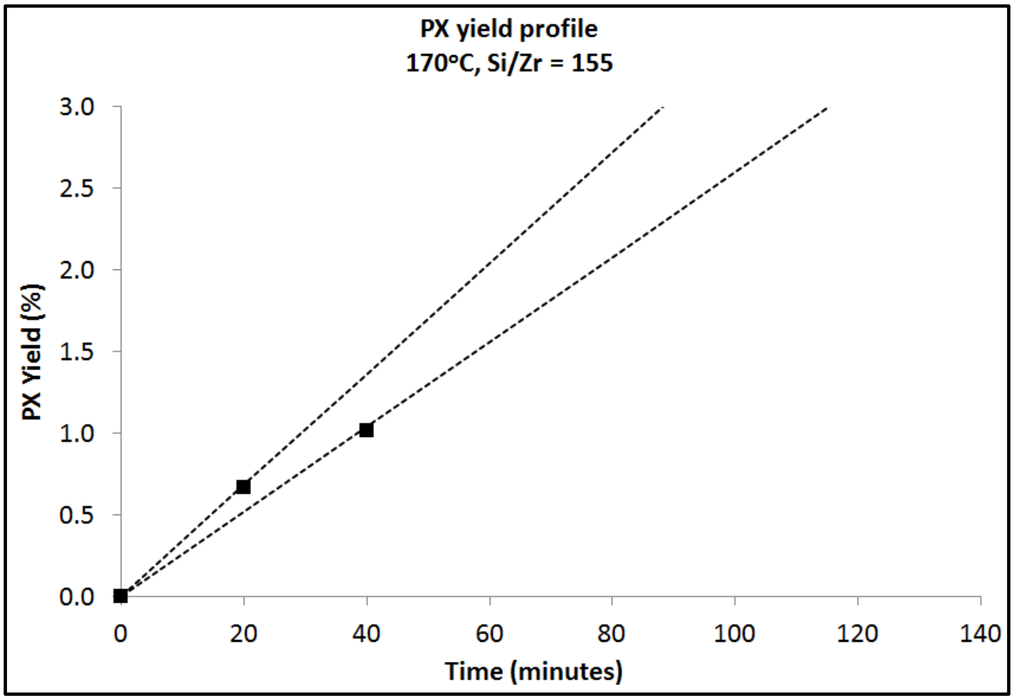

Fig. 7.14 continued. Plots used for measuring the initial rates from the collected PX yield profiles.

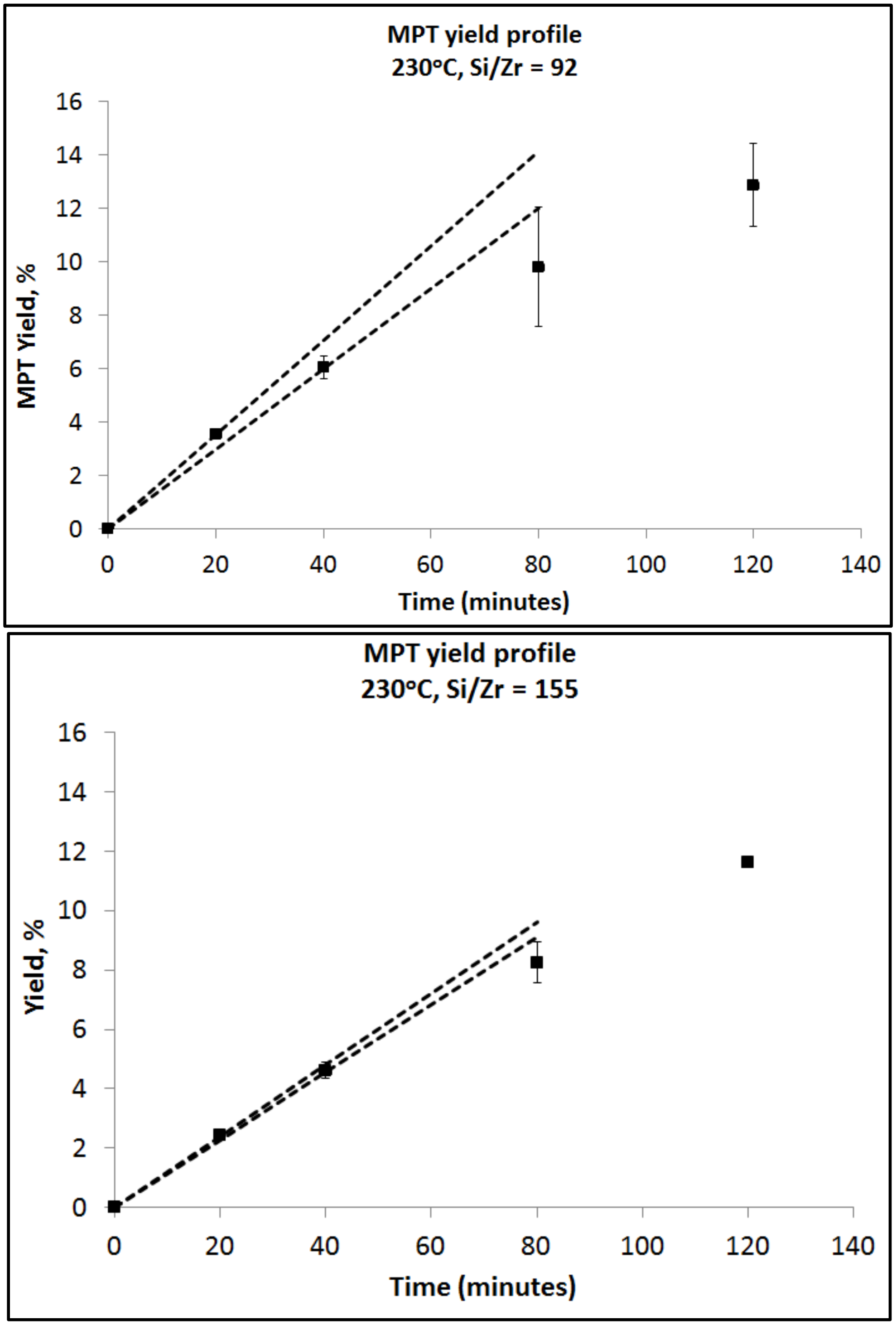

Fig. 7.15 Plots used for measuring the initial rates from the collected MPT yield profiles. Error bars are +/- standard deviation for multiple injections on GC.

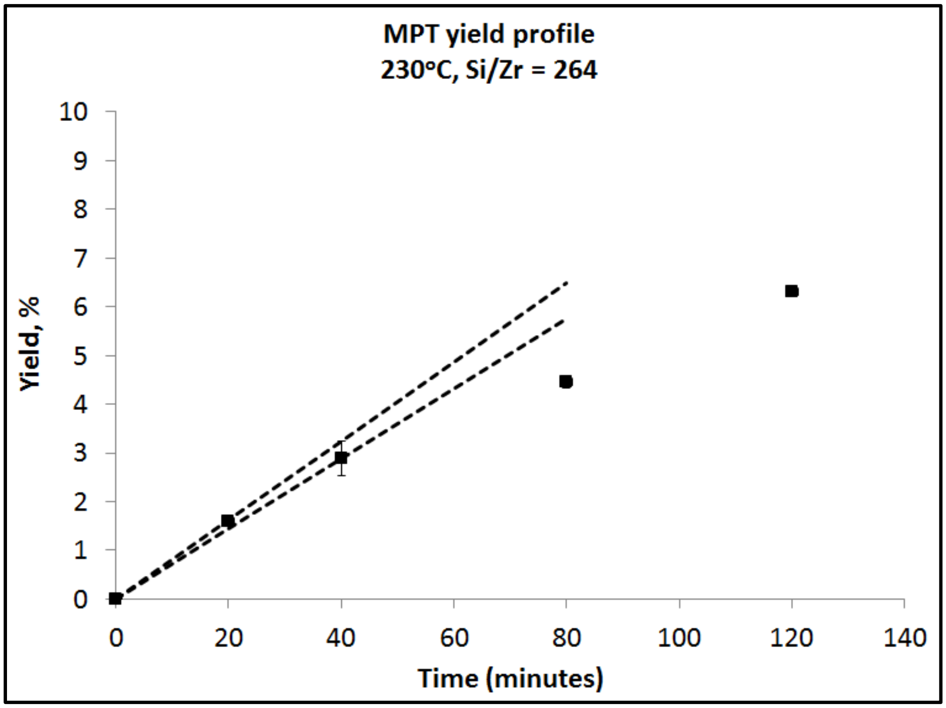

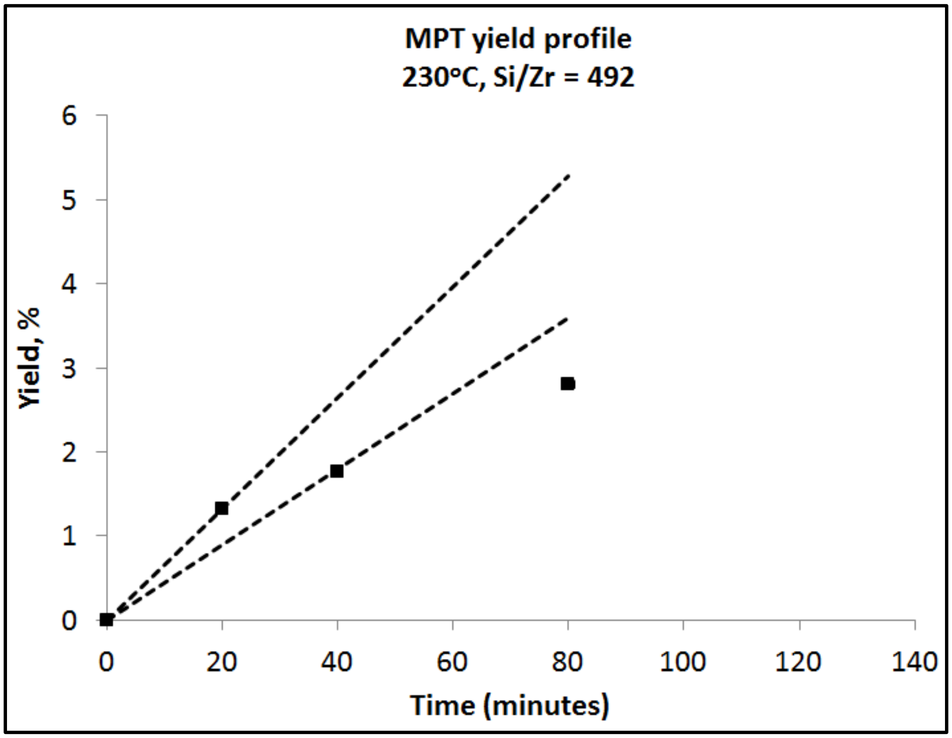

Fig. 7.15 continued Plots used for measuring the initial rates from the collected MPT yield profiles. Error bars are +/- standard deviation for multiple injections on GC.

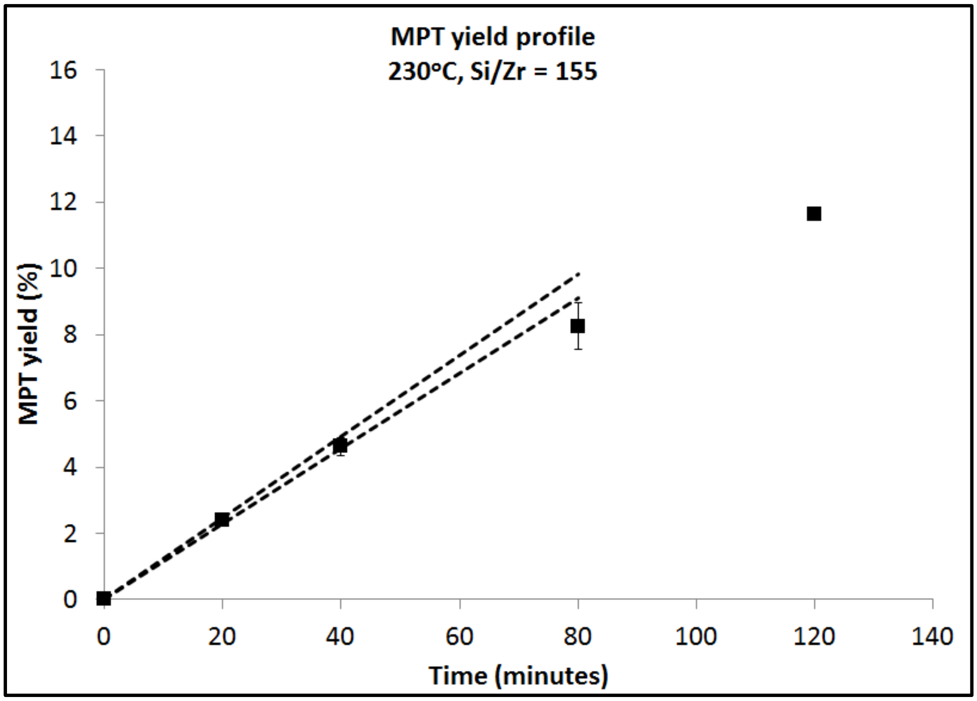

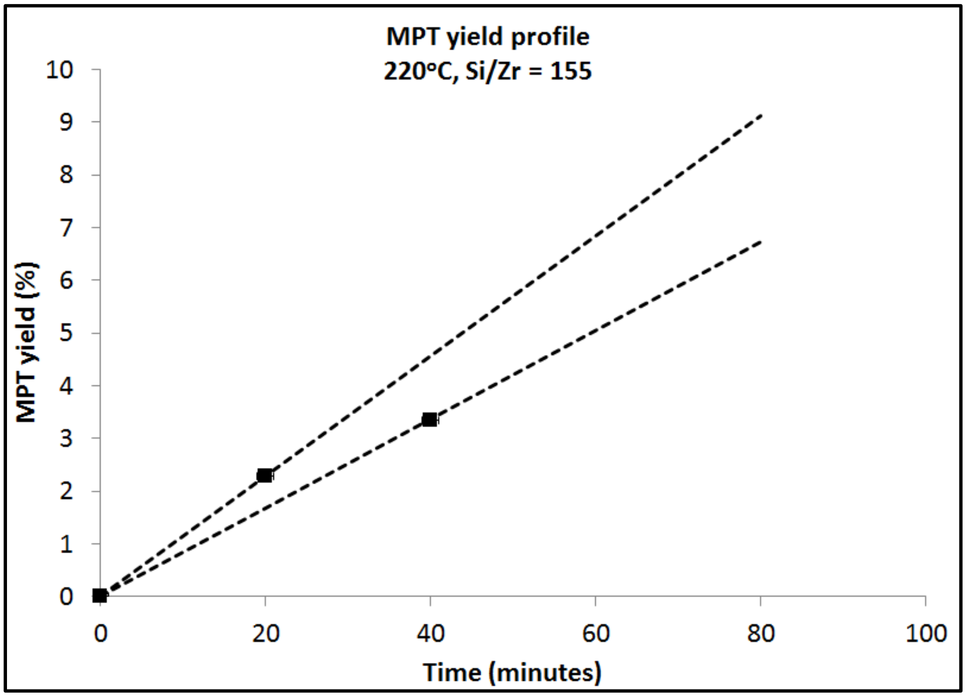

Fig. 7.15 continued Plots used for measuring the initial rates from the collected MPT yield profiles. Error bars at +/- standard deviation for yield determined by multiple injections on GC.

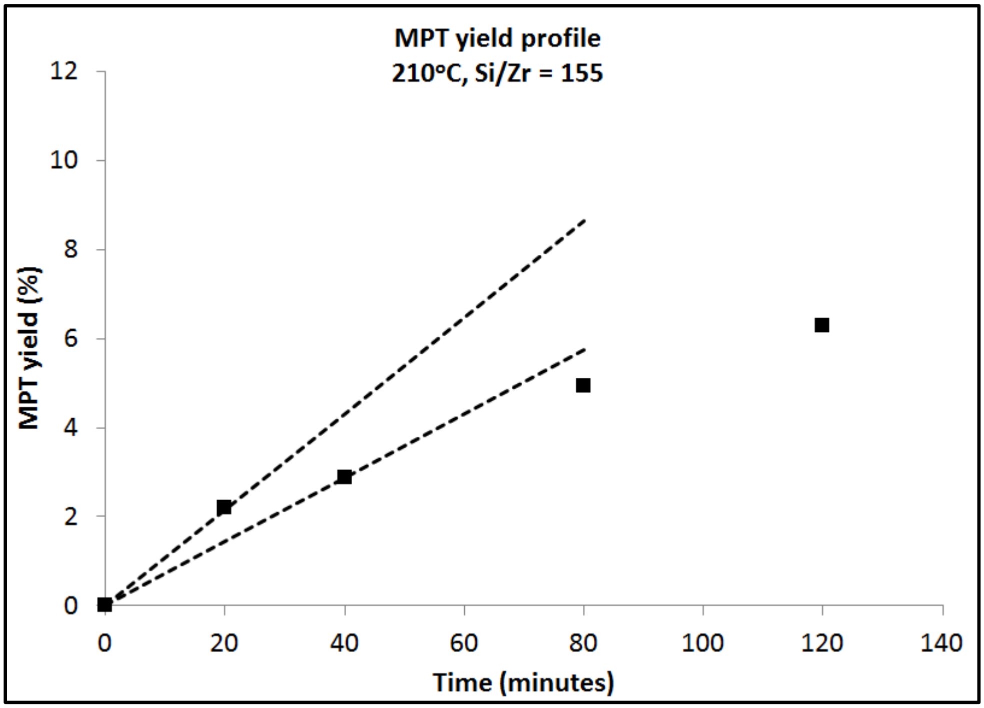

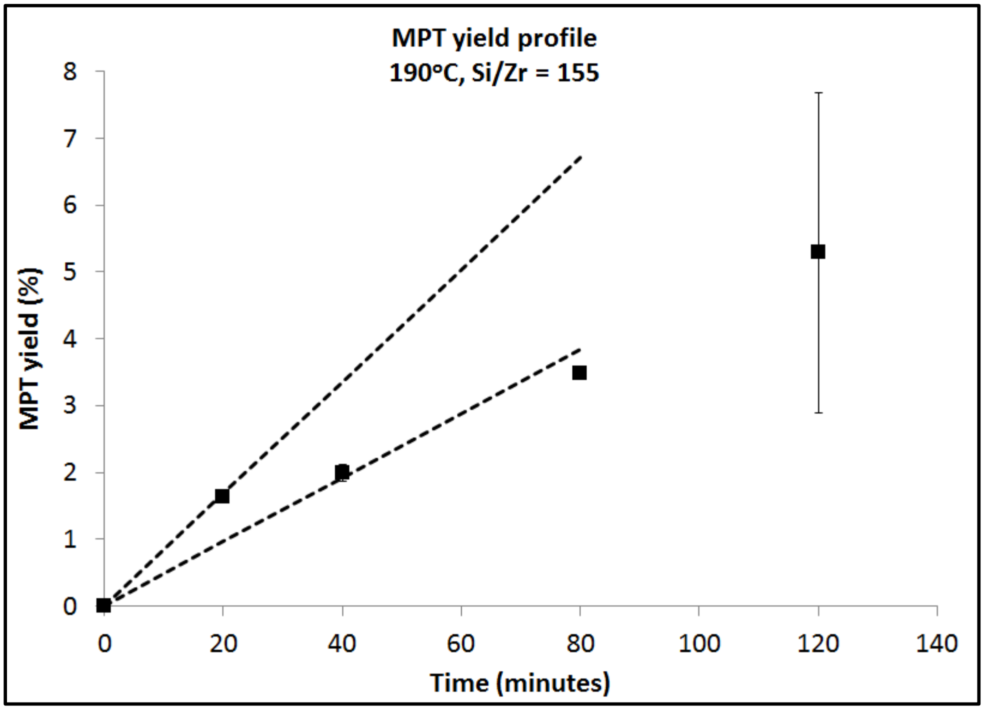

Fig. 7.15 continued Plots used for measuring the initial rates from the collected MPT yield profiles. Error bars at +/- standard deviation for yield determined by multiple injections on GC.

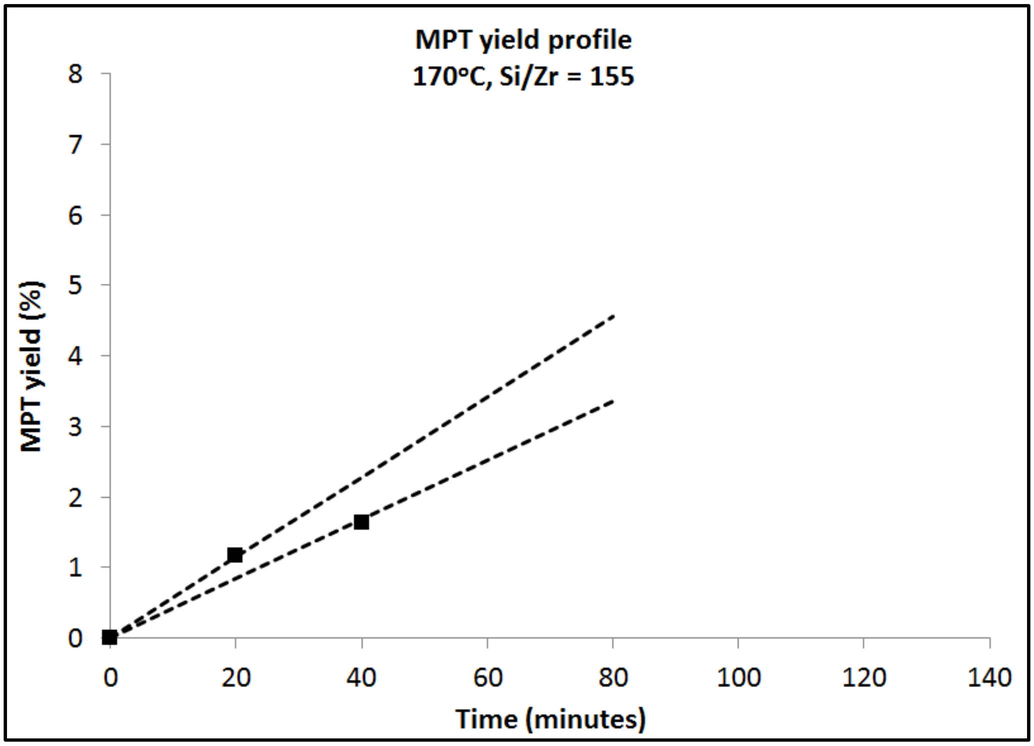

Fig. 7.15 continued Plots used for measuring the initial rates from the collected MPT yield profiles. Error bars at +/- standard deviation for yield determined by multiple injections on GC.

7.5 References

[1] Boudart, M.; *Chem. Rev.* **1995**, *95*, 661 – 666.

[2] Patet, R.E.; Nikbin, N.; Williams, C.L.; Green, S.K.; Chang, C-C.; Fan, W.; Caratzoulas, S.; Dauenhauer, P.J.; Vlachos, D.G.; *ACS. Catal.* **2015**, DOI: 10.1021/cs5020783.

CHAPTER 8

CONCLUSION AND FUTURE RESEARCH

8.1 Conclusion

The motivation of this work was to develop new methods for the production of PTA for renewable PET polymers starting from biomass-derived HMF. New Diels-Alder reactions between oxidized variants of HMF and ethylene that are catalyzed by Lewis acid molecular sieves were discovered, and have opened a new pathway for the synthesis of PTA that does not require reduction steps (Fig. 8.1). The pathway allows for a novel method for the production of 100% renewable PET from biomass (Fig. 2).

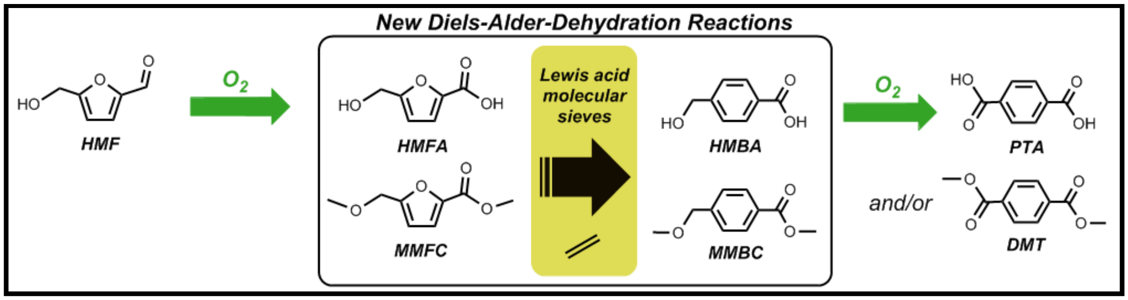

Fig. 8.1 New Diels-Alder-dehydration reactions possible using Lewis acid molecular sieves catalysts.

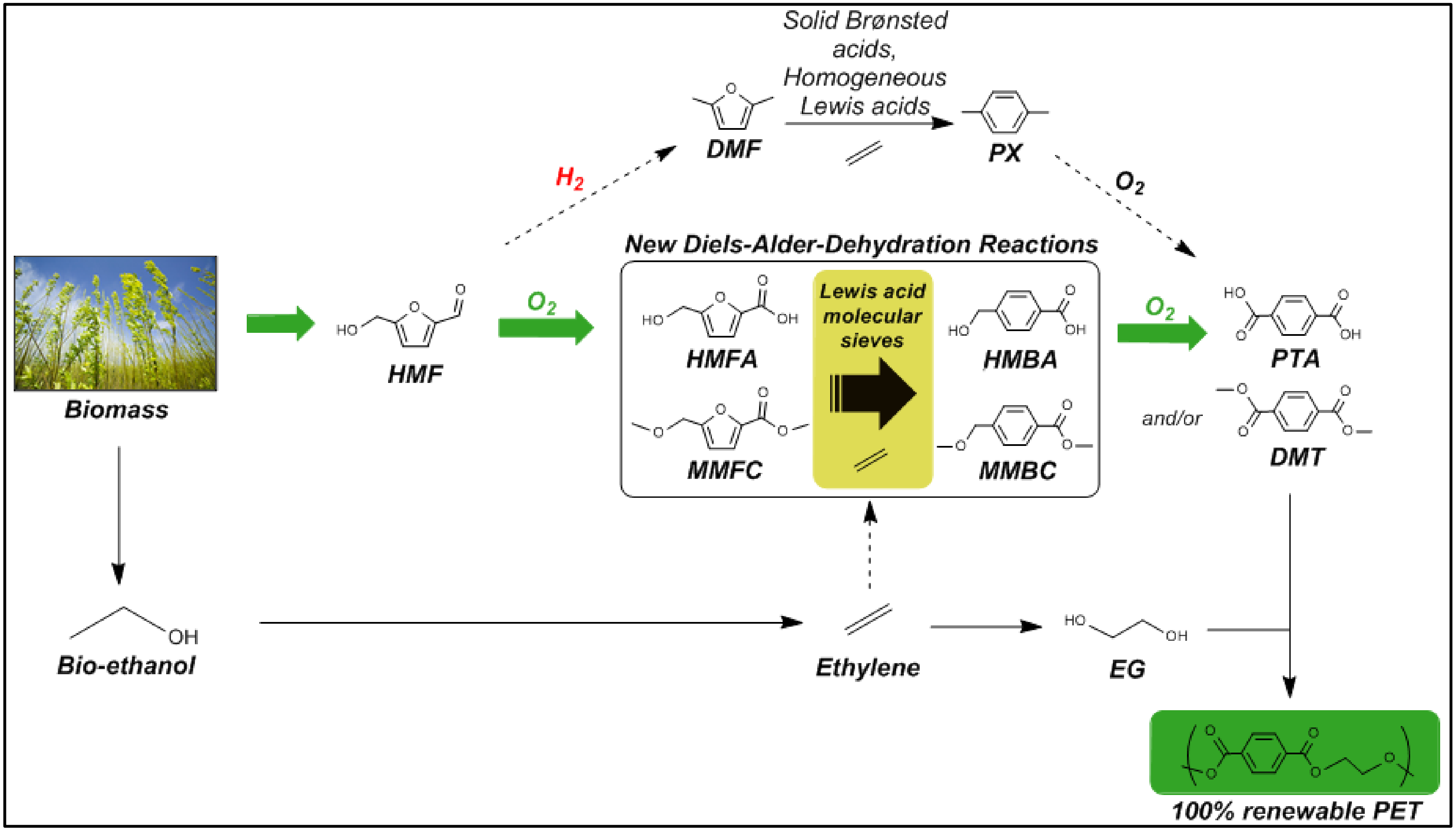

Fig. 8.2 New route to 100% renewable PET.

The work presented in this thesis has included synthesis of microporous materials for Lewis acid catalysis, exploratory research and development of new Diels-Alder-dehydration chemistry involving ethylene, and characterizations of the Diels-Alder-dehydration reaction systems that included side product identification and measurement of kinetic data (apparent activation energies).

Although there are numerous previous examples of Lewis acidic solid materials catalyzing Diels-Alder reactions, this is the first use of the series of pure silica molecular sieves containing Lewis acid metal centers in the zeolite framework (Sn-Beta, Zr-Beta, Ti-Beta) for catalyzing Diels-Alder reactions. The new Diels-Alder-dehydration reactions are unusual reactions involving furanic dienes with carboxylate group substituents that are known to usually deactivate the diene in Diels-Alder cycloadditions. These reactions are the first examples of oxygenated furans reacting at high temperatures and pressures with ethylene in Diels-Alder cycloadditions. The catalyst plays a key role in allowing the reactions to occur and an important characteristic of the catalyst is the lack of any strong Bronsted acidity since Bronsted acidity causes significant conversion and degradation of the oxygenated furans at the high temperature/pressure conditions required for ethylene to react. Confinement effects within the microporous environment of the Lewis acid molecular sieves may also be important for catalysis of some reactions since it was found that the Beta materials were the only effective catalysts for the reaction between MMFC and ethylene (the mesoporous and amorphous materials did not catalyze the reaction).

The elucidation of the key side products in the new Diels-Alder-dehydration reaction system involving MMFC and ethylene has resulted in the identification of novel cyclohexadiene-type compounds, that is methyl 4-formylcyclohexa-1,3-diene-1-carboxylate and methyl 4-formylbicyclo[2.2.2]oct-2-ene-1-carboxylate. These compounds may be considered PTA precursors and, therefore , are not necessarily undesired side products. These compounds may be included when calculating an overall selectivity to PTA precursors (MMBC, etc.) from HMF-derived MMFC.

The measurement of E_a's for two different Diels-Alder-dehydration systems (DMF/PX, MMF/MPT) catalyzed by Zr-Beta reveal low apparent E_a values that are likely too low to be activation energies of a single chemical step. Instead, these data suggest the apparent E_a's of the processes under the studied conditions may include a collection of terms that could result in low overall values. Since two reactions in tandem (Diels-Alder cycloaddition and dehydrative aromatization) occur over a heterogeneous surface, it is possible for the apparent E_a's to be a combination of terms that may include the ΔH_{rxn} for the reversible Diels-Alder reaction, the true E_a for the dehydrative aromatization of the Diels-Alder adduct, the ΔH_{ads} terms for adsorption steps in equilibrium (reactants or intermediates adsorbing reversibly onto the catalyst surface or active site), or others.

The exact mechanism of how the Lewis acid centers catalyze the Diels-Alder-dehydration reactions of oxygenated furans and ethylene is not clear at this time. Computational studies aimed at elucidating the role of different acid sites in the Diels-Alder-dehydration reaction between DMF and ethylene have suggested that Lewis acids can coordinate with ethylene to catalyze the [4 + 2]-Diels-Alder reaction, but there is no prior experimental evidence of the catalysis of ethylene in Diels-Alder cycloadditions.[1,2] Additionally, the computational studies suggested the usefulness of Lewis acids in the dehydration of cycloadducts between ethylene and furans. Several examples of Lewis acid catalysis of dehydrative aromatizations of oxabicyclic compounds, including the use of heterogeneous Lewis acids involving Fe^{3+}-exchanged montmorillonite K10 clay, have been reported.[3-5] Elucidation of the mechanism may allow for the creation of even more selective catalysts for the Diels-Alder-dehydration of the oxidized variants of HMF and ethylene for the synthesis of renewable PTA from biomass.

As mentioned, the new Diels-Alder reactions are very unusual since the furanic dienes have carboxylate group substituents that are known to typically deactivate the diene towards Diels-Alder cycloadditions. A previous system that appears to have similarities to the current Diels-Alder reactions involve 5-amino furoates reacting with mono- and diactivated dienophiles at elevated temperatures.[6,7] Specifically, each of these furans have an electron-donating group on the 5-position of the ring (amino-, hydroxymethyl-, methoxymethyl-, methyl-) that may help compensate the deactivating effect the carboxylate group has on the ability of the diene to react with dienophiles. Additionally, both the 5-amino furoate and HMFA/MMFC/MFA/MMF furoates not only require temperatures that are higher than usual for Diels-Alder chemistry (the 5-amino furoates react at $80^{o}C$ and the HMFA/MMFC/MFA/MMF furoates react at

>170^{o}C), but also involve a subsequent reaction that occurs in tandem. The 5-amino furoates react with dienophiles and spontaneously ring-open to generate cyclohexadienols, while the HMFA/MMFC/MFA/MMF furoates react with ethylene in the presence of a solid Lewis acid to form the dehydrated Diels-Alder adducts (1,4-substituted benzenes). Interestingly, when the cyclohexadienols were contacted with a Lewis acid ($BF_3 \bullet OEt_2$) the dehydration to the polysubstituted aniline product occurred.

8.2 Future research directions

Currently, the key issues regarding the new Diels-Alder pathways to PTA from oxidized derivatives of HMF and ethylene that are hindering the commercial viability include slow reaction rates and low product yields (~25% MMBC yield after several hours), and low reaction concentrations (2 wt%). The conversion of DMF and ethylene to PX is currently being pursued commercially. Methods are reported in the patent application for producing high yields (>80%) of PX within several hours using DMF concentrations of up to 9 wt%.[8] Further research is required to develop reaction conditions, methods, and catalysts for producing the PTA intermediates (HMBA or MMBC) at yields and concentrations closer to those reported for the DMF/PX system. Since the reduction of HMF to DMF is not required for the new pathways, the yields and concentrations may not need to be as high as those for the DMF/PX system to be competitive. Although the selectivity for the MMFC/MMBC conversion using Zr-Beta is high (>70-80 %), the development of preparation methods for catalysts that allow for selectivities even closer to 100% would also be important. To improve the catalysis of the new Diels-Alder-dehydration reactions, future research efforts should be aimed at improving the understanding of (1) the reaction mechanism, including rate-determining step, and (2) the nature of the catalytic active site and deactivation mechanisms. This work will prove helpful in designing faster, more robust, and more selective catalysts.

8.3 References

[1] Nikbin, N.; Do, P.T.; Caratzoulas, S.; Lobo, R.F.; Dauenhauer, P.J.; Vlachos, D.G.; *J. Catal.* **2013**, *297*, 35 – 43.

[2] Nikbin, N.; Feng, S.; Caratzoulas, S.; Vlachos, D.G.; *J. Phys. Chem. C* **2014**, *118*, 24415 – 24424.

[3] Ilyin, A.; Kysil, V.; Krasavin, M.; Kurashvili, I.; Ivachtchenko, A.V.; *J. Org. Chem.* **2006**, *71*(25), 9544 – 9547.

[4] Wong H.N.C.; Ng, T.; Wong, T.; Xing, Y.D.; *Hetero* **1984**, *22*(4), 875 – 890.

[5] Claeys, D.D.; Stevens, C.V.; Roman, B.I.; Van De Caveye, P.; Waroquier, M.; Speybroeck, V.V.; *Org Biomol Chem* **2010**, *8*(16), 3644 – 3654.

[6] Cochran, J.E.; Wu, T.; Padwa, A.; *Tetrahedron Lett.* **1996** *37*(17), 2903 – 2906.

[7] Padwa, A.; Dimitroff, M.; Waterson, A.G.; Wu, T.; *J. Org. Chem.* **1997**, *62*, 4088 – 4096.

[8] Masuno, M.N.; Smith, P.B.; Hucul, D.A.; Dumitrascu, A.; Brune, K.; Smith, R.L.; Bissell, J.; Foster, M.; Methods of producing para-xylene and terephthalic acid. U.S. Patent Appl. No. 13/838,761, **2013**.

APPENDIX

Chapter 2

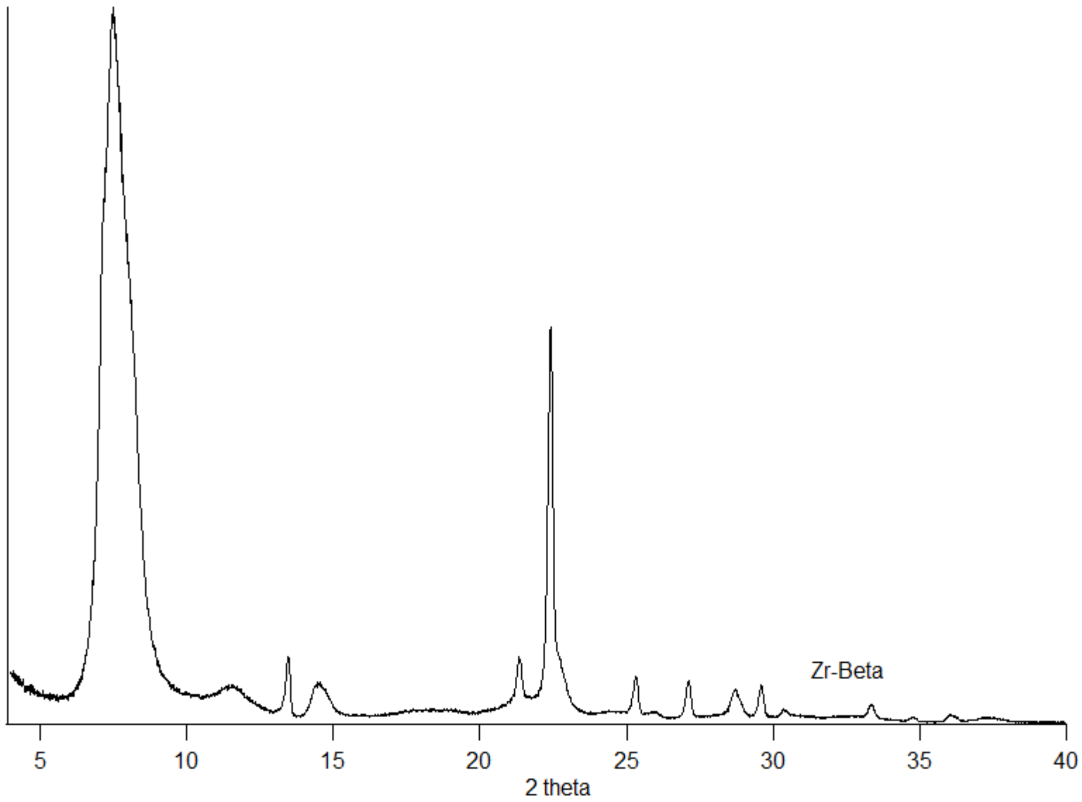

Fig. 2.1-A XRD pattern of Zr-Beta.

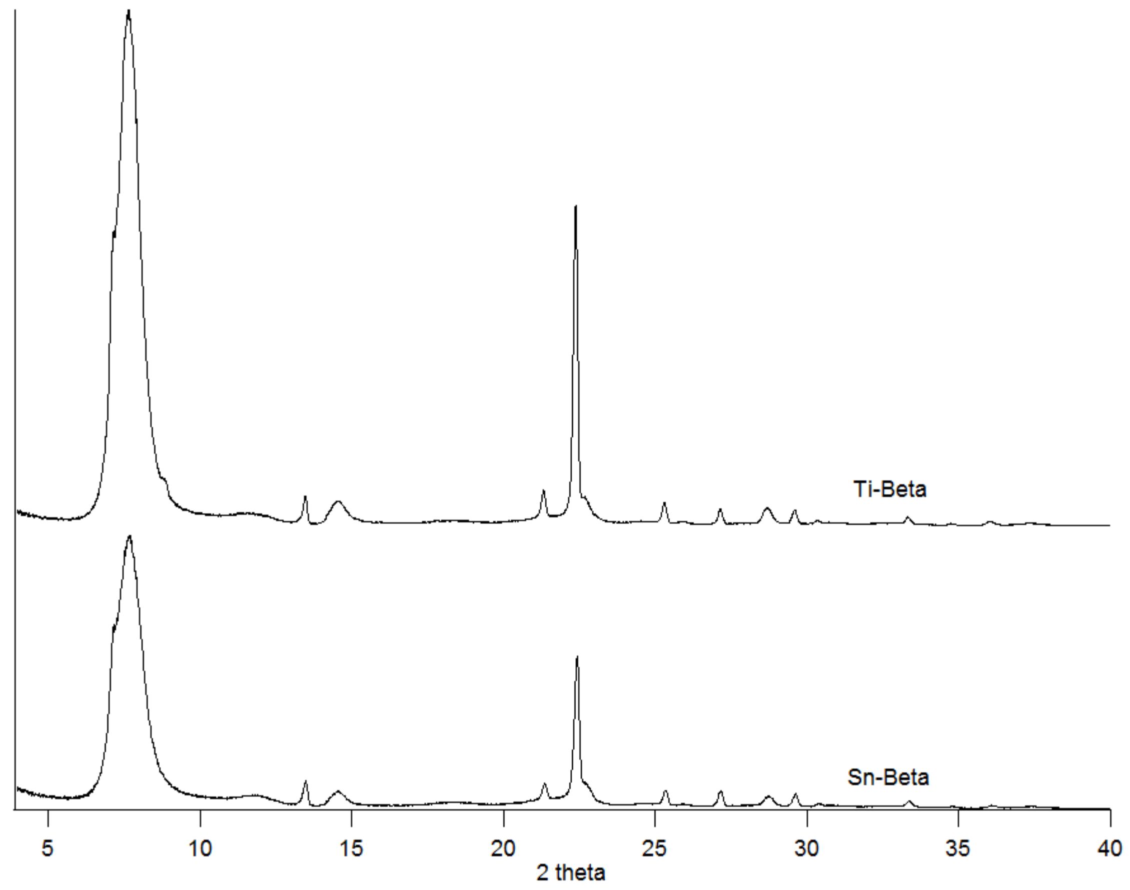

Fig. 2.2-A XRD patterns of Sn-Beta and Ti-Beta.

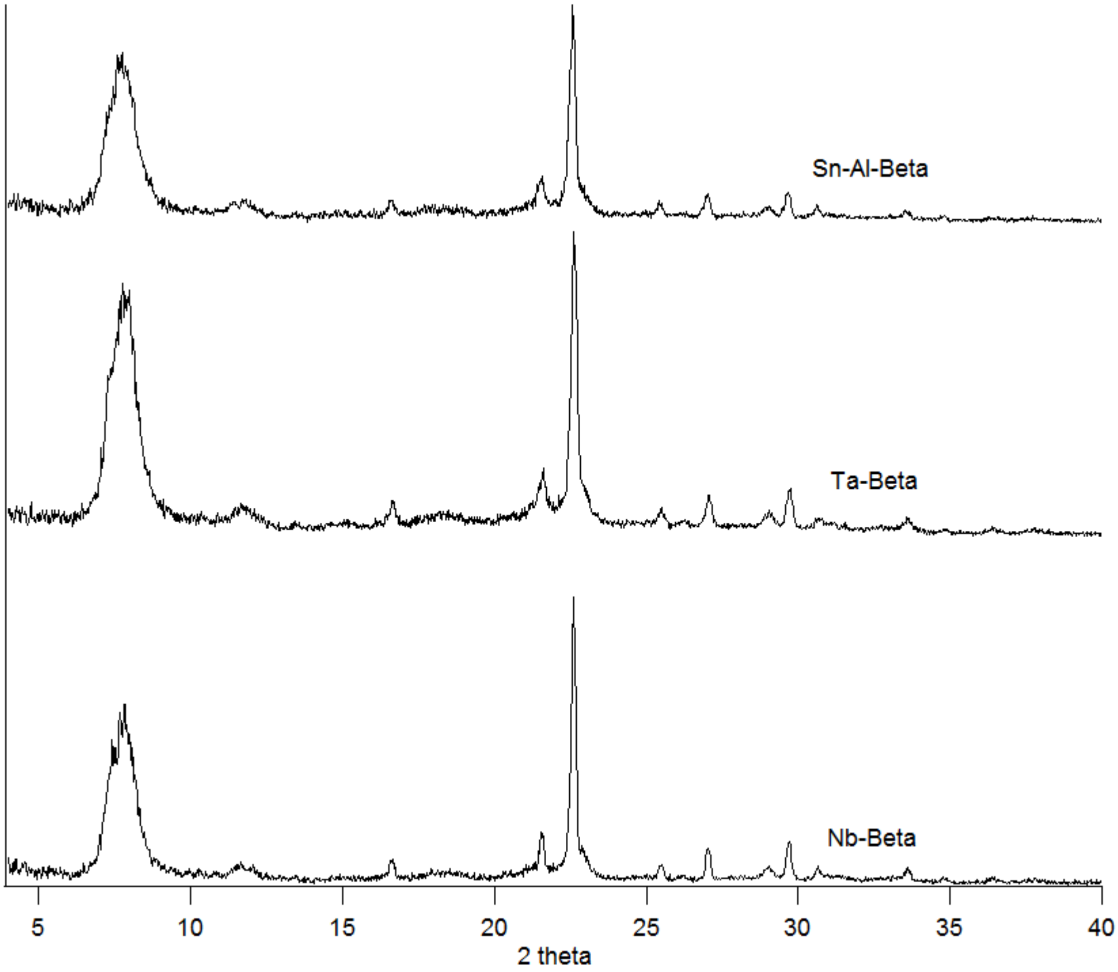

Fig. 2.3-A XRD patterns of Sn-Al-Beta, Ta-Beta, and Nb-Beta.

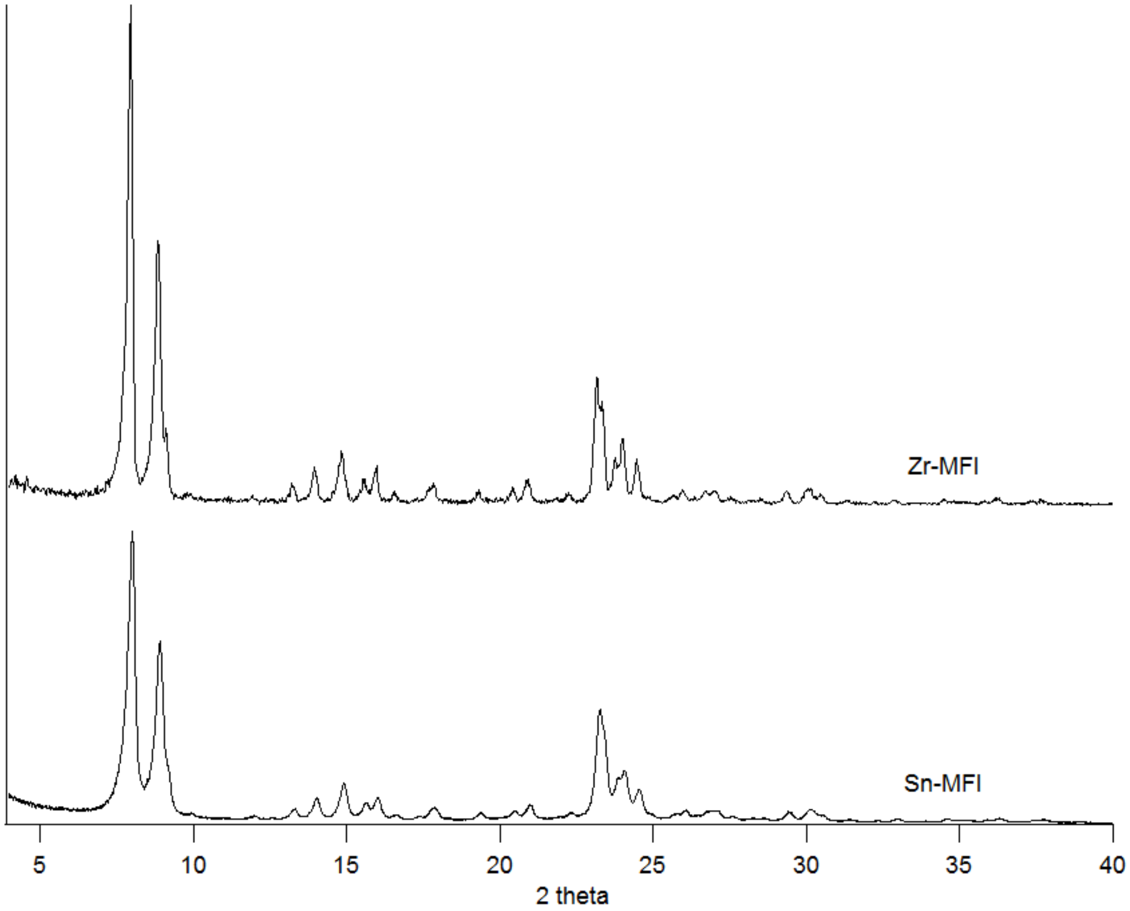

Fig. 2.4-A XRD patterns of Zr-MFI and Sn-MFI.

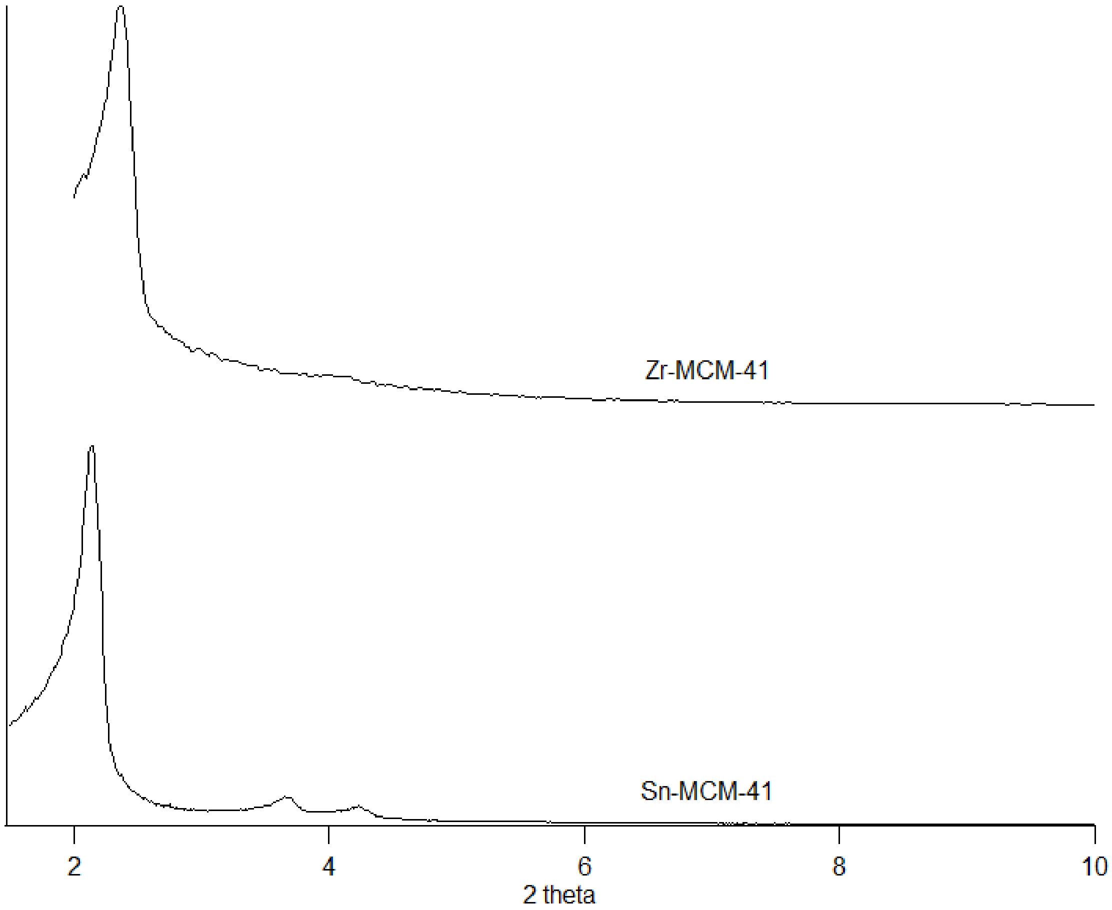

Fig. 2.5-A XRD patterns of Zr-MCM-41 and Sn-MCM-41.

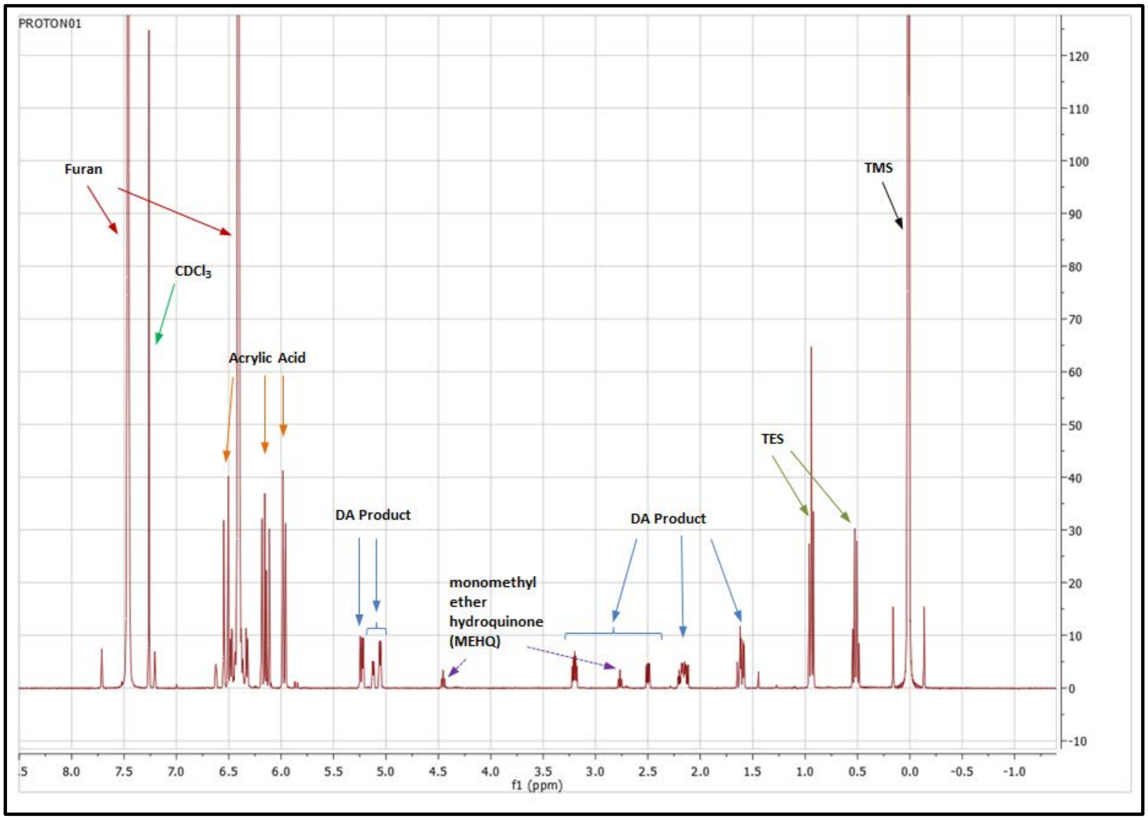

Fig. 2.6-A Example ^{1}H NMR spectrum taken in $CDCl_3$ of product solution of the Diels-Alder reaction between furan and acrylic acid with each of the peaks identified. The DA product, 7-oxa-bicyclo[2.2.1]hept-5-ene-2-carboxylic acid, was identified by using the product standard obtained from Matrix Scientific. All shifts are relative to TMS (tetramethylsilane). Monomethyl ether hydroquinone (MEHQ) was a stabilizer in the acrylic acid obtained from Sigma-Aldrich and no effort was made to remove the MEHQ prior to use.

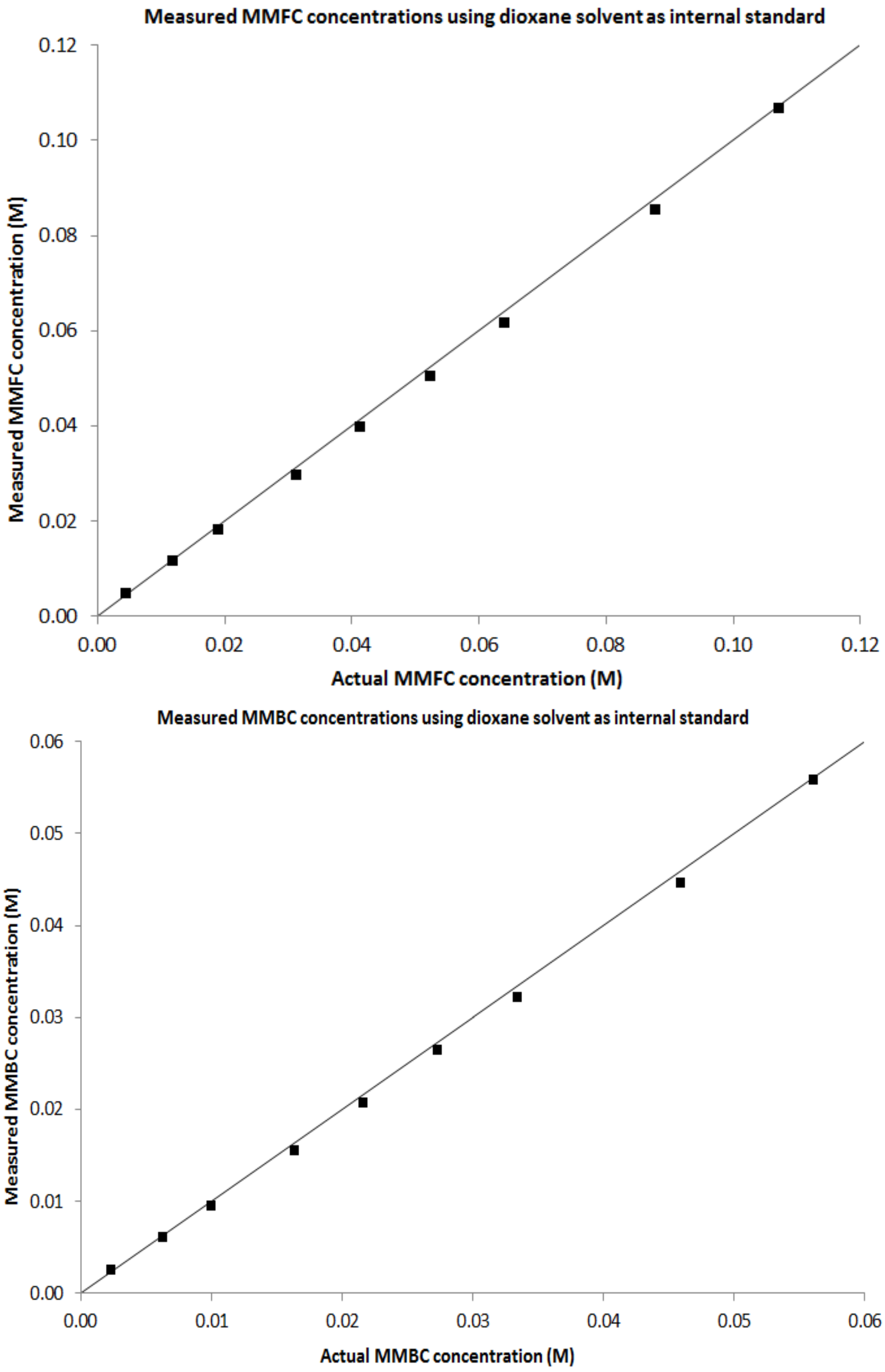

Fig. 2.7-A Measured MMFC and MMBC concentrations in dioxane by using the dioxane peak as internal standard for a series of solutions of known concentrations.

Table 2.1-A. Comparison of reaction results for the ethylene Diels-Alder-dehydration conversion of MMFC to MMBC using TES as external standard and the dioxane solvent as internal standard. Reaction conditions: 0.1 M MMFC solution in dioxane, 100 mg catalyst, 190°C, 1000 psig C_2H_4.

Entry	Catalyst	Time (hr)	^{1}H NMR method	MMFC conversion (%)	MMBC yield (%)	MMBC selectivity (%)
1	Zr-Beta-185	4	TES external standard	21.6	16.3	75.5
			Dioxane internal standard	21.5	16.3	75.8
2	Zr-Beta-185	6	TES external standard	25.6	20.8	81.3
			Dioxane internal standard	27.6	19.9	72.1
3	Zr-Beta-185	12	TES external standard	42.1	32.2	76.5
			Dioxane internal standard	41.6	32.3	77.6
4	Zr-Beta-116	6	TES external standard	33.9	28.8	85.0
			Dioxane internal standard	32.2	30.0	93.2

Chapter 3

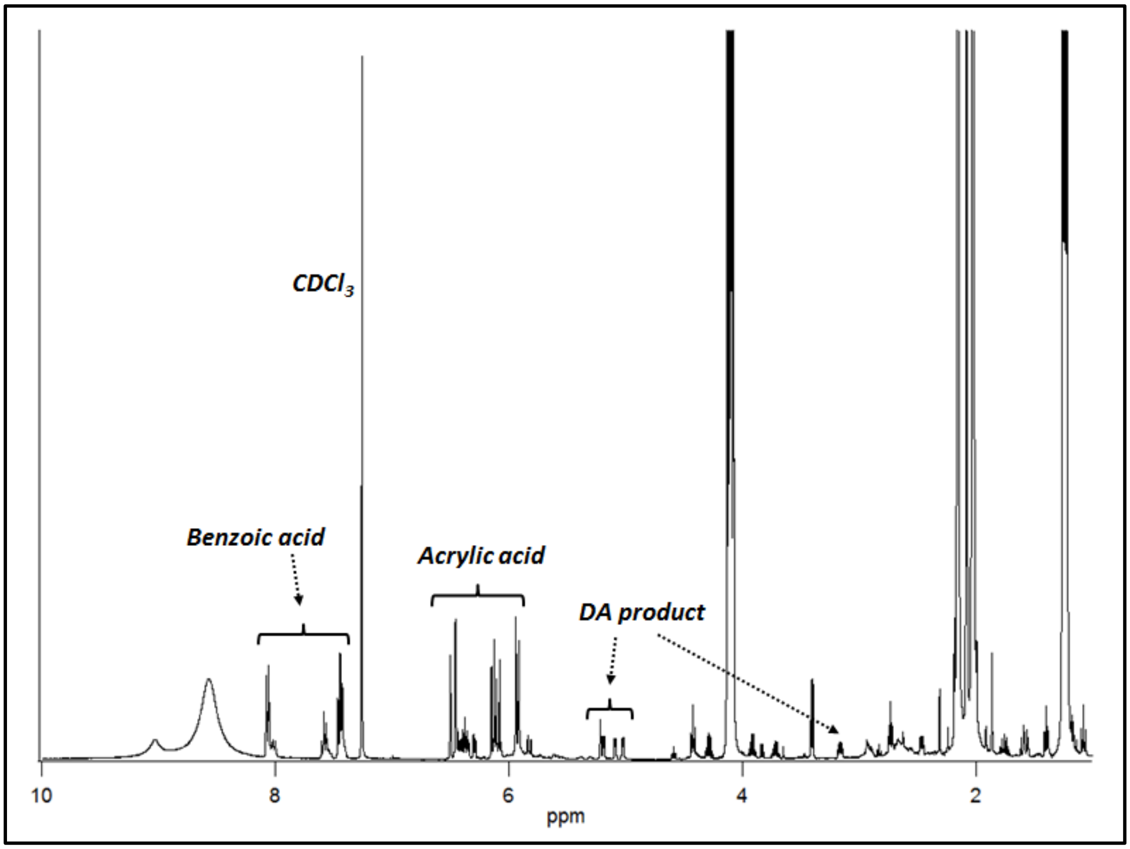

Fig. 3.1-A ^{1}H NMR spectrum (in $CDCl_3$) of the product obtained from the conversion of 7-oxa-bicyclo[2.2.1]hept-5-ene-2-carboxylic acid to benzoic acid using concentrated sulfuric acid at 0^{o}C. The benzoic acid product, acrylic acid (formed by the retro-Diels-Alder reaction), and unreacted 7-oxa-bicyclo[2.2.1]hept-5-ene-2-carboxylic acid are identified.

Chapter 4

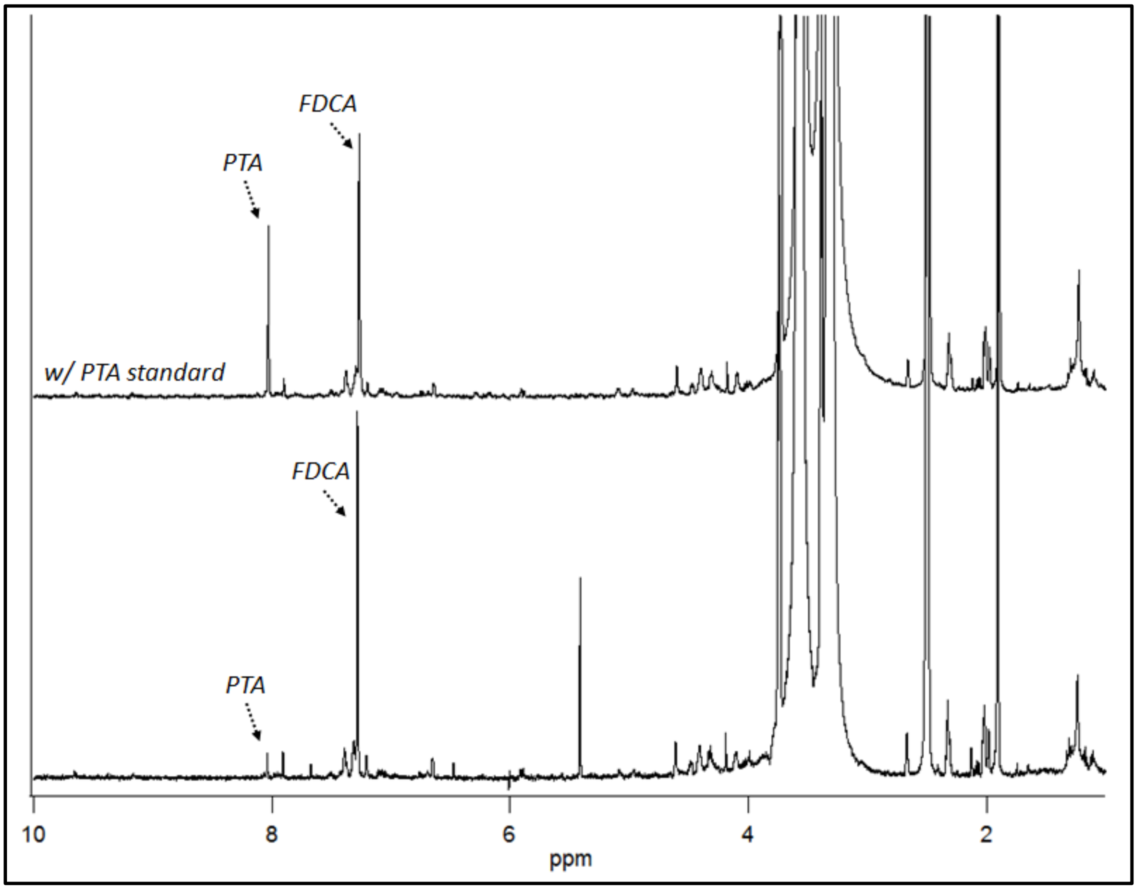

Fig. 4.1-A Diels-Alder-dehydration of FDCA and ethylene to PTA. ^{1}H NMR (in DMSO-d_6) of crude product solution (bottom) and product solution spiked with PTA product standard (top). Dioxane solvent shows up at 3-4 ppm. Reaction conditions: 0.1 M FDCA in dioxane, 200 mg Sn-Beta, 250^{o}C, 1000 psig C_2H_4, 14 hours.

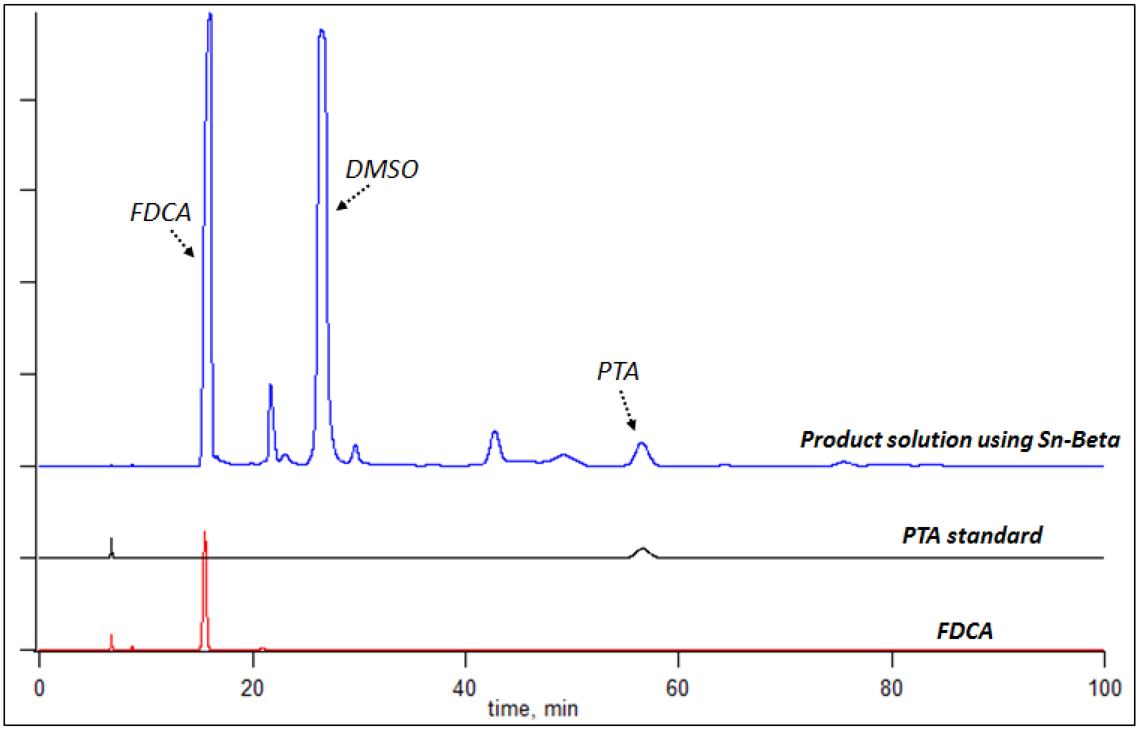

Fig. 4.2-A Diels-Alder-dehydration of FDCA and ethylene to PTA. HPLC chromatograms of reaction product solution using Sn-Beta catalyst (top), PTA product standard (middle), and FDCA reactant (bottom). DMSO is present in the product solution since DMSO was used to solubilize all of the FDCA and PTA while recovering from reactor. Reaction conditions: 1 M FDCA in dioxane, 200 mg Sn-Beta, 225^{o}C, 1000 psig C_2H_4, 16 hours.

Chapter 5

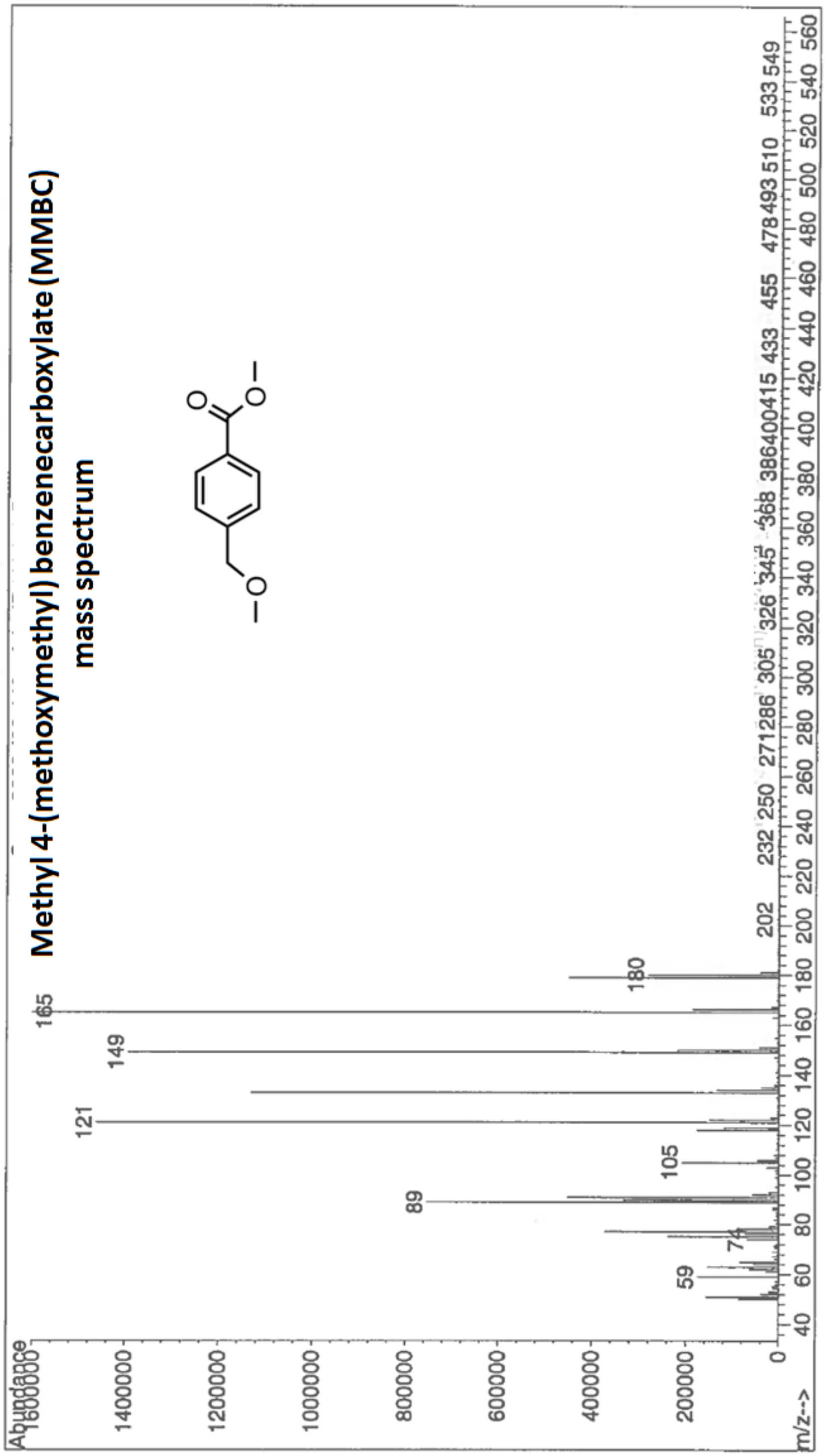

Fig. 5.1-A EI mass spectrum of methyl 4-(methoxymethyl) benzenecarboxylate (MMBC) product in the Diels-Alder-dehydration of MMFC and ethylene.

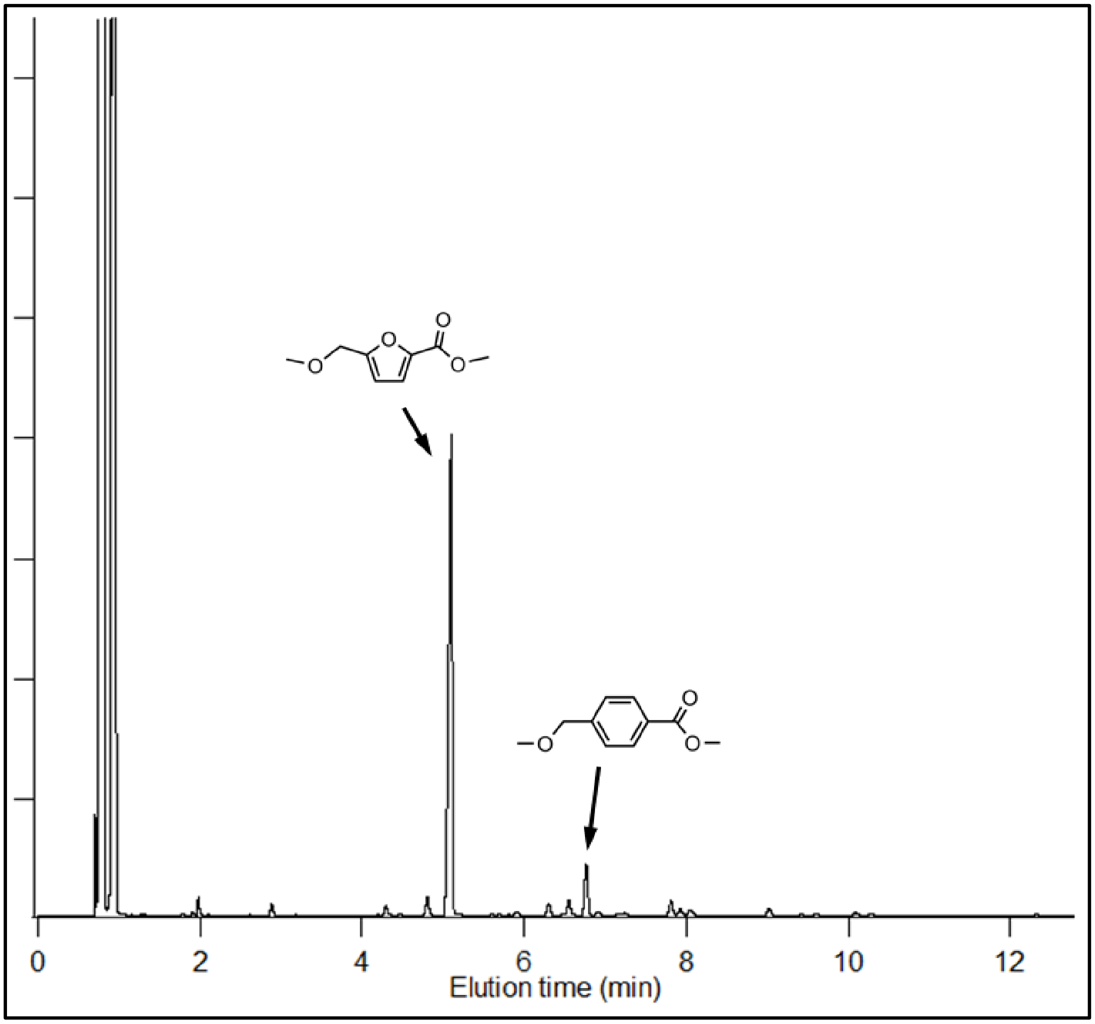

Fig. 5.2-A GC-FID chromatogram of product solution for ethylene Diels-Alder-dehydration of MMFC using high MMFC concentrations. Reaction conditions: 10 wt % MMFC in dioxane, 190°C, 6 hr, 1000 psig C_2H_4.

Chapter 6

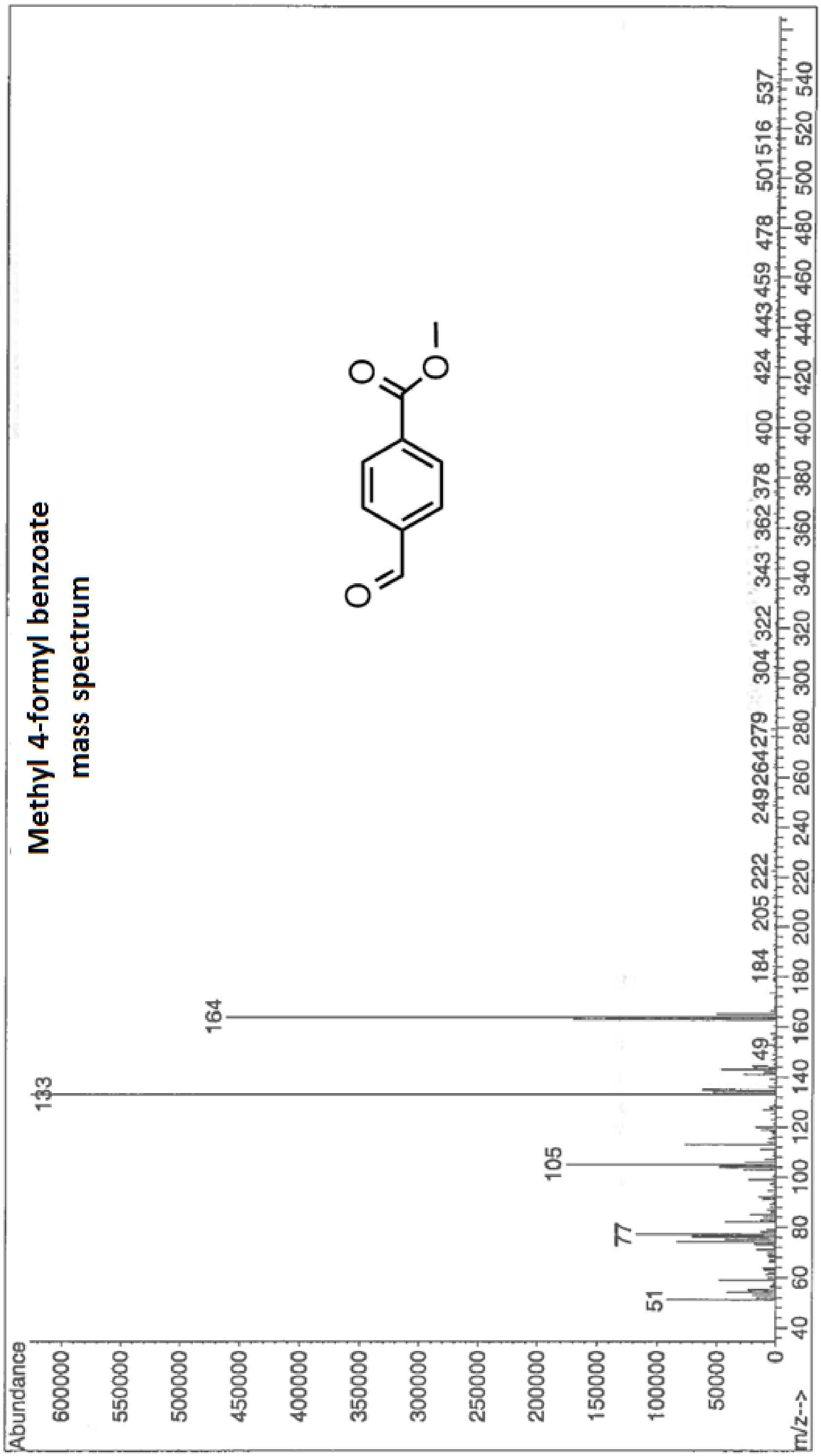

Fig. 6.1-A EI mass spectrum of methyl 4-formyl benzoate in Fig. 6.11.

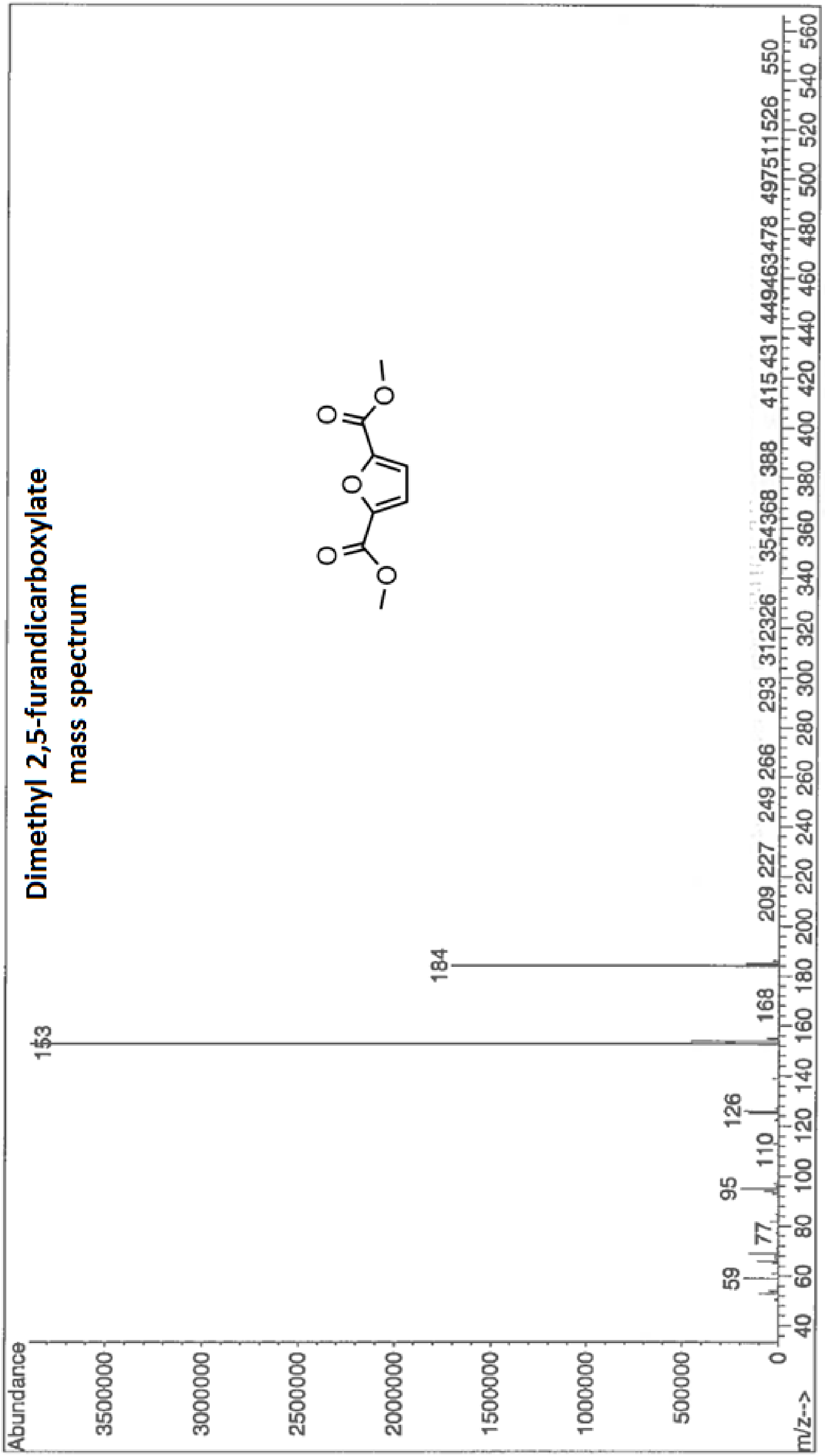

Fig. 6.2-A EI mass spectrum of dimethyl 2,5-furandicarboxylate in Fig. 6.11.

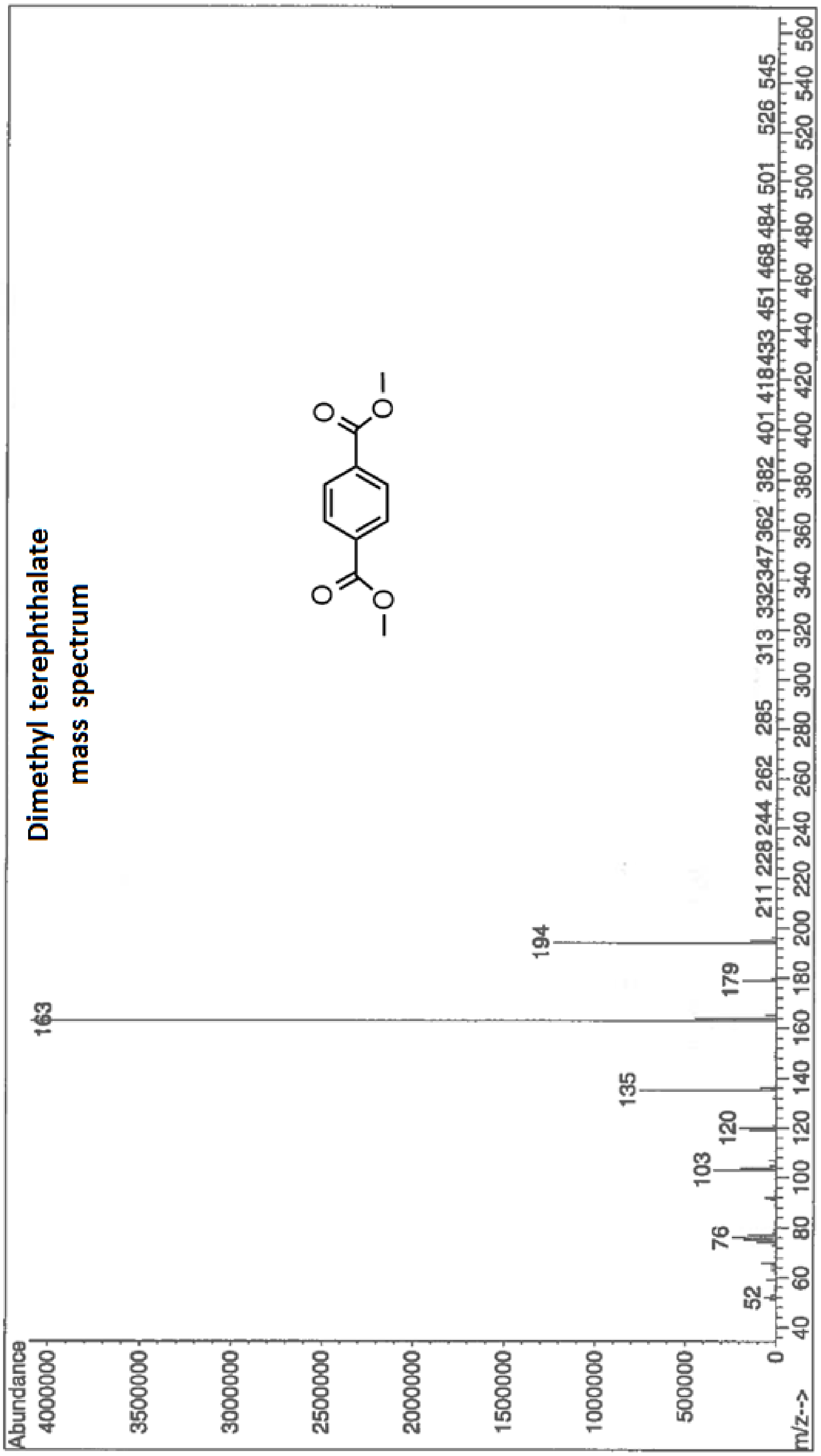

Fig. 6.3-A EI mass spectrum of dimethyl terephthalate in Fig. 6.11.

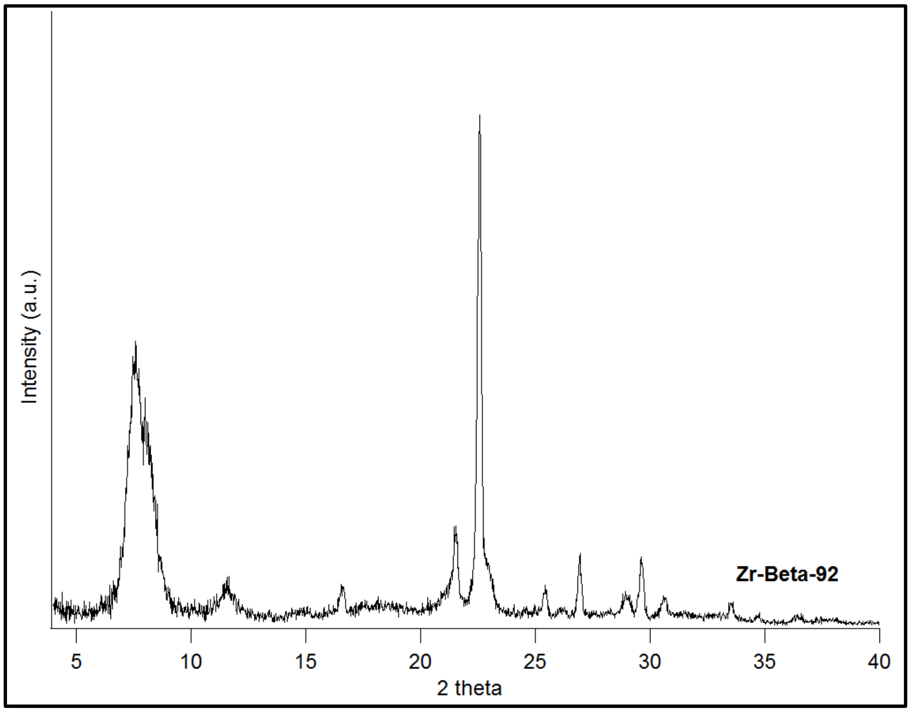

Fig. 7.1-A XRD pattern of Zr-Beta-92.

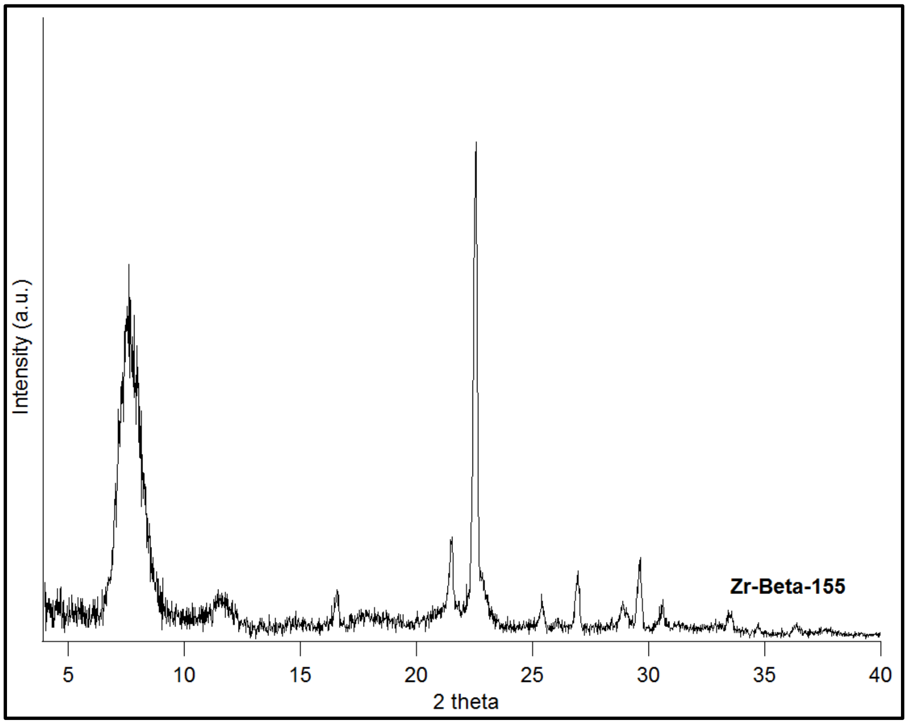

Fig. 7.2-A XRD pattern of Zr-Beta-155.

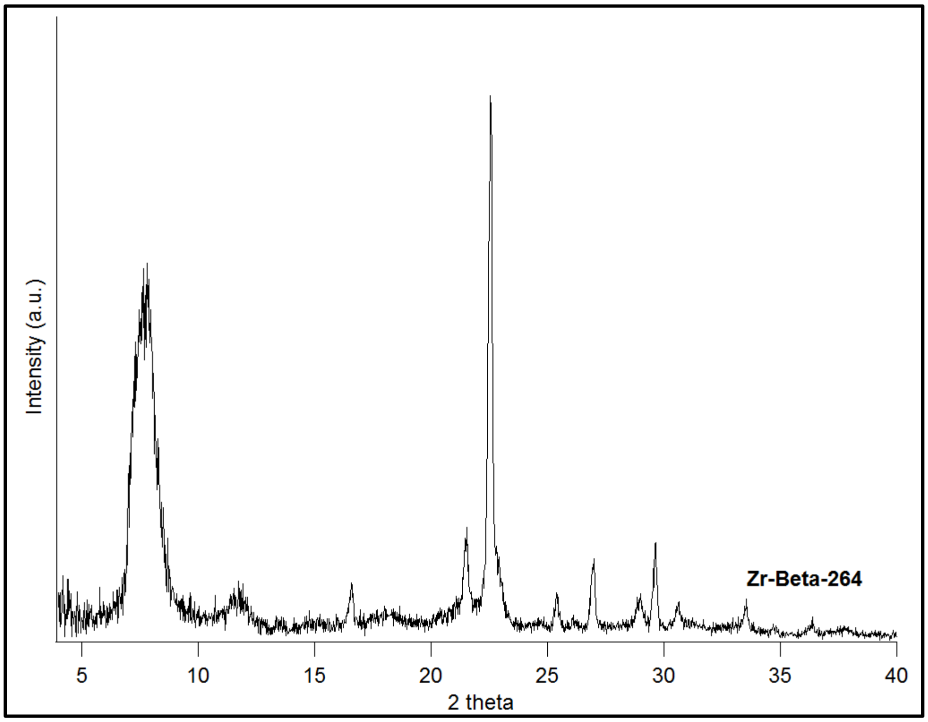

Fig. 7.3-A XRD pattern of Zr-Beta-264.

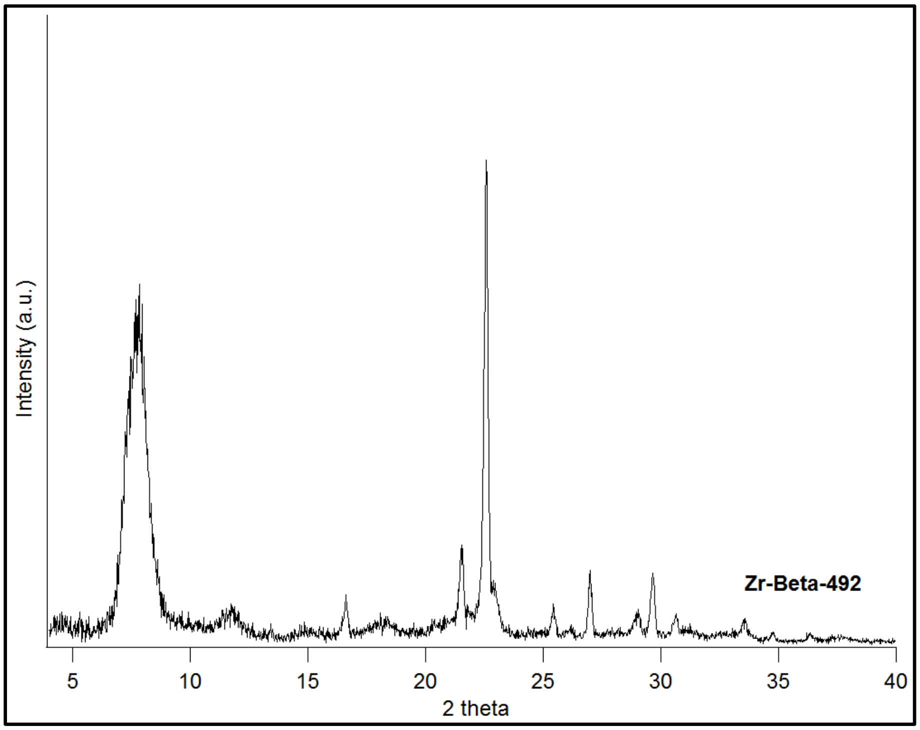

Fig. 7.4-A XRD pattern of Zr-Beta-492.

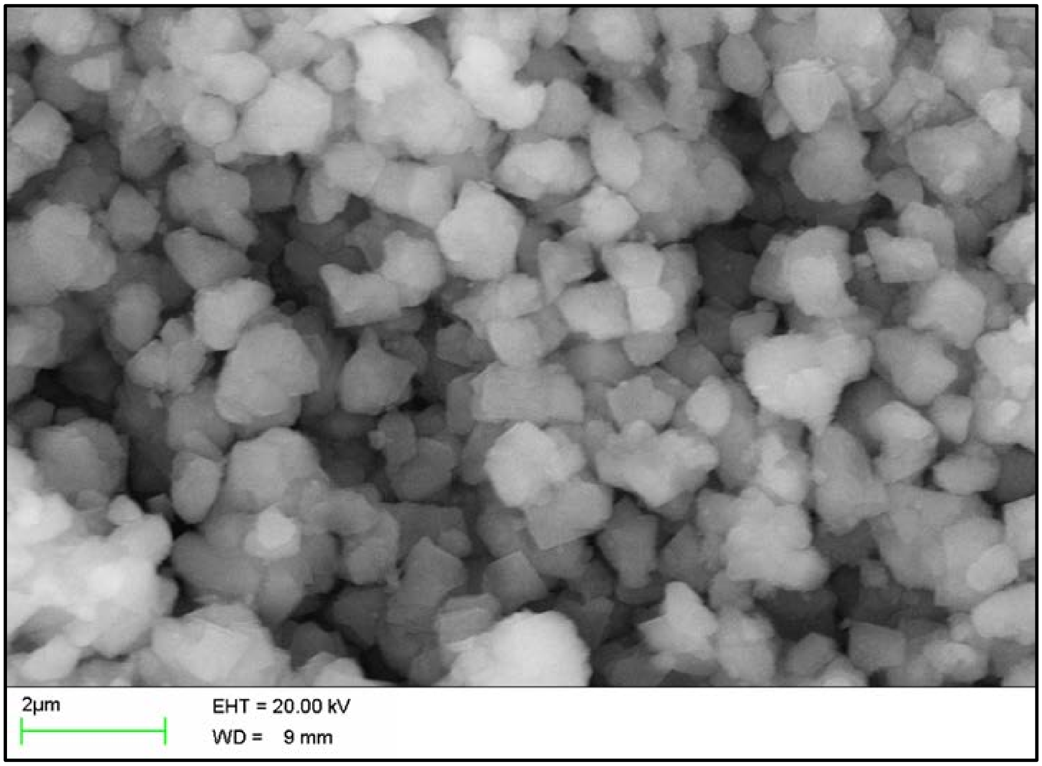

Fig. 7.5-A SEM image of Zr-Beta-92.

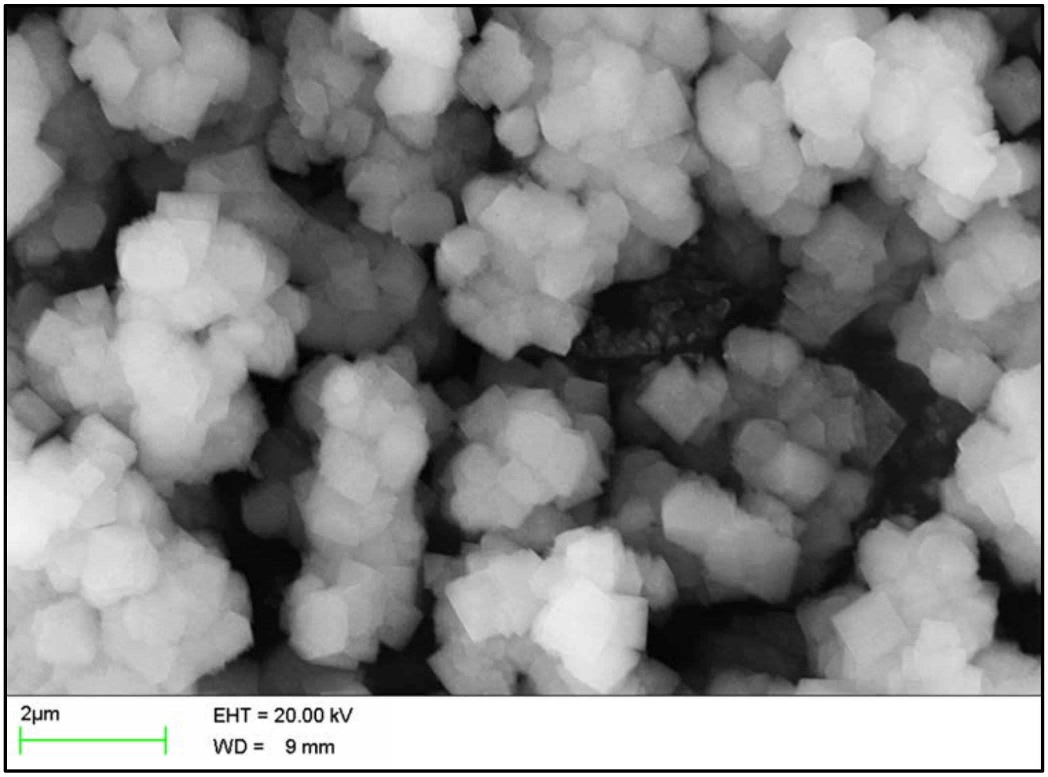

Fig. 7.6-A SEM image of Zr-Beta-155.

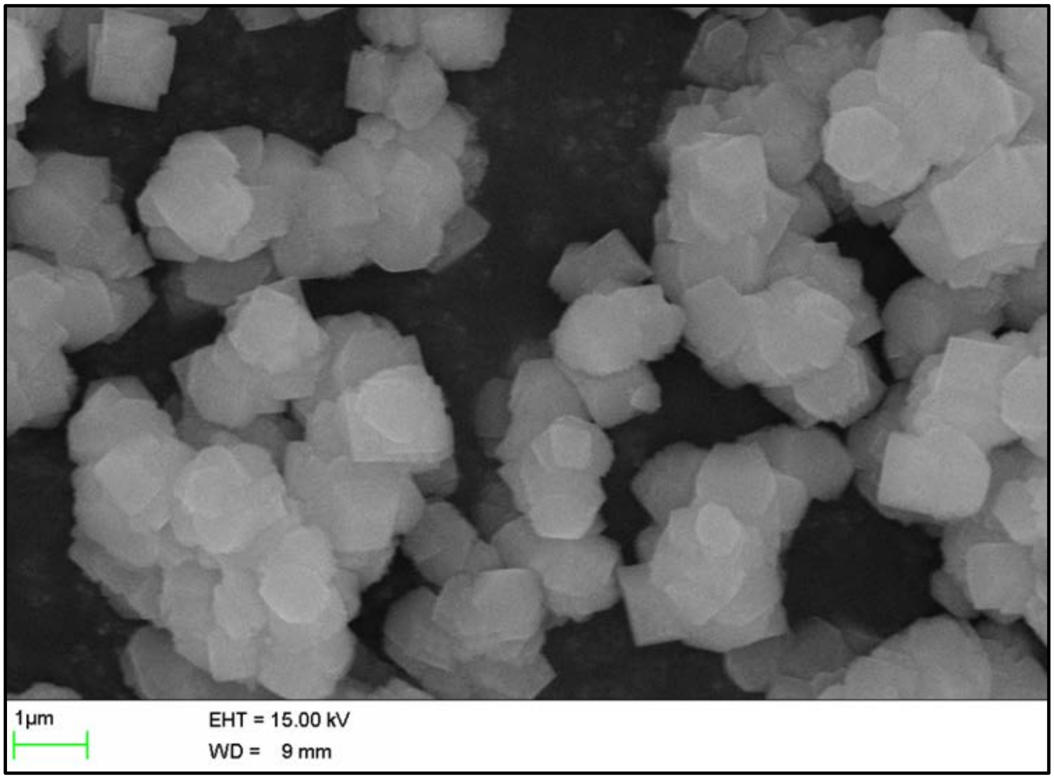

Fig. 7.7-A SEM image of Zr-Beta-264.

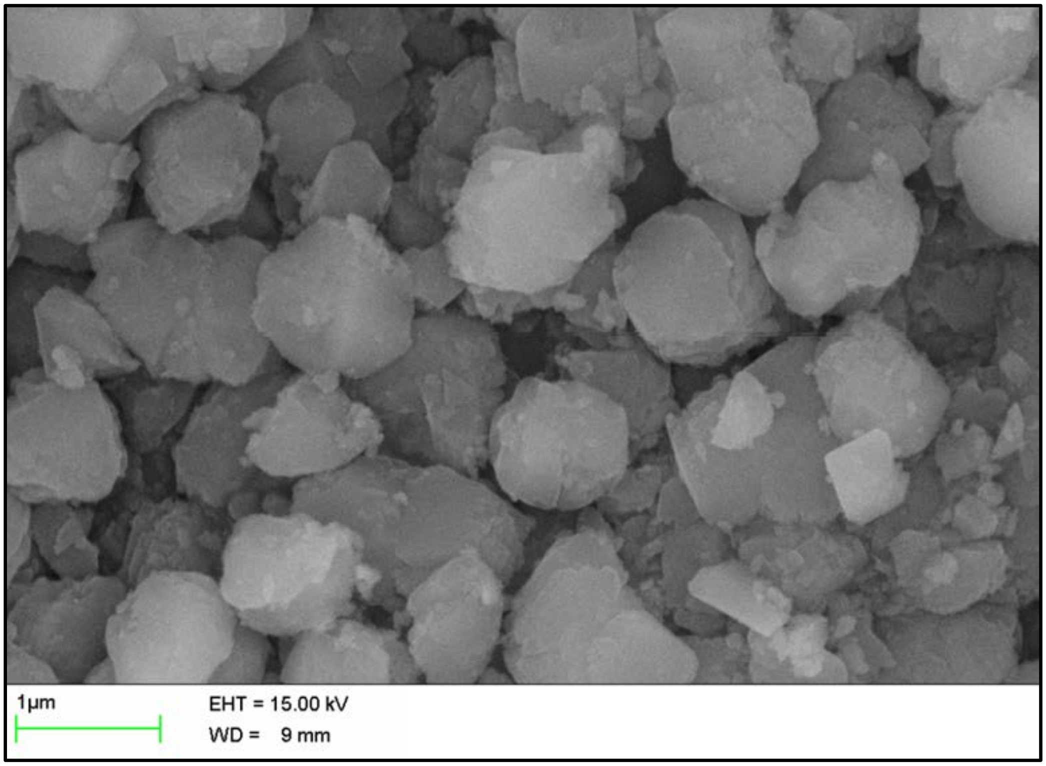

Fig. 7.8-A SEM image of Zr-Beta-492.